

“

INTERNATIONAL STUDIES AND EVALUATIONS IN THE FIELD OF

MECHANICAL ENGINEERING

December 2024

EDITORS

PROF. DR. COŞKUN ÖZALP

PROF. DR. SELAHATTN BARDAK

”

Genel Yayın Yönetmeni / Editor in Chief • C. Cansın Selin Temana

Kapak & İç Tasarım / Cover & Interior Design • Serüven Yayınevi

Birinci Basım / First Edition • © Aralık 2024

ISBN • 978-625-5955-74-6

© copyright

Bu kitabın yayın hakkı Serüven Yayınevi'ne aittir.

Kaynak gösterilmeden alıntı yapılamaz, izin almadan hiçbir yolla çoğaltılamaz. The right to publish this book belongs to Serüven Publishing. Citation can not be shown without the source, reproduced in any way without permission.

Serüven Yayınevi / Serüven Publishing

Türkiye Adres / Turkey Address: Kızılay Mah. Fevzi Çakmak 1. Sokak

Ümit Apt No: 22/A Çankaya/ANKARA

Telefon / Phone: 05437675765

web: www.seruyenyayinevi.com

e-mail: seruyenyayinevi@gmail.com

Baskı & Cilt / Printing & Volume

Sertifika / Certificate No: 47083

INTERNATIONAL RESEARCH
AND EVALUATIONS IN THE
FIELD OF MECHANICAL
ENGINEERING

EDITORS

PROF. DR. COŞKUN ÖZALP

PROF. DR. SELAHATTİN BARDAK

Contents

Chapter 1

DESIGN AND EXPERIMENTAL STUDIES OF BIO-INSPIRED WING MODEL

<i>Samet Giray TUNCA</i>	1
<i>Mustafa Arif ÖZGÜR</i>	1
<i>Onur KOŞAR</i>	1

Chapter 2

A STUDY ON FLUIDS USED IN PVT SYSTEMS

<i>Rahim Aytug Ozer</i>	13
<i>Merve Demirci</i>	13

Chapter 3

AN OVERVIEW OF COMPOSITE COATINGS: TYPES, MECHANICAL PROPERTIES, PRODUCTION METHODS, AND APPLICATION AREAS

<i>Abdulkerim FIRAT</i>	33
<i>Sakine KIRATLI</i>	33

Chapter 4

BIBLIOMETRIC ANALYSIS FOR ROBOTS USING ARTIFICIAL INTELLIGENCE

<i>Tayfun Abut</i>	47
<i>İhsan Tuğal</i>	47

Chapter 5

THE EFFECTS OF USING GRAPHENE NANOFUIDS AND ITS DERIVATIVES ON THERMAL PERFORMANCE IN HEAT EXCHANGER

<i>Fatma OFLAZ</i>	67
--------------------------	----

Chapter 6

**WIND TURBINE DESIGNS AND NUMERICAL ANALYSES AT
VERY LARGE POWERS**

Faruk KÖSE83

Mohamed DWEDAR.....83

Chapter 7

**ENERGY AND EXERGY ANALYSIS OF A 1 MW
MONOCRYSTALLINE PHOTOVOLTAIC SOLAR POWER PLANT
PROPOSED FOR INSTALLATION IN ORDU PROVINCE**

Oguz Ozan YOLCAN103

Ahmet DAYANÇ103

Chapter 8

WIND TUNNEL EXPERIMENTAL APPLICATIONS

Samet Giray TUNCA.....119

Kadir OLCAI.....119

Mustafa Arif ÖZGÜR.....119

Chapter 1

DESIGN AND EXPERIMENTAL STUDIES OF BIO-INSPIRED WING MODEL

Samet Giray TUNCA¹

Mustafa Arif ÖZGÜR²

Onur KOŞAR³

1 Dr., Kütahya Dumlupınar University Dumlupınar Vocational School Department of Electricity and Energy sgiray.tunca@dpu.edu.tr ORCID: 0000-0002-7632-8745

2 Prof.Dr., Kütahya Dumlupınar University, Faculty of Engineering, Department of Mechanical Engineering, arif.ozgur@dpu.edu.tr ORCID: 0000-0001-5877-4293

3 Asst. Prof., Kütahya Dumlupınar University, Faculty of Engineering, Department of Mechanical Engineering, onur.kosar@dpu.edu.tr ORCID: 0000-0001-7335-7076

Bio-Inspiration

Bio-inspiration is a multidisciplinary approach that enables the development of engineering solutions inspired by nature. By examining the aerodynamic performances of wing structures inspired by nature, information about their energy efficiency is used in the emergence of technological designs. In particular, the wing structures of creatures with good flying ability, such as birds, bats and extinct pterosaurs, have been optimized aerodynamically and made adaptable to environmental conditions. Aerodynamic studies contribute to the emergence of more efficient and sustainable developments in modern engineering applications.

Inspired by owl feathers, studies have been conducted on reducing noise at wing tips. The study offers a solution to control the noise generated by turbine blades in aircraft (Hassanalain & Abdelkefi, 2017; Ghimire et al., 2020). In another study, serrated edge designs inspired by owl feathers were explored to improve aerodynamic performance. (Karan & Singh, 2019). In addition, studies on flapping wings have shown that insect wings can increase the lift coefficient at low Reynolds numbers in micro air vehicles (MAVs). These designs seem to have good potential in developing high maneuverability in future vehicles (Gao et al., 2019; Mittal & Iaccarino, 2021). Inspired by the wing morphology of birds, flexible wing technologies were developed. These designs positively affected the stability of flights while also reducing energy consumption. 3D printing technology has accelerated the work done in this area (Zhang et al., 2023). Efforts to increase efficiency in wind turbines have progressed by taking inspiration from the movement mechanisms in the natural structures of birds and fish. With nature-inspired approaches, aerodynamic advantages are identified and higher efficiency is targeted in the produced wings. Innovative designs contribute to the development of environmentally friendly wind turbines and energy efficiency (Chi et al., 2020; Narayan & Pillai, 2018). Optimizing the aerodynamic performance of wing geometries facilitates energy production at low wind speeds. In addition, in bio-inspired wing structures, imitating the aerodynamic skills of the inspired creature in nature increases efficiency. In this way, improvements can be made in newly designed turbines. Such developments are especially important for the future of renewable energy systems. The performance of unmanned aerial vehicles is improved with nature-inspired designs. The ability of birds to dynamically shape their wings during flight reduces aerodynamic drag and increases lift. By imitating these natural mechanisms, UAV wings achieve more flexible flight dynamics and energy efficiency (Li, Wang & Sun, 2022). These designs provide improved adaptability and performance by allowing flight modes to be adjusted according to specific mission requirements.

Turbulence control mechanisms in nature are important natural

strategies that inspire engineering to reduce friction and increase flow efficiency. The smooth skin of whales reduces friction by allowing flow to be directed more efficiently.

Natural turbulence control mechanisms are significant natural strategies that inspire engineering solutions for reducing friction and improving flow efficiency. The smooth skin of whales facilitates more efficient flow direction, thereby reducing friction. Similarly, the soft curvatures in the body structures of fish allow fluids to adhere with less resistance, minimizing energy losses (Song, Ji & Shen, 2021). The application of these turbulence control mechanisms is expected to extend beyond aircraft to other engineering fields requiring energy efficiency. In wind turbines, turbulence-reducing surfaces enhance energy efficiency. The integration of these natural turbulence management strategies into engineering systems contributes to the development of more efficient and environmentally friendly designs.

Bio-inspired designs play a critical role in the development of sustainable and environmentally friendly technologies. Their applications span a broad range of fields, including wind turbines, unmanned aerial vehicles, automotive aerodynamics, and acoustic control systems. It is anticipated that such studies will receive increasing attention in the future and expand into even wider areas of application.

Pterosaurs and Wing Structure

Pterosaurs, known as flying reptiles, are known to be the creatures with the best flight characteristics in history. These creatures, known as the rulers of the skies, emerged approximately 220 million years ago in the Triassic Period and became extinct approximately 66 million years ago following the Cretaceous-Paleogene mass extinction event. Their characteristics have been revealed with fossils obtained in studies conducted by paleontologists, but their origins and flight capabilities are still debated (Ezcurra et al., 2020).

Since the 19th century, studies by paleontologists have developed different theories about the evolutionary periods of pterosaurs and their ability to fly. The focus of these theories is on their wing structures, skeletal systems and muscular systems (Ezcurra et al., 2020).

According to the findings obtained in the studies, Pterosaurs vary in different sizes. It has been revealed that even the largest species had good flight abilities. Fossil evidence has determined that the wingspan was around 11 m. It is considered that an important factor in their flight abilities is the lightness of their bone structures. Due to their lightweight skeletal structure, the weight of such large pterosaurs has been estimated to range between 200 and 250 kilograms (Witton, 2013; Witton & Habib,

2010). Considering that these creatures likely traveled intercontinental distances, it is evident that their wing structures significantly influenced their flight performance. Table 1 presents the physical characteristics of selected pterosaur species.

Table 1. Pterosaur Species and Physical Characteristics

Species	Body Length (l) (m)	Mass (m) (kg)	Wing Area (S) (m ²)	Wingspan (b) (m)	Aspect Ratio (AR = b ² /S)	Wingspan/Body Length Ratio (b/l)	Wing Loading (WL = mg/S) (N/m ²)	Current Power (P) (W)	Cruising Speed (m/s)
Eudimorphodon ranzii	0,075	0,015	0,021	0,412	8,08	5,49	7	0,608	3,8
Pterodactylus antiquus	0,108	0,0386	0,0274	0,538	10,56	5,23	13,6	1,13	5
Rhamphorhynchus muensteri	0,156	0,134	0,072	0,864	10,34	5,52	18,25	2,62	6,4
Dorygnathus banthensis	0,188	0,232	0,104	0,92	8,14	4,89	21,88	3,776	8
Tapejara wellnhoferi	0,229	0,418	0,166	1,35	10,98	5,91	24,7	5,59	8
Nyctosaurus gracilis	0,376	1,86	0,409	2,72	18,08	7,23	44,6	15,12	9,6
Dsungaripterus weii	0,512	4,7	0,747	3,24	14,05	6,33	61,7	28,1	13
Anhanguera piscator	0,7	7,58	2,118	4,69	10,39	6,69	35,1	38,59	11,6
Pteranodon longiceps	0,78	16,6	2,65	6,18	14,42	7,91	61,4	65,1	13
Quetzalcoatlus northropi	1,76	70	9,55	10,39	11,3	8,25	71,88	170	16

(Chatterjee ve Templin, 2004).

In the study conducted by Chatterjee and Templin, the flow of air over the pterosaur wing was illustrated. Cross-sectional views taken from different parts of the wing model are shown in Figure 1.

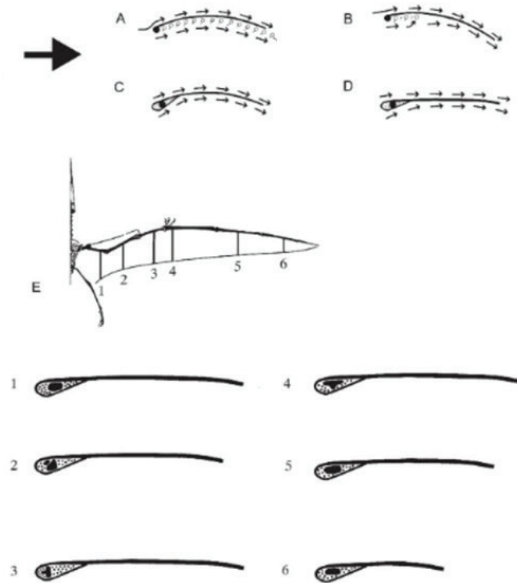


Figure 1: *Pterosaur Wing Structure (Chatterjee and Templin, 2004).*

In the study conducted by Hone and colleagues in the field of paleontology, they created a top view of the pterosaur wing (Figure 2).

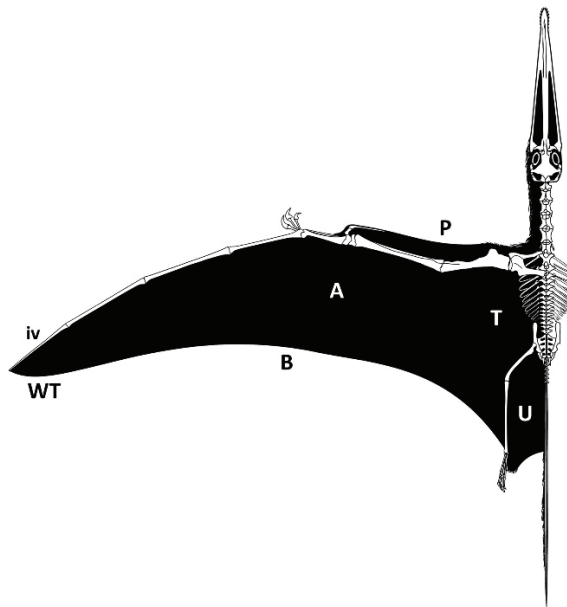


Figure 2. *Top View of the Pterosaur Wing Structure (Hone, Van Rooijen, and Habib, 2015).*

The most important equipment used in the manufacturing of the wing profile prototype is the Creality K1 3D printer. This printer, equipped with FDM (Fused Deposition Modeling) technology, is 12 times faster than a conventional FDM 3D printer, capable of reaching printing speeds of up to 600 mm/s. It operates by melting a thermoplastic filament and extruding it layer by layer onto a base to form an object (Table 2).

Table 2. Technical Specifications of the 3D Printer

Specification	Details
Printing Technology	FDM (Fused Deposition Modeling)
Print Bed	PC-coated spring steel magnetic bed
Print Area	220 x 220 x 250 mm
Nozzle Diameter	0.4 mm
Maximum Print Speed	600 mm/s
Print Accuracy	±0.1 mm
Layer Thickness	0.05-0.35 mm
Hotend Type	Brass Nozzle
Extruder	Bowden
Max Nozzle Temperature	300°C
Max Bed Temperature	100°C
Input Voltage	AC 115-230V
Output	DC 24V 350W
Printer Dimensions	355 x 355 x 480 mm

The wing profile models to be used in the study were obtained by printing the drawings with the Creality K1 3D printer after they were created. The simulation of wing printing using a 3D printer is shown in Figure 4.

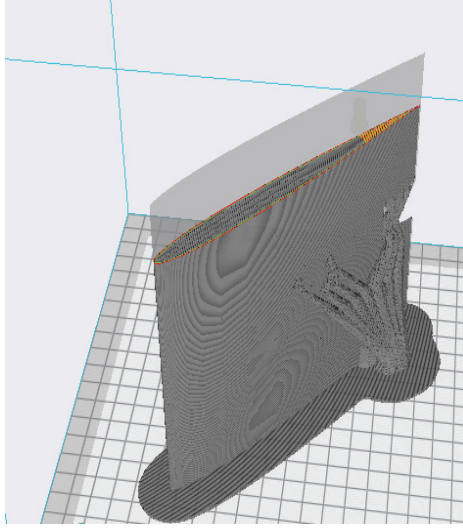


Figure 4. Wing printing simulation for 3D printers

Pterosaur Wing Prototype Parameters

There are studies related to pterosaurs in the fields of paleontology and biology. Based on these studies, which focus on their physical structures, the wing model from which the wing cross-sections to be used in our experiments will be obtained is shown in Figure 3.

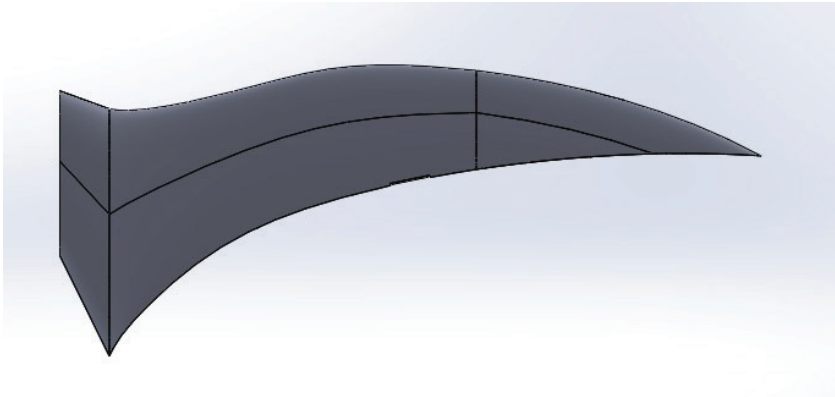
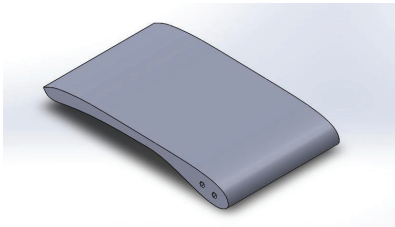
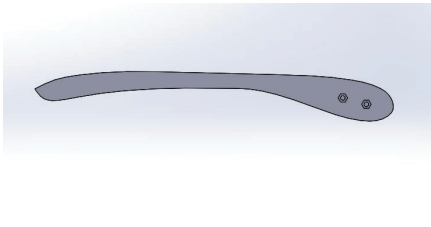
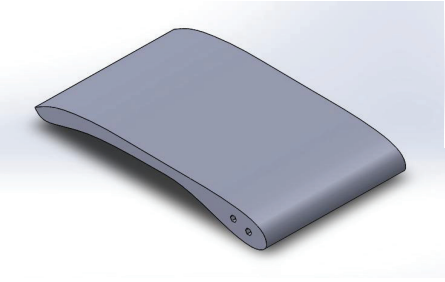
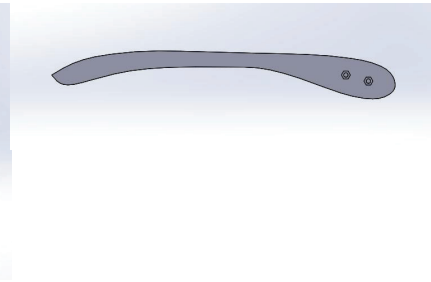
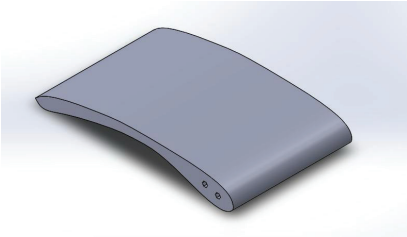
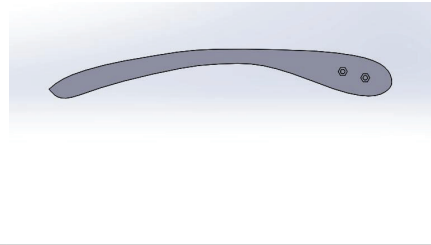


Figure 4. Pterosaur Wing Model Created in SolidWorks

In Figure 3, cross-sections were taken from three different sections of the pterosaur wing, from the body to the wingtip, to create the wing sections to be used in the experiments. The wing sections are coded as PT01, PT02, and PT03, as shown in Table 3. As seen in the drawings, the angle of the wing increases progressively from PT01 to PT03. The effect of this angle is discussed in the analysis of the experiments.

Table 3. Pterosaur Wing Sections Used in the Experimental Study

	
PT01 Pterosaur Wing Profile	
	
PT02 Pterosaur Wing Profile	
	
PT03 Pterosaur Wing Profile	

When examining the information related to pterosaurs, it was found that the length of the leading edge (forewing) decreases towards the wingtip. However, the size of the bone structure on the front side (the enlarged lump structure on the humeral side) changed less compared to the length of the leading edge. It was observed that the slope of the upper surface of the wing increased towards the wingtip. Since the comparisons between the wing profiles will be conducted at the same Reynolds numbers, the leading edge lengths have been equalized. In this case, it is observed that the slope on the upper surface of the wing model obtained from the point closer to the wingtip is more pronounced compared to the others.

Aerodynamic Force Experiments

Subsonic wind tunnel aerodynamic force experiments were conducted using the PT01, PT02, and PT03 wing profiles. The wing profiles were attached to the force measurement system using connecting elements. Experiments were then performed at a Reynolds number of 50,000, starting

from 0 and increasing by increments of 20. The obtained data are related to the lift (CL) and drag (CD) coefficients (Tunca et al., 2024).

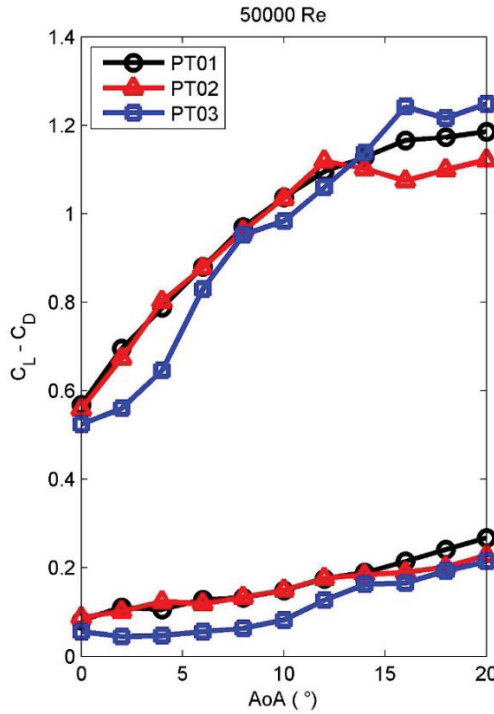


Figure 5. Aerodynamic Force Coefficients of the Wing Models

In the graph shown in Figure 4, the lift coefficients generally increase linearly up to the critical angles of attack. The lift coefficient slopes for the PT02 and PT01 wing profiles are steeper compared to PT03. The maximum lift coefficients for PT01 exceed 1.2 at an angle of attack of 16°, for PT02 the maximum lift coefficient is 1.1 at 11°, and for PT03 it ranges between 1.1 and 1.2 at 16°. At the angles of attack where the maximum lift coefficients are observed, the wing profiles experience a loss of lift. Due to the turbulence intensity, the expected continuous decrease in CL values after stall is not observed. The drag coefficient values increase with a low slope, ranging approximately from 0.2 to 0.3. Similar to the lift coefficient, the PT03 wing profile also shows a gradual increase in drag coefficient with a low slope. It is observed that the drag coefficient values exhibit a nearly horizontal slope at the angles where stall occurs.

Conclusion

Wing structures inspired by nature play an important role in improving energy efficiency, aerodynamic performance and maneuverability in different weather conditions. These studies provide improvements in performance criteria such as detection of laminar separation bubbles and improvement of aerodynamic forces according to flight conditions. In addition, these studies provide advantages for creating stable performance in flights at low Re numbers.

Thanks to the studies carried out in this field, faster improvements are achieved in technological developments. With methods such as aerodynamic force tests in the wind tunnel, smoke imaging experiments and oil experiments, the aerodynamic properties of wing structures inspired by nature are determined. In this way, developments are made in engineering solutions. Thanks to innovative approaches, designs that increase energy efficiency and aerodynamic performance are made.

In conclusion, bioinspiration is a way to learn from nature within the developing technology. These designs contribute to technological developments in engineering studies. In this context, the biologically inspired approach is an indisputable method for developing sustainable and high-performance engineering solutions.

Note: It was produced from Samet Giray Tunca's PhD thesis.

Reference

- Chatterjee, S., & Templin, R. J. (2004). Posture, locomotion, and paleoecology of pterosaurs. *Geological Society of America Special Papers*, 376, 1–64. <https://doi.org/10.1130/0-8137-2376-4.1>
- Chi, Q., Pan, G., Zhang, C., & Zhang, Z. (2020). Bio-inspired aerodynamic design of wind turbine blades based on bird and fish structures. *Renewable Energy*, 153, 780–792. <https://doi.org/10.1016/j.renene.2020.02.045>
- Ezcurra, M., Nesbitt, S., Bronzati, M., Vecchiha, F., Agnolin, F., Benson, R., . . . Max, L. Enigmatic dinosaur precursors bridge the gap to the origin of Pterosauria. *Nature*.2020;588; 445-449.
- Gao, H., Wu, J., & Wen, Z. (2019). Bio-inspired micro air vehicle designs based on insect flight mechanics. *Journal of Bionic Engineering*, 16(5), 865–879. <https://doi.org/10.1016/j.jbe.2019.04.005>
- Ghimire, R., Subramanian, S., & Mohan, R. (2020). Aerodynamic noise reduction inspired by owl feathers. *Journal of Sound and Vibration*, 481, 115442. <https://doi.org/10.1016/j.jsv.2020.115442>
- Hassanalian, M., & Abdelkefi, A. (2017). A review on bio-inspired flight systems. *Progress in Aerospace Sciences*, 91, 99–131. <https://doi.org/10.1016/j.paerosci.2017.04.003>
- Hone, D. W. E., Van Rooijen, J., & Habib, M. B. (2015). Wing shape and aerial performance in pterosaurs. *PeerJ*, 3, e1491. <https://doi.org/10.7717/peerj.1491>
- Karan, S., & Singh, S. P. (2019). Analysis of bio-inspired serrated trailing edge designs for aerodynamic performance improvement. *Journal of Fluids Engineering*, 141(7), 071101. <https://doi.org/10.1115/1.4043473>
- Li, W., Wang, Y., & Sun, L. (2022). Adaptive morphing technologies in nature-inspired UAV designs. *Aerospace Science and Technology*, 125, 107624. <https://doi.org/10.1016/j.ast.2022.107624>
- Mittal, R., & Iaccarino, G. (2021). Bio-inspired aerodynamics: From insects to vehicles. *Annual Review of Fluid Mechanics*, 53(1), 331–365. <https://doi.org/10.1146/annurev-fluid-010720-105600>
- Narayan, R., & Pillai, R. K. (2018). Bio-inspired fluid-structure interaction for energy harvesting. *Applied Energy*, 224, 277–289. <https://doi.org/10.1016/j.apenergy.2018.04.086>
- Song, Z., Ji, X., & Shen, Y. (2021). A review of bio-inspired turbulence control for drag reduction. *Physics of Fluids*, 33(11), 115102. <https://doi.org/10.1063/5.0069372>

Tunca S.G. Investigation of Aerodynamic Characteristics of Bio-Inspired Airfoil in Subsonic Wind Tunnel. Kütahya Dumlupınar University Graduate Education Institute Doctoral Thesis. Kütahya.2024.

Tunca, S., Özgür, M., Koşar, O. (2024) Flow Imaging Analysis on Bio-Inspired Airfoil Surface. Ankara International Congress On Scientific Research-X.. ISBN:978-625-8254-55-6.

Witton, M. P. (2013). Pterosaurs: Natural History, Evolution, Anatomy. Princeton University Press.

Witton, M., Habib, M. On the Size and Flight Diversity of Giant Pterosaurs, the Use of Birds as Pterosaur Analogues and Comments on Pterosaur Flightlessness. PLoS One. 2010;5;11. <https://doi.org/10.1371/journal.pone.0013982>

Zhang, T., Yang, L., & Wu, Y. (2023). 3D printed morphing wings for UAV applications: Bio-inspired designs. *Additive Manufacturing*, 51, 102539. <https://doi.org/10.1016/j.addma.2023.102539>

Chapter 2



A STUDY ON FLUIDS USED IN PVT SYSTEMS

Rahim Aytug Ozer¹

Merve Demirci²

1 Assist. Prof. Dr. Rahim Aytug Ozer, Kafkas University, <https://orcid.org/0000-0002-3162-5551>, aytug.ozerkafkas.edu.tr

2 Assist. Prof. Dr. Merve Demirci, Kafkas University, <https://orcid.org/0000-0001-8192-7366>, merve.demircikafkas.edu.tr

1. Introduction

Energy consumption on a global scale and, in parallel, energy demand are accelerating with increasing momentum every day. In response to this unavoidable rise, governments are not only seeking new energy sources but also striving to utilize existing resources more effectively and efficiently. The finite nature of fossil fuel reserves, in particular, has brought about global energy crises and associated tensions. Renewable energy sources, being both inexhaustible and environmentally friendly, stand out as a strong alternative to fossil-based energy systems.

Solar energy is one of the prominent alternative energy sources. Direct current (DC) can be generated as a result of the absorption of solar radiation by the cells in photovoltaic (PV) panels, leading to the movement of electrons that complete the circuit. Traditional photovoltaic panels produce only electricity, but they cannot operate at maximum efficiency, making it impossible to convert all incoming solar radiation into electrical energy. Consequently, the portion of solar radiation that is not converted into electricity causes the panel surface to heat up. This phenomenon reduces the efficiency of PV panels, which is an undesirable outcome for energy systems. To address this issue and remove the accumulated waste heat from the panel surface, photovoltaic-thermal (PVT) systems have been developed. Photovoltaic-thermal (PVT) systems are hybrid energy technologies that enable the simultaneous production of both electricity and thermal energy. By utilizing this waste heat, PVT systems enhance energy efficiency and provide an integrated solution.

In these hybrid systems, the fluids used to collect and transfer heat play a critical role in the performance of PVT systems. Fluids are utilized to effectively remove, store, or transport thermal energy to other locations. Therefore, the selection of fluid type has a direct impact on system efficiency, durability, and economic sustainability.

This section will address the various types of fluids used in PVT systems, the criteria for their selection, and their impacts on PVT designs.

2. Definition of PVT Systems and the Role of Fluids

Photovoltaic-thermal (PVT) systems enable the simultaneous utilization of two energy forms by integrating the electricity generated from photovoltaic panels with thermal systems. These systems facilitate the transfer and utilization of excess heat accumulated on the surface of photovoltaic panels through heat transfer fluids. PVT systems are generally classified based on the type of fluid, system configurations, heat transfer mechanisms, and the method of solar concentration (see Fig. 1). This classification can also be extended to include residential, industrial, and

portable applications depending on the heating and energy requirements at the point of use.

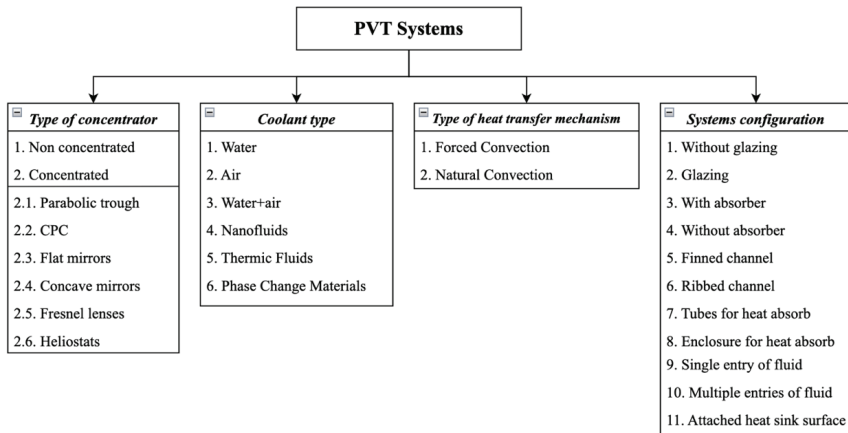


Figure 1. Classification of PVT Systems [1].

A basic PVT system is illustrated in Figure 2. This section will focus on the cooling fluids preferred for removing the waste heat accumulated on the PV panel surface and utilizing it effectively. The primary functions of the fluids used in PVT systems are outlined and explained below in bullet points.

- Increasing PV panel efficiency;** Photovoltaic panels lose their efficiency as temperature increases. The fluids used in PVT systems reduce the temperature on the surface of the PV panels, leading to more efficient electricity generation. Studies presented in the literature on PVT system performance support this effect. For example, in a study conducted by Stropnik and Stritih [2], it was concluded that the electricity generated from PV panels could be increased by 7.3% using Phase Change Materials (PCMs). On the other hand, a study by Popovici et al. [3] highlighted a power production increase of up to 7.55% in air-cooled PV systems. In a study conducted by Alzaabi et al. [4], the electrical efficiency of PV systems in a water-based system showed an increase of 15%-20%. Similarly, Khanjari et al. [5] concluded that the use of nanofluids as a cooling fluid resulted in a 13.2% increase in electricity production efficiency. As observed in the literature, air- and liquid-based PVT systems can achieve an increase in electrical efficiency ranging from 5% to 20%.

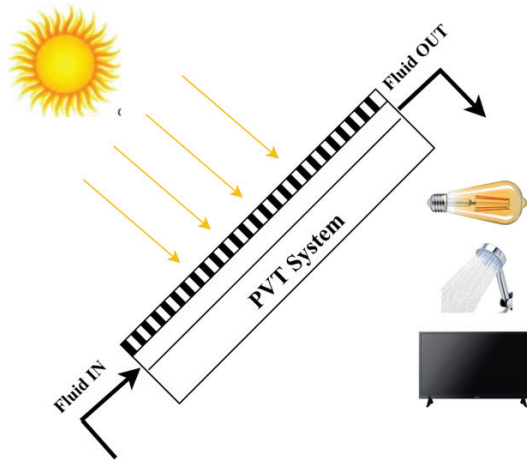


Figure 2. Typical PVT System Diagram.

- **Storage and use of thermal energy;** In PVT systems, fluids collect the waste heat generated during electricity production and make this energy available for other purposes. The collected heat can be used for hot water production, space heating, or process heat. This increases the overall system efficiency by saving energy. All materials in nature have a carbon footprint, particularly in terms of pollution during the production phase [6]. Recycling processes and applications are the most effective approaches to mitigate this impact. In PVT systems, the utilization of waste energy not only enhances the energy conversion efficiency of the system but also reduces the overall carbon footprint [7].

- **Temperature control and thermal stability;** Uniform temperature distribution prevents the system from overheating and ensures the long lifespan of both electrical and thermal components. In PVT systems, fluids maintain the thermal stability of the panels and system components [8]. Reducing temperature fluctuations minimizes physical deformations and performance losses that may occur in the system.

- **Efficiency-Economy balance;** The thermophysical properties of the fluid used in PVT systems, such as heat retention capacity, thermal conductivity, and viscosity, directly affect system costs and energy efficiency. For example, air-based PVT systems have simple and low-cost installations, but their thermal energy capacities are quite limited [9]. In water-based PVT systems, higher thermal performance can be achieved, but issues such as corrosion and freezing during winter months may occur [10]. In applications where further improvement of heat transfer performance is desired, nanofluids, although costly, can be used to provide long-term economic benefits [11].

- **Energy storage and seasonal performance;** The energy storage capacity of a PVT system can be increased depending on the heat retention capacity of the fluid used. For example, PCM fluids can store heat during phase change and release this energy when needed [12]. In terms of seasonal use, glycol-water mixtures are commonly employed fluids [13].

- **Impact on system design;** The physical and chemical properties of the fluid are crucial factors influencing system design, including pump power, corrosion, and material compatibility. The viscosity of the fluid is a key parameter in determining the amount of energy required to drive the fluid. The use of fluids with lower viscosity reduces pump power requirements and, consequently, energy consumption. On the other hand, the chemical properties of the fluid affect the materials used for pipes and tanks in the system. Incorrect fluid selection can lead to corrosion and system damage over the long term.

- **Environmental impact and sustainability;** The type of fluid used in the system plays a role in determining the environmental impact of the PVT system. For instance, systems using natural fluids such as water can be considered environmentally friendly due to their low carbon footprint. On the other hand, next-generation fluids developed through nanotechnology can contribute to sustainability by providing higher performance with lower energy consumption.

- **Efficiency increase in high-performance systems;** Fluids with advanced technologies can enhance energy conversion rates by increasing thermal conductivity [14]. For example, fluids containing copper or aluminum oxide nanoparticles provide much higher heat transfer efficiency compared to traditional liquids. Similarly, supercritical fluids can improve heat transfer performance in systems operating under high temperature and pressure conditions [15].

3. Types of Fluids Used in PVT Systems

Photovoltaic-thermal (PVT) systems are an innovative renewable energy technology that enhances energy efficiency by integrating both electricity and thermal energy production on the same platform. In these systems, solar energy is converted into electricity through photovoltaic cells, while the waste heat generated in the same process is collected and utilized. The success and performance of PVT systems depend not only on the system design but also on the selection and properties of the fluids used. Fluids, responsible for the thermal management of the system, optimize heat transfer, energy storage, and the overall energy conversion efficiency of the system. The types of fluids preferred in PVT systems vary according to the system's intended use and operating conditions. While traditional

fluids include air and water, advanced applications often employ antifreeze mixtures, nanofluids, phase change materials (PCMs), and supercritical fluids.

These fluids are evaluated not only based on their heat transfer capacities but also on their chemical stability, environmental sustainability, and cost-effectiveness. For example, innovative fluids such as nanofluids and phase change materials (PCMs) offer significant advantages over traditional fluids by providing high thermal conductivity and energy storage capacity. Moreover, supercritical fluids have become an ideal choice for industrial-scale PVT applications, as they enhance energy conversion under high-pressure and high-temperature conditions.

The correct selection of fluids not only enhances heat transfer efficiency but also directly impacts the longevity, reliability, and environmental effects of the system. Therefore, a detailed analysis of the thermophysical properties of fluids is critical for both theoretical studies and practical designs. A comprehensive examination of the role of fluids in PVT systems is considered a key step in optimizing energy conversion processes and supporting renewable energy goals.

3.1. Air-Based PVT Systems

Air-based PVT systems are hybrid energy systems that stand out for their simple design and low-cost structure, utilizing air as the heat transfer fluid. In these systems, the waste heat generated during electricity production from photovoltaic cells is collected and transported through an air channel beneath the system. Despite air's low density and thermal capacity, efficient heat transfer can be achieved using natural convection or forced air flow methods. In these systems, air can be directed through channels in a single-pass or multi-pass configuration, and by increasing the time spent within the channel, system performance can be enhanced. One of the main advantages of air-based systems is the elimination of risks such as freezing, boiling, or leakage, which are commonly seen in liquid-based systems. Additionally, these systems offer an ideal solution for small-scale applications due to their simple maintenance requirements and long service life. However, due to air's low thermal conductivity, optimized designs and advanced materials must be employed to enhance thermal efficiency. Literature studies suggest that air-based PVT system efficiency can be increased up to a certain level. Therefore, air-based PVT systems are considered a suitable option, particularly for low-temperature applications such as energy production and building heating in temperate climates. For example, in a study conducted by Choi [16], a 5.89% increase in electrical efficiency was achieved in the application of air-based PVT systems, while Boulhidja et al. [17] reported a 9.88% increase.

3.2. Liquid-Based Fluids

These are PVT systems where cooling is achieved using liquids. In these systems, fluids such as water, antifreeze mixtures, or nanofluids are typically used to remove the waste heat generated from photovoltaic cells. The high specific heat capacity and thermal conductivity of liquids enable them to provide higher energy collection efficiency compared to air-based systems. However, liquid-based systems require more careful design and maintenance to prevent issues such as freezing, boiling, and leakage. The advantages and disadvantages of various types of liquids are assessed based on the system's intended use, environmental conditions, and cost criteria. Liquid-based PVT systems have a wide range of applications, especially in areas such as hot water production, heating, and industrial energy, making them an important component of renewable energy technologies. When evaluating liquid-based fluids, both advantages and disadvantages should be considered;

- **Water;** It stands out as a low-cost, easily accessible, and environmentally friendly fluid. Additionally, water's high thermal storage capacity is one of the primary reasons for increasing the thermal efficiency of PVT systems and effectively utilizing waste heat [18]. However, water's critical temperature limits, such as freezing and boiling points, present an important constraint that must be considered in system design. In cold climates, antifreeze additives are required to prevent freezing, which may slightly affect water's specific heat capacity and environmental properties [7]. Moreover, the risk of corrosion and leakage in pipes of water-based systems negatively impacts long-term performance. However, these disadvantages can be minimized through appropriate material selection and design optimizations. Furthermore, the sustainability of water as a fluid increases its desirability [19].

- **Glycol-Water Mixtures:** Glycol-water mixtures are effective heat transfer fluids used in PVT systems to minimize the risks of freezing and boiling. By adding glycol to water, the freezing point of the mixture is significantly reduced, allowing the system to operate safely even at low temperatures. Propylene glycol and ethylene glycol are particularly common components used in these mixtures. While ethylene glycol is a more effective option due to its high thermal conductivity, it must be used with caution due to its toxic properties. Propylene glycol, on the other hand, offers advantages due to its lower toxicity and greater environmental friendliness, but it is somewhat limited in terms of thermal conductivity and viscosity compared to ethylene glycol. Glycol-water mixtures may slightly increase energy consumption due to their high viscosity; therefore, pump power requirements and system design should be optimized with these factors in mind [20]. These mixtures enhance the

reliability of PVT systems, particularly in cold climates with a high risk of freezing, ensuring long-term performance.

- **Thermal oils:** Thermal oils are specialized fluids that provide stable performance over a wide temperature range in heat transfer and storage applications. Due to their high thermal stability and boiling points, they are preferred in applications that require higher temperatures compared to water or glycol-based fluids. Thermal oils, particularly used in concentrating PVT systems and industrial-scale projects, offer advantages such as low evaporation rates and chemical stability [21]. However, these fluids are relatively expensive, and the heavy metals and chlorine compounds found in oils disposed of as waste can be released into the atmosphere, causing environmental issues. This is an important consideration in the fluid selection process [22].

3.3. Innovative fluids

As previously emphasized in earlier sections, PVT systems are hybrid systems that offer the possibility of utilizing the waste heat from PV panels for various purposes. Although researchers have implemented numerous design applications to enhance both thermal and electrical efficiency, the low thermal conductivity of cooling fluids remains one of the key factors limiting the heat transfer capability and, consequently, the combined efficiency of PVT systems. Improving the thermal properties of energy transfer fluids could provide an additional gain in heat transfer. In recent years, innovative fluids used in PVT systems have been developed in various forms to provide higher performance and efficiency.

3.3.1. Nanofluids

Conventional heat transfer fluids have low thermal conductivity, which negatively affects efforts to improve thermal performance. However, it is a fact that suspending solid-phase metals in the fluid results in a mixture with improved thermal conductivity. Many studies in the literature support this observation. In a study conducted by Sathish et al. [23], they observed a 70.4% increase in thermal conductivity of the next-generation fluid they developed, which consisted of water-based Al_2O_3 , Cu, multi-walled carbon nanotubes (MWCNT), and SiO_2 nanofluids. Mixing nanoparticles of metal particles into conventional fluids increases both the turbulence effects and the intermolecular heat transfer surface area due to the suspended particles in the fluid. This leads to an increase in thermal conductivity [24]. Furthermore, the nanoparticles on the nanoscale generate microconvection within the liquid, further enhancing the heat transfer capability [24].

Nanofluids are innovative heat transfer fluids obtained by

homogeneously dispersing nanoparticles into a base fluid (such as water, oil, or glycol). The nanoparticles used are typically metal, metal oxide, carbon-based materials, or composite nanomaterials. These nanoparticles enhance the thermal conductivity, viscosity, and other physical properties of the base fluid. The chemical formulas of nanofluids vary depending on the composition of the nanoparticles and the base fluid. The nanoparticles commonly used are listed below.

- **Metal-Based Nanoparticles;** They are highly suitable particles for nanofluid production due to their high thermal and electrical conductivity. Copper (Cu), Silver (Ag), and Gold (Au) metal particles are commonly used. The main disadvantage is their high cost.

- **Metal Oxide Nanoparticles;** These particles are more cost-effective compared to metal-based nanoparticles. Aluminum oxide (Al_2O_3), titanium dioxide (TiO_2), and silicon dioxide (SiO_2) fall within this category. Due to their chemical stability, they are compatible with base fluids and can form a homogeneous structure within the fluid. Additionally, they are preferred for their environmentally friendly properties. Nanofluids containing Al_2O_3 nanoparticles are widely used in solar energy systems to enhance thermal energy transport [23–25].

- **Carbon-Based Nanoparticles;** Graphene (C) and carbon nanotube (CNT) particles can be manufactured at the nanoscale and suspended into the base fluid. The primary advantages of these particles are their very high thermal conductivity and their high mechanical strength despite the light weight of the particles. PVT systems using nanofluids containing multi-wall carbon nanotubes (MWCNT), graphene, and CNT can achieve improvements in both electrical and thermal performance [23].

- **Magnetic Nanoparticles:** Magnetic nanoparticles are particles manufactured from materials, typically based on iron oxide (Fe_3O_4 or $\gamma\text{-Fe}_2\text{O}_3$), that exhibit magnetic properties at the nanoscale. These particles, in addition to their high surface area, are widely used in various fields such as energy storage systems, medical applications, and heat transfer applications due to their magnetic alignment capabilities and chemical stability [26–28]. The use of magnetic nanoparticle-based nanofluids in PVT systems is quite common. The ability of these particles to align in a magnetic field significantly increases the thermal conductivity and, consequently, the heat transfer coefficient of the fluid. Furthermore, their high stability and controlled reactivity make them an ideal choice for long-term energy applications. On the other hand, the use of magnetic nanoparticles also involves challenges such as production costs, potential agglomeration, and environmental impacts. With advancements in

nanotechnology and materials science, these particles have the potential to offer a broader range of applications in the future.

It is incorrect to simply consider nanofluids as a solid-liquid suspension. The efficiency of these fluids depends on the stable distribution of the particles within the base fluid, the negligible level of particle agglomeration, and chemical stability. Therefore, the nanofluid preparation process is crucial and involves a series of steps that must be carefully considered. Two methods are applied in the preparation of nanofluids, depending on the particle production method. These are the single-step and two-step methods. In the single-step method, nanoparticles are produced within the base fluid. However, in this method, evaporation is required to separate the nanoparticles from the liquid. This method was developed by Akoh et al. [29] and introduced to the literature. In the two-step method, pre-prepared nanoparticles are suspended into the base fluid through various techniques to complete the fluid production. Compared to the single-step method, this method is more suitable for metal oxide particles than for metal-based nanoparticles [30]. In the two-step method, techniques such as altering the suspension's pH, using surfactants, and applying ultrasonic vibrations are employed to suspend the nanoparticles into the base fluid. These processes prevent the agglomeration of nanoparticles and maintain the homogeneous structure of the fluid.

3.3.2. Phase Change Materials (PCM)

Phase Change Materials (PCMs) are materials that can store large amounts of energy when transitioning from solid to liquid or from liquid to solid at specific temperatures. Due to these properties, they are innovative materials that contribute to energy efficiency. PCMs are widely used in applications that require heat management, as they can store or release significant amounts of energy during the melting and freezing processes. In PVT systems, PCMs are commonly used to prevent the overheating of photovoltaic modules, store thermal energy more efficiently, and enhance system performance. PCMs are classified into organic, inorganic, and composite types. Organic PCMs (e.g., paraffin and fatty acids) are notable for their chemical stability and non-toxicity, while inorganic PCMs (e.g., salt hydrates, metallic compounds) offer higher heat storage capacity. On the other hand, composite PCMs (e.g., organic-inorganic mixtures, carbon-based composites) are distinguished by their thermal stability and physical stability (resistance to separation), although their production processes are more complex. However, the low thermal conductivity of PCMs can limit heat transfer rates, posing a design challenge; therefore, these properties are improved using metallic additives or nanotechnology-based solutions. In this regard, PCMs stand out as a strategic component that enhances energy conversion efficiency in PVT systems and contributes to sustainable energy solutions [31].

PCMs enable the storage of waste heat generated during electricity production in PVT systems. The energy collected throughout the day becomes available for use during the night or on cloudy days. Additionally, the temperature stability that occurs during phase change helps maintain the temperature of the PV panels, thereby reducing electrical efficiency losses [31]. PCMs are typically integrated into the system, such as behind the panels or in fluid storage tanks.

3.3.3. Supercritical Fluids

It is a phase state where the fluid exhibits both gas and liquid phase properties simultaneously by surpassing the critical temperature and pressure values. The critical point is defined as the combination of temperature and pressure at which the liquid and gas phases of a substance become indistinguishable. Supercritical fluids provide exceptional performance in heat transfer by combining the low viscosity and high diffusion capacity of gases with the density and high heat capacity of liquids. These properties allow for efficient energy conversion under high temperature and pressure conditions, especially in concentrating designs in PVT systems. Supercritical fluids such as carbon dioxide (CO₂) are widely preferred in this field due to their environmentally friendly nature, low cost, and broad operating range [32].

Supercritical fluids are not only used in PVT systems but also have a wide range of applications across many different industries. Supercritical CO₂ plays a significant role in applications such as power generation in energy plants, solvent use in the chemical industry, and decaffeination in the food sector. Additionally, it is used in processes like supercritical water oxidation (SCWO) for waste disposal and clean energy production. Although supercritical fluids require compact heat exchangers and advanced engineering systems capable of withstanding high temperatures and pressures, their capacity to increase energy density and thermal efficiency makes them a strong option for innovative energy technologies and PVT systems.

4. Fluid Selection Criteria

One of the critical components that directly affects both the thermal and electrical efficiency and long-term reliability of PVT systems is the fluid used. Therefore, the selection of the fluid to be used as absorber, storage and transfer medium in the system is a critical process. Various criteria such as thermophysical properties, environmental factors, cost and application conditions should be taken into consideration for the selection of the appropriate fluid. This selection process can be detailed in line with the following basic criteria.

4.1. Thermophysical properties

Thermophysical properties of the fluid are one of the most important factors determining the heat transfer capacity in PVT systems [22, 26- 27]. Thermal conductivity coefficient, specific heat capacity (c_p), viscosity (μ), heat of vaporization and melting point are among the thermophysical properties. Thermal conductivity coefficient (k) is a parameter that shows the heat transfer ability of the fluid. Therefore, fluids with high thermal conductivity are preferred to increase thermal performance. On the other hand, viscosity (μ) is defined as the resistance of the fluid to flow. Therefore, it is appropriate to use low viscosity fluids to reduce pump power and minimize friction energy losses. In addition, in cases where the amount of energy that the fluid can carry per unit temperature change is desired to be high, the fluid is desired to have a high specific heat capacity.

4.2. Operating temperature

The system operating temperature range is one of the factors to be considered in the selection of the fluid to be used. Fluids with low freezing points (e.g. glycol-water mixtures) should be preferred against the risk of freezing at low temperatures, while in high temperature applications it may be appropriate to use oil-based or supercritical fluids with high thermal stability.

4.3. Chemical stability and compatibility

The chemical properties of the fluid are a factor that affects the life and durability of the elements in the system. Therefore, the fluid must be compatible with the seal, pipe and other components. Although homogeneous temperature distribution is desired in PVT systems, fluids with high resistance to deterioration should be preferred against the possibility of sudden temperature jumps. In addition, the fluid should not cause corrosion damage in case of contact with metal surfaces. Therefore, mixtures containing inhibitors or corrosion-resistant materials should be preferred.

4.4. Environmental effects

The selection of fluids used in PVT systems is critical in terms of energy efficiency and system performance, as well as environmental impacts. The environmental impacts of fluids are often assessed in terms of their greenhouse gas emission potential, ozone layer damage risk, toxicity levels, and waste management requirements. For example, chlorofluorocarbon (CFC) and hydrochlorofluorocarbon (HCFC) based fluids were widely used in the past but have largely been abandoned due to their high global warming potential (GWP) and ozone layer damage. Today, environmentally friendly options include natural fluids, CO_2 , hydrocarbons (e.g. propane and isobutane) and synthetic fluids with low GWP values. However, some environmentally friendly alternatives,

such as hydrocarbons, require additional safety measures due to their flammability. In order to ensure environmental sustainability in fluid selection, priority should be given not only to low emission values, but also to options that consume less energy in the energy conversion process and offer a longer lifespan. In this context, the use of environmentally friendly fluids contributes to the sustainability goals of renewable energy systems by reducing the total carbon footprint of PVT systems [7].

4.5. Economic effects

The selection of fluids used in PVT systems has a direct impact on the total cost of the system and its long-term economic sustainability. Fluid costs should be evaluated across a wide spectrum, from initial costs such as purchasing, transportation, and storage to maintenance and replacement requirements during the system's operation. For example, common, low-cost fluids such as water and glycol-water mixtures reduce initial investments, while special fluids such as thermal oils or supercritical fluids require higher initial costs but may provide long-term economic advantages by offering higher efficiency. Additionally, when selecting fluids, choosing solutions that increase energy efficiency can shorten the amortization period. However, some environmentally friendly fluids may have higher initial costs but can benefit from renewable energy incentives and provide economic advantages by reducing carbon emission costs in the long term. Therefore, fluid selection in PVT systems should be based not only on technical and environmental factors, but also on cost-effectiveness and economic sustainability goals.

As explained up to this section, it is seen that the fluids commonly used in PVT systems have superior properties compared to each other. The comparative evaluation is given in Table 1. Therefore, when selecting the fluid to be used in the PVT system, all evaluation criteria should be taken into consideration together and the fluid that best suits the system requirements should be preferred.

Table 1. Comparative evaluation of fluids used in PVT systems.

Fluid Type	Productivity	Cost	Application Area	Specific Requirements
Air	Low	Low	Heating (Low temperature)	Fan and large volume are required.
Water	Medium-high	Low	Hot water, space heating	Frost protection
Glycol-Water mixture	High	Medium	Cold climate	Corrosion prevention
Nanofluids	Very high	High	Industrial applications	Cost of nanotechnology
PCM	Medium high	Medium	Energy storage	Special design

5. Recent Studies

As emphasized in previous sections, PVT systems are hybrid systems that use solar energy to obtain electrical and thermal energy. The limited availability of fossil fuels and the resulting global crises have increased the interest in alternative energy sources. Therefore, it is inevitable to improve PVT system efficiency as much as possible in order to obtain maximum efficiency from solar energy. One way to increase efficiency is to improve heat transfer fluids. Researchers have conducted a series of studies trying to increase system efficiency by using traditional fluids and new generation fluids. Some recent studies in the literature using different fluids and the results obtained from these studies are presented in Table 2.

6. Conclusions

Photovoltaic-thermal (PVT) systems are innovative hybrid technologies that enable the production of both electrical and thermal energy from solar energy. The effectiveness of these systems depends not only on their design, but also on the thermophysical properties and selection of the fluids used. The role of different fluid types in PVT systems is examined in detail in the study; the advantages and disadvantages of air, liquid, nanofluids, phase change materials (PCM) and supercritical fluids are discussed. It is emphasized how the fluid selection directly affects system performance, economic sustainability and environmental impacts.

As a result, the selection of fluids in PVT systems should be made carefully depending on criteria such as the intended use of the system, operating conditions and cost-effectiveness. While traditional fluids offer low-cost and accessible solutions, innovative options such as nanofluids and supercritical fluids provide significant increases in energy efficiency. Considering the need for environmentally friendly and sustainable energy solutions, it is of great importance to develop innovative approaches to reduce the carbon footprint of fluids used in PVT systems. In this context, the integration of advanced material science and engineering technologies will play a key role in optimizing the performance of PVT systems in the future and reaching wider application areas.

Table 2. Recent studies on fluids used in PVT systems and their effects on performance.

Ref.	Fluid	System parameters	Remarks
[33]	CaCl ₂ ·6H ₂ O (PCM)	PCM, TE and aluminum fins were used to cool the PV panel.	The highest power output was obtained in the finned case (47.88 W) while the lowest power output was obtained in the hybrid system (44.26 W). The maximum energy efficiency was obtained in the finned case (9.23%).
[34]	Air, water, paraffin	A new PVT system was created by combining the air channel and water pipe and performance analysis was performed.	PVT-PCM systems have improved energy efficiency. It was emphasized that the combined efficiency of the PVT-PCM system was 39.4% and the energy saving efficiency was 64.2%.
[35]	(Al ₂ O ₃ , TiO ₂ , ZnO)/water	Performance evaluation and economic effects of different types of nanofluids were evaluated.	The best performance was obtained with ZnO-water nanofluid. This fluid, the annual average electrical efficiency was determined as 14.65% and the thermal efficiency was determined as 47.63%. The payback period was determined as 5.12 years.
[36]	CuO-Water	Performance comparison was made using water and copper oxide nanofluid in the PVT system with serpentine coil and thermal absorber.	Water based PVT system performance compared to uncooled PV system electrical efficiency increased by 12.32%, while cooling with CuO nanofluid provided 35.67% increment.
[37]	GnP-water nanofluid	Concentration, fluid mass flow rate were used as experimental parameters.	The thermal conductivity of the base fluid increased by 11% and the PV panel efficiency increased by 23%.
[38]	MWCNT-water/EG, Paraffin wax	Performance analysis	Electrical efficiency increased by 4.22% with MWCNT/water based PVT/PCM.
[39]	(SiO ₂ , Al ₂ O ₃ , CuO)/Water	Concentration, flow rate and solar irradiation.	MTE was found to be 66.49% with the use of CuO nanofluid. MEE was found to be 21.18% with the use of Al ₂ O ₃ nanofluid.
[40]	TiO ₂ -water, air	PVT system analysis with efficient MLI topology was performed.	It was determined that the panel proposed by the researchers ITE by 27% and showed a 1.17% improvement in PE compared to the air-cooled system.
[41]	TiO ₂ -CuO/Deionized water hybrid nanofluid	Energy and exergy analysis was performed using ionized water based hybrid nanofluid.	When the hybrid nanofluid volume concentration was 0.3%, the electrical power increased by 77.5% and the system efficiency increased by 58.2%.
[42]	Cu, CuO, TiO ₂ , Al ₂ O ₃ , Fe ₃ O ₄ , MWCNT, PCM	The effect of hybrid nanofluids at different concentrations and combinations on system performance was investigated.	Using PCM composite increased the system performance by 31.1% in thermal efficiency and 5.4% in electrical efficiency compared to the case without PCM.
[43]	Coconut oil- Graphene nanoplatelets	Bio-nanofluids were prepared and performance analysis was performed using the surfactants PVP, SDS, CTAB.	The bio-nanofluid prepared using Polyvinylpyrrolidone (PVP) surfactant showed maximum efficiency (25.169% thermal and 8.632% electrical).
[44]	Al ₂ O ₃ -Cu/water hybrid nanofluid	The PVT system designed using single and double serpentine absorber channels.	The highest overall efficiency was obtained as 84.30% and 90.47% in the use of single and double serpentine, respectively.

EG: Ethylene Glycol, **PCM:** Phase change material, **TE:** Thermoelectric, **MLI:** Multi-level inverter, **ITC:** Increased Thermal Efficiency, **PE:** Panel Efficiency, **MEE:** Maximum Electrical Efficiency, **MTE:** Maximum Thermal Efficiency, **PVP:** Polyvinylpyrrolidone, **SDS:** Sodium dodecyl sulfate, **CTAB:** Cetyltrimethylammonium bromide.

References

- [1] Joshi, S. S., & Dhoble, A. S. (2018). Photovoltaic-Thermal systems (PVT): Technology review and future trends. *Renewable and Sustainable Energy Reviews*, 92, 848-882. <https://doi.org/10.1016/J.RSER.2018.04.067>
- [2] Stritih, U. (2016). Increasing the efficiency of PV panel with the use of PCM. *Renewable Energy*, 97, 671-679. <https://doi.org/10.1016/J.RENENE.2016.06.011>
- [3] Popovici, C. G., Hudişteanu, S. V., Mateescu, T. D., & Cherecheş, N. C. (2016). Efficiency improvement of photovoltaic panels by using air cooled heat sinks. *Energy procedia*, 85, 425-432. <https://doi.org/10.1016/J.EGYPRO.2015.12.223>
- [4] Alzaabi, A. A., Badawiyeh, N. K., Hantoush, H. O., & Hamid, A. K. (2014). Electrical/thermal performance of hybrid PV/T system in Sharjah, UAE. *International Journal of Smart Grid and Clean Energy*, 3(4), 385-389.
- [5] Khanjari, Y., Pourfayaz, F., & Kasaeian, A. B. (2016). Numerical investigation on using of nanofluid in a water-cooled photovoltaic thermal system. *Energy Conversion and Management*, 122, 263-278.
- [6] Berge, B. (2007). *Ecology of building materials*. Routledge. <https://doi.org/10.4324/9780080504988/ecology-building-materials-bj>
- [7] Lamnatou, C., & Chemisana, D. (2017). Photovoltaic/thermal (PVT) systems: A review with emphasis on environmental issues. *Renewable energy*, 105, 270-287. <https://doi.org/10.1016/J.RENENE.2016.12.009>
- [8] Sopian, K., Al-Waeli, A. H., & Kazem, H. A. (2020). Energy, exergy and efficiency of four photovoltaic thermal collectors with different energy storage material. *Journal of EnergyStorage*, 29, 101245. 29, 101245 (2020). <https://doi.org/10.1016/J.EST.2020.101245>
- [9] Rukman, N. S. B., Fudholi, A., Taslim, I., Indrianti, M. A., Manyoe, I. N., Lestari, U., & Sopian, K. (2019). Electrical and thermal efficiency of air-based photovoltaic thermal (PVT) systems: An overview. *Indonesian Journal of Electrical Engineering and Computer Science*, 14(3), 1134-1140.
- [10] Hazi, A., Hazi, G., Grigore, R., & Vernica, S. (2014). Opportunity to use PVT systems for water heating in industry. *Applied thermal engineering*, 63(1), 151-157.
- [11] Aberoumand, S., Ghamari, S., & Shabani, B. (2018). Energy and exergy analysis of a photovoltaic thermal (PV/T) system using nanofluids: An experimental study. *Solar Energy*, 165, 167-177.

- [12] Yang, X., Sun, L., Yuan, Y., Zhao, X., & Cao, X. (2018). Experimental investigation on performance comparison of PV/T-PCM system and PV/T system. *Renewable energy*, 119, 152-159.
- [13] Lotfi, M., Shiravi, A. H., Bahrami, T., & Firoozzadeh, M. (2022). Cooling of PV Modules by Water, Ethylene-Glycol and Their Combination; Energy and Environmental Evaluation. *Journal of Solar Energy Research*, 7(2), 1047-1055.
- [14] Jabeen, N., Haider, H. A., Waqas, A., & Ali, M. (2024). An effective parametric sensitivity analysis to improve electrical and thermal energy/exergy efficiency of PVT system using nanofluid. *Process Safety and Environmental Protection*, 189, 1037-1051.
- [15] Ratnakar, R. R., Gupta, S. S., Hackbarth, J., Livescu, S., & Dindoruk, B. (2024, September). Assessment of Geothermal and Hydrocarbon Wells Using Supercritical Fluids for Heat Production. In *SPE Annual Technical Conference and Exhibition?* (p. D011S006R008). SPE.
- [16] Choi, Y. (2024). Increasing the Utilization of Solar Energy through the Performance Evaluation of Air-Based Photovoltaic Thermal Systems. *Buildings*, 14(5), 1219.
- [17] Boulhidja, S., Bourouis, A., Boukelia, T. E., & Omara, A. (2024). Mixed convection air-cooled PV/T solar collector with integrate porous medium. *Journal of the Brazilian Society of Mechanical Sciences and Engineering*, 46(3), 144.
- [18] Dong, S., Long, H., Guan, J., Jiang, L., Zhuang, C., Gao, Y., & Di, Y. (2024). Performance investigation of a hybrid PV/T collector with a novel trapezoidal fluid channel. *Energy*, 288, 129594.
- [19] Yildirim, M. A., & Cebula, A. (2024). A numerical and experimental analysis of a novel highly-efficient water-based PV/T system. *Energy*, 289, 129875.
- [20] Kazemian, A., Taheri, A., Sardarabadi, A., Ma, T., Passandideh-Fard, M., & Peng, J. (2020). Energy, exergy and environmental analysis of glazed and unglazed PVT system integrated with phase change material: An experimental approach. *Solar Energy*, 201, 178-189. <https://doi.org/10.1016/J.SOLENER.2020.02.096>
- [21] Dong, X., Zhao, Z., Yang, D., & Jia, N. (2024, March). Quantification of Gas Exsolution Dynamics for CO₂/CH₄-Heavy Oil Systems with Population Balance Equations. In *SPE Canadian Energy Technology Conference* (p. D021S016R005). SPE.
- [22] Kenfack, A. Z., Nematchoua, M. K., Simo, E., Konchou, F. A. T., Babikir, M. H., Pemi, B. A. P., & Chara-Dackou, V. S. (2024). Techno-economic and

- environmental analysis of a hybrid PV/T solar system based on vegetable and synthetic oils coupled with TiO₂ in Cameroon. *Heliyon*, 10(1).
- [23] Sathish, T., Giri, J., Saravanan, R., Ubaidullah, M., Shangdiar, S., Iikela, S., ... & Amesho, K. T. (2024). Amplifying thermal performance of solar flat plate collector by Al₂O₃/Cu/MWCNT/SiO₂ mono and hybrid nanofluid. *Applied Thermal Engineering*, 252, 123692.
- [24] Gelis, K., & Akyurek, E. F. (2021). Factorial design for convective heat transfer enhancement of hybrid nanofluids based on Al₂O₃-TiO₂ in a double pipe mini heat exchanger. *Heat Transfer Research*, 52(15).
- [25] Prasetyo, S. D., Arifin, Z., Prabowo, A. R., & Budiana, E. P. (2024). Examining various finned collector geometries in the Water/Al₂O₃ based PV/T system: An analysis using computational fluid dynamics simulation. *International Journal of Heat and Technology*, 42(3), 851-864.
- [26] Tong, Y., Wang, R., Wang, S., & Zhu, Z. (2024). Experimental study on the influence of operating parameters of plug flow on thermal efficiency of direct absorption solar collector with Fe₃O₄ nanofluid. *Process Safety and Environmental Protection*.
- [27] Adil, A., Farrukh, A., Hassan, F., Jamil, F., Khiadani, M., Saeed, S., ... & Ali, H. M. (2024). Magnetic nanofluids preparation and its thermal applications: a recent review. *Journal of Thermal Analysis and Calorimetry*, 149(17), 9001-9033.
- [28] Wang, Q., Yu, C., Li, T., Wang, J., Liu, Y., Shi, Y., ... & Niu, Y. (2024). Enhancing the performance of PVT-TEG power generation systems by heat pipes and Fe₃O₄ nanofluids. *Energy Conversion and Management*, 319, 118938.
- [29] Akoh, H., Tsukasaki, Y., Yatsuya, S., & Tasaki, A. (1978). Magnetic properties of ferromagnetic ultrafine particles prepared by vacuum evaporation on running oil substrate. *Journal of Crystal Growth*, 45, 495-500.
- [30] Wang, X. Q., & Mujumdar, A. S. (2007). Heat transfer characteristics of nanofluids: a review. *International journal of thermal sciences*, 46(1), 1-19.
- [31] Emam, M., Hamada, A., Refaey, H. A., Moawed, M., Abdelrahman, M. A., & Rashed, M. R. (2024). Year-round experimental analysis of a water-based PVT-PCM hybrid system: Comprehensive 4E assessments. *Renewable Energy*, 226, 120354.
- [32] Yuan, J., Xue, K., Gao, X., Chen, Y., Zhao, L., & Hu, D. (2024). Green preparation of biodegradable poly (butylene adipate-co-terephthalate) foam modified with bio-based epoxidized cardanol using supercritical fluid foaming. *The Journal of Supercritical Fluids*, 214, 106391.

- [33] Bayrak, F., Oztop, H. F., & Selimefendigil, F. (2020). Experimental study for the application of different cooling techniques in photovoltaic (PV) panels. *Energy Conversion and Management*, 212, 112789.
- [34] Li, J., Zhang, W., Xie, L., Li, Z., Wu, X., Zhao, O., ... & Zeng, X. (2022). A hybrid photovoltaic and water/air based thermal (PVT) solar energy collector with integrated PCM for building application. *Renewable Energy*, 199, 662-671.
- [35] Sohani, A., Shahverdian, M. H., Sayyaadi, H., Samiezadeh, S., Doranehgard, M. H., Nizetic, S., & Karimi, N. (2021). Selecting the best nanofluid type for A photovoltaic thermal (PV/T) system based on reliability, efficiency, energy, economic, and environmental criteria. *Journal of the Taiwan Institute of Chemical Engineers*, 124, 351-358.
- [36] Menon, G. S., Murali, S., Elias, J., Delfiya, D. A., Alfiya, P. V., & Samuel, M. P. (2022). Experimental investigations on unglazed photovoltaic-thermal (PVT) system using water and nanofluid cooling medium. *Renewable Energy*, 188, 986-996.
- [37] Venkatesh, T., Manikandan, S., Selvam, C., & Harish, S. (2022). Performance enhancement of hybrid solar PV/T system with graphene based nanofluids. *International Communications in Heat and Mass Transfer*, 130, 105794.
- [38] Naghdbishi, A., Yazdi, M. E., & Akbari, G. (2020). Experimental investigation of the effect of multi-wall carbon nanotube-Water/glycol based nanofluids on a PVT system integrated with PCM-covered collector. *Applied Thermal Engineering*, 178, 115556.
- [39] Gelis, K., Ozbek, K., Ozyurt, O., & Celik, A. N. (2023). Multi-objective optimization of a photovoltaic thermal system with different water based nanofluids using Taguchi approach. *Applied Thermal Engineering*, 219, 119609.
- [40] Mustafa, U., Qeays, I. A., BinArif, M. S., Yahya, S. M., & Md. Ayob, S. B. (2024). Efficiency improvement of the solar PV-system using nanofluid and developed inverter topology. *Energy Sources, Part A: Recovery, Utilization, and Environmental Effects*, 46(1), 14657-14673.
- [41] Alktranee, M., Shehab, M. A., Németh, Z., Bencs, P., & Hernadi, K. (2023). Experimental study for improving photovoltaic thermal system performance using hybrid titanium oxide-copper oxide nanofluid. *Arabian Journal of Chemistry*, 16(9), 105102.
- [42] Jasim, D. J., Al-Asadi, H. A., Alizadeh, A. A., Nabi, H., Albayati, T. M., Salih, I. K., ... & Ganji, D. D. (2023). Evaluation of different methods to ameliorate the performance of PV/T systems using hybrid nanofluids and PCM in a spiral tube with different cross sections. *Results in Engineering*, 20, 101514.

- [43] Permanasari, A. A., Rosli, M. A. M., Habibi, I. A., Puspitasari, P., Sukarni, S., Herawan, S. G., & Rafaizul, N. I. A. M. (2023). Efficiency of a Photovoltaic Thermal (PVT) System using Bio-nanofluid based on Virgin Coconut Oil-Graphene with Additive Surfactant: An Experimental Study. *Journal of Advanced Research in Applied Sciences and Engineering Technology*, 34(2), 287-304.
- [44] Ali, A., Alhussein, M., Aurangzeb, K., & Akbar, F. (2023). The numerical analysis of Al₂O₃Cu/water hybrid nanofluid flow inside the serpentine absorber channel of a PVT; the overall efficiency intelligent forecasting. *Engineering Analysis with Boundary Elements*, 157, 82-91.

Chapter 3



AN OVERVIEW OF COMPOSITE COATINGS: TYPES, MECHANICAL PROPERTIES, PRODUCTION METHODS, AND APPLICATION AREAS

Abdulkerim FIRAT¹

Sakine KIRATLI²

¹ (Graduate student), Çankırı Karatekin University, Faculty of Engineering, Department of Mechanical Engineering

² (Asst. Prof. Dr.), Çankırı Karatekin University, Faculty of Engineering, Department of Mechanical Engineering, skiratli@karatekin.edu.tr, ORCID: 0000-0001-6292-5605

1. Introduction

Composite coatings combine the properties of two or more different materials to create a more durable and high-performance material. Usually, a matrix and a reinforcing material (fiber or particle) combine to form these coatings. By modifying the interface characteristics of solid materials, composite coatings help to make surfaces self-cleaning, self-healing, and resistant to corrosion [1]. Furthermore, low-shear-strength composite coatings can offer exceptionally low coefficients of friction and wear under certain or carefully regulated test conditions. They also exhibit good self-lubrication and wear resistance. In applications where cost, weight, corrosion resistance, and biocompatibility are crucial, self-lubricating composite coatings are especially appealing because they combine a number of qualities not seen in other solid lubricant coatings [2].

However, self-lubricating composite coatings have many limitations. These limitations can be due to design, usage conditions, and material properties. The most common limitations are low load-carrying capacity, temperature resistance, surface hardness and wear resistance, limited application areas, and cost [3].

Composite coatings are less robust than carbon-based and ceramic coatings, and they produce more wear debris and have a shorter lifespan. Coatings are more likely to melt and degrade at high temperatures when they have low thermal conductivity and poor heat resistance. Furthermore, the environment greatly affects their tribological performance. Because of the chemical reaction between the surface and its surroundings, a worn surface may display distinct chemistries, microstructures, and crystallographic textures from the overall coating. In a different setting, it might not be feasible to achieve extremely low friction and long wear life [4]. Oxidation and degradation brought on by aging also provide difficulties for some applications. The qualities of materials can be optimized and customized by combining materials with diverse properties and effectively utilizing the advantages of two or more components. Functional fillers have therefore been used to enhance the performance of composite coatings. These include a stable and low coefficient of friction, high heat resistance and thermal conductivity, enhanced mechanical properties for increased loads, and optimal adhesion between the substrate and the coating. For low friction and wear resistance, fillers like graphite and polytetrafluoroethylene are utilized; for high thermal conductivity and heat resistance, ceramics, copper, and boron nitride are employed; and for increased load-carrying capacity, carbon fiber and titanium carbide are utilized [5].

Composite coatings are one of the most widely used coating materials in

the industry, providing exceptional liquid insulation and corrosion resistance. Composite coatings are advantageous in areas such as the petroleum industry, where structures such as drawn pipes are common. Some of these advantages include acting as thermal protectors and providing protection from gas and heat. For example, they provide fire resistance and protect composites from resin melting. Composite coatings provide electromagnetic compatibility. They also provide a smooth and clean appearance on textures and surfaces [6]. This wide range of applications for composite coatings is expanding with the continuous development of new material technologies and manufacturing methods. These coatings have the potential to offer industries more durable, lightweight, and customizable solutions. Table 1 shows previous studies on composite coatings.

Table 1. *Investigations into composite coatings*

Authors	Composite coatings	Mechanical properties	Results	Reference
Liu et al.	Epoxy composite	High tensile strength and wear resistance	They found the positive effects of incorporating two differently functionalized fullerenes, C60 and graphene, into the polymer matrix, on the tribological performance of the epoxy coating.	[7]
Yang et al.	Polyurethane composite	High impact strength and wear resistance	They observed that the polyurethane composite coating filled with microcapsules had a lower coefficient of friction compared to unfilled composite coatings.	[8]
Han et al.	UHMWPE/Graphene sheet composite	High wear and friction resistance	They found that new UHMWPE-graphene composite coatings produced by flame spraying were successful in protecting engineering components against corrosion.	[9]
Nemati et al.	Polytetrafluoroethylene composite	Low coefficient of friction and heat resistance	They applied a composite coating consisting of PTFE and graphene oxide on stainless steels and claimed that the wear resistance was successful.	[10]
Lim et al.	Polytetrafluoroethylene-carbon composite	Low friction, high wear resistance and high hardness	They proposed that the composite coating made with carbon nanotubes and a polytetrafluoroethylene matrix had more wear and friction resistance than pure PTFE.	[11]
Wang et al.	Polymer composite	High impact resistance and flexibility	They discovered that the wear and corrosion resistance of polymer composite coatings were enhanced by the inclusion of oily functional fillers.	[12]

2. Types of Composite Coatings

2.1 Fiber-reinforced composite coatings

Fiber-reinforced composite coatings generally use reinforcing materials such as carbon, glass, aramid, or natural fiber. Sectors such as aviation, automotive, marine, and sports equipment widely prefer these coatings due to their excellent strength properties and lightness [13]. Various processing methods allow for the flexible production of fiber-reinforced coatings, enabling the creation of special designs and complex forms. Different fiber types offer different strengths, flexibility, and weight properties, enabling the selection of the coating based on specific application requirements. It also combines the high-strength properties of reinforcing fiber materials with the low-density property of the polymer matrix. This allows the material to have an excellent strength/weight ratio [14].

2.2 Polymer matrix composite coatings

Polymeric matrix coatings typically use polymeric materials. Automotive, construction, and medical applications generally prefer such coatings due to their lightness and flexibility. In addition to providing a range of color and texture possibilities, polymeric matrix coatings can be applied throughout a broad temperature range. Due to the nature of polymer resins, they also possess flexible properties. This feature facilitates the application of coatings to various surfaces and offers a wide range of applications. High-strength materials like glass, carbon, or aramid fiber are typically used as reinforcing materials. This provides durability and strength to polymer matrix coatings [15]. Applications for polymer matrix coatings include spraying, dipping, baking, vacuum infusion, 3D printing, brushing, rolling, and plasma coating. Figure 2 illustrates some methods of applying polymer matrix coatings.



Figure 1. Various methods used in the preparation of polymer matrix composite coatings [16].

2.3 Particle-reinforced composite coatings

Generally, the matrix material integrates ceramic, metal, or polymer particles to form particle-reinforced composite coatings. These coatings are used especially to increase wear resistance, regulate thermal conductivity, or add electrical conductivity. For instance, industrial applications often prefer coatings containing aluminum oxide due to their ability to withstand high temperatures. The particles used in particle-reinforced coatings can generally be ceramic (e.g., alumina), metal (e.g., aluminum), or polymeric (e.g., thermoplastic microparticles) [17]. The distinct advantages of each particle type dictate the coating's particular characteristics. For a given application, these coatings are seen to be an effective way to enhance the performance of engineering materials [18].

2.4 Ceramic composite coatings

Ceramic coatings typically resist high temperatures, wear, and chemicals. In industrial applications, they provide surface protection, thermal insulation, and friction resistance. These coatings are essential components, particularly in the energy production and defense sectors. Ceramic coatings generally have high-temperature resistance. High-temperature applications such as industrial furnaces, engine parts, or spacecraft can utilize this property. Ceramics generally have wear

resistance due to their high hardness [19]. This enables their application on surfaces subjected to wear conditions, such as industrial equipment parts, cutting tools, or automotive parts. Ceramic coatings can resist chemicals. This property makes the coatings suitable for use in chemical industries or applications where they might encounter acids and bases. These properties have led to the widespread use of ceramic coatings across various industries. Depending on the application context, one can select different ceramic types and produce coatings suitable for specific requirements [20]. Figure 3 shows the superhydrophobic image of the TiO_2 ceramic composite coating applied on 316L stainless steel.

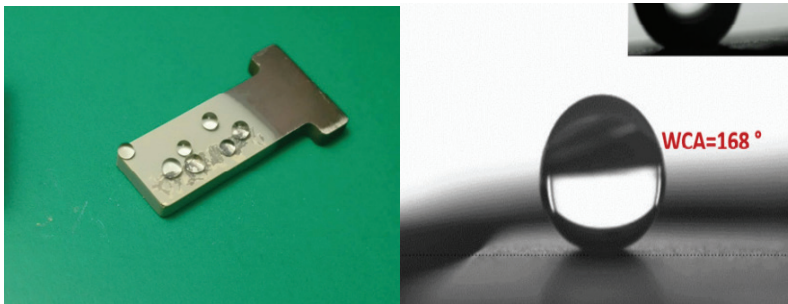


Figure 2. Superhydrophobic effect of $\text{TiO}_2/\text{TMOSi}$ ceramic composite coating on 316L stainless steel [21].

2.5 Metal matrix composite coatings

Metal matrix composite coatings combine a metal matrix material with a reinforcing material. Aerospace applications specifically use them to ensure resistance to high temperatures and heavy loads. Special alloys' excellent mechanical properties can strengthen these coatings. The metal matrix gives the coating high overall strength, while the reinforcing materials enhance its hardness. This increases the durability and wear resistance of the coating. Metal matrix coatings generally have high thermal conductivity properties. This property is advantageous in applications requiring heat management, especially in electronic devices. Reinforcing materials can increase the wear resistance of the coating. Therefore, applications requiring wear resistance on the surfaces of mechanical parts use these materials. Metal matrix coatings generally resist corrosion. This property guarantees a long lifespan for the coatings in a variety of environments [22]. There are multiple methods of applying metal matrix composite coatings, such as thermal spray, molecular mixing, electrochemical deposition, sputtering, vapor deposition, and plasma spray coating. Figure 5 illustrates the most common application method, the

thermal spray coating method, which involves spraying molten or semi-molten metal onto the product's surface to form a coating.

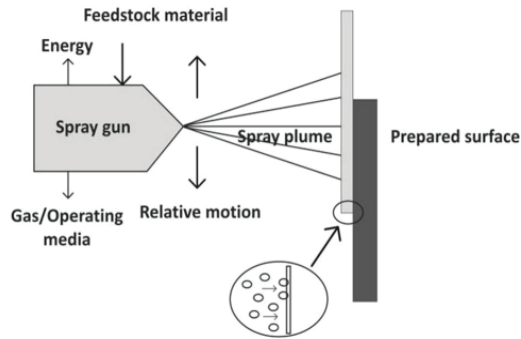


Figure 3. Application of thermal spray coating [23].

2.6 Nanocomposite coatings

Nanocomposite coatings take advantage of nanotechnology. The addition of nano-sized materials usually provides excellent mechanical properties, high electrical conductivity, or special optical properties. Various fields, from electronic devices to medical imaging equipment, use them. The nanomaterials used in nanocomposite coatings provide the ability to control the properties of the material at the nanoscale. Nanomaterials generally have high strength properties despite their small size [24]. This can increase the durability of nanocomposite coatings. The high surface area of nanoparticles can increase the surface interactions of the coatings. This property can be advantageous in areas such as adhesion, catalytic interactions, or sensor applications. Nanoparticles can increase the thermal and electrical conductivity of the coating. This property enables the use of nanoparticles in areas that require electrical conductivity or in heating applications. For instance, coating an aluminum alloy surface involves applying three layers: chromate conversion coating, primer coating, and topcoat. Figure 4 illustrates the protective coatings applied to an aluminum alloy aircraft. In this case, chromate conversion coatings are good at resisting corrosion, the primer coat makes the coating stick better and last longer, and the last layer is a polymeric topcoat made of polyurethane, polyamide, polyester, resin, or epoxy that protects the other layers from chemicals, oxygen, and light [25].

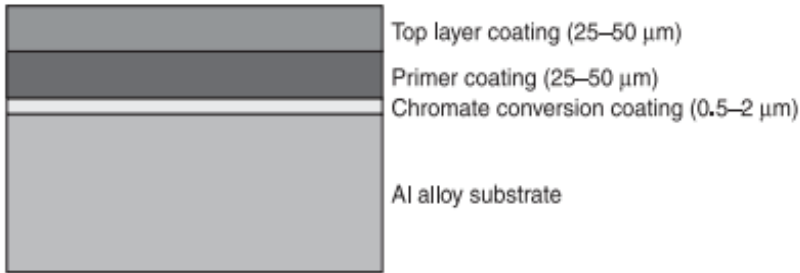


Figure 4. *Coating on aluminum alloys used in aircraft [25].*

3. Manufacturing Methods and Application Areas

It is necessary to guarantee the strength and stability of the contact between the substrate and the composite layers. Thus, substrate surface treatment is becoming more and more important. High and complex demands on the material necessitate the application of composite coatings. Coatings provided:

- Strength and binding effects are increased (for example, high-strength phases in a tough, uncured matrix).
- Development of various phase ranges and compositions that can trap or bridge cracks, reduce and direct stress, and absorb or dissipate energy
- Enhanced tribological characteristics (wear reduction, friction modification), enhanced corrosion resistance, enhanced thermal resistance, enhanced catalytic capabilities,
- Increased roughness and porosity, enhanced ornamental effects, and the creation of barrier effects (such thermal insulation) are some of the benefits [26].

Figure 5 displays examples of matrix and dispersion materials. The qualities of the coating are impacted by the aggregated particles in several ways. During growth, they may have an impact on the material's coating structure, and their presence in the coating may have an impact on its attributes. Small, hard, uniformly distributed particles with a fine distribution should be included into the coating to provide the highest possible hardness, according to the dispersion hardening theory [27].

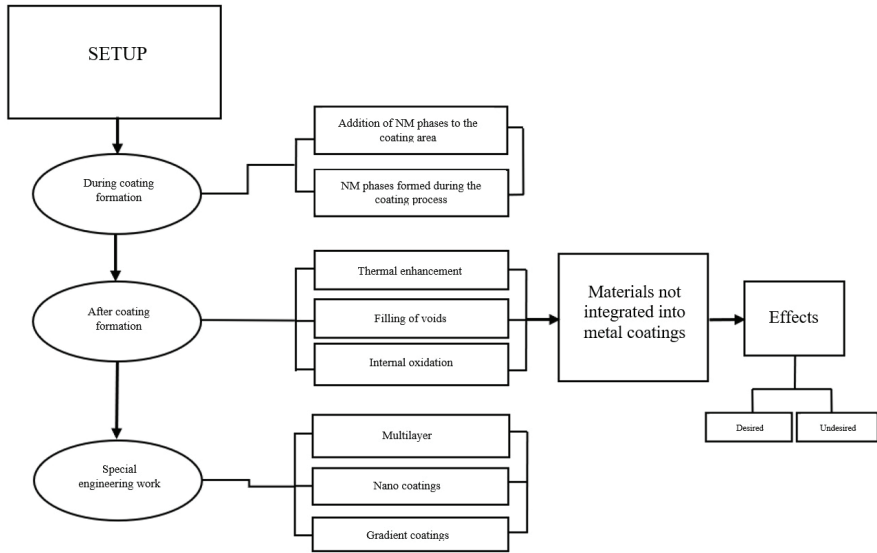


Figure 5. Matrix and dispersion materials in composite coatings [28]

There are two guiding concepts of the technological production approach. The first technique uses tiny particles scattered throughout the electrolyte. Due to externally driven conduction and potentially minor electrophoresis effects, the particles arrive at the electrolyte/cathode surface near the phase boundary. Migration and electrostatic forces cause the particles to travel to a location near the surface where they can gather. Until the particles become part of the matrix, they must remain in this area for a sufficient amount of time. In the second way, the usage of bigger particles requires that they either be placed in a fixed bed where they integrate into the developing layer or sink to the cathode surface using the proper technical techniques. Depending on the particle size and technological equipment, one or both methods may be used. It is possible to use the dispersion method up to a particle diameter of 10 μm (perhaps greater). Both coarse and very fine particles can be used to create coatings [29]. Materials used for matrix and dispersion in composite coatings are listed in Table 2 [28].

Table 2. *The use of materials in composite coatings [28]*

Matrix materials
Metals (Ni, Cu, Fe, Cr, Co, Ag, Au, Zn, Sn, Cd, Pb, Pd, Al)
Metal alloys (NiCr, NiAg, CuNi, CuAg, NiCrBSi, steel alloys)
Polymers (PA)
Ceramics (Al_2O_3 , $\text{MgO} \times \text{ZrO}_2$, SiC, BN, S_4 , Ti-Si-C, Ti-Ge-C)
Carbon
Dispersion Materials
Carbides (SiC, TiC, Cr_3C_2 , WC, B_4C , ZrC, HfC)
Oxides (Al_2O_3 , SiO_2 , TiO_2 , Cr_2O_3 , ZrO_2 , UO_2 , BeO)
Borides and nitrides (Cr_3B_2 , TiB_2 , ZrB_2 , HfB ₂ , BN, B_4N , TiN, AlN)
Graphite (MoS_2)
Polymers (polytetrafluoroethylene, polyethylene, polyvinyl chloride, acrylonitrile styrene)
Metals (Cr, W)
Others (Glass, CaF_2)

Vacuum plasma spraying is one of the thermal technologies that can be used to create a variety of composite coatings. Other approaches are also feasible. The particles are either agglomerated or combined with other spray powder ingredients either prior to or during the spraying process. This can lead to issues, such as an uneven distribution of particles in the coating or a significant difference in the particle ratio between the powder and the coating [30]. Because tiny particles (less than 1 μm) cannot be used, dispersion hardening cannot be accomplished.

Alternatively, dispersion-hardened material can be made into spray powder particles. The method's issues are the workability of the thermal spray process and the creation of powder.

TiC- and TiN-reinforced titanium coatings can be produced via reactive plasma spraying, which is an additional technique. These days, aluminum or aluminum alloy composite coatings and Si_3N_4 coatings are a major area of research interest. In order to reduce the weight of construction, light metals like aluminum or aluminum alloys are crucial. Nevertheless, their poor sliding qualities and inadequate resistance to wear and corrosion frequently restrict their use. The use of aluminum composite coatings as lightweight structural components is very desirable. Successful thermal spraying of carbon short fiber-reinforced aluminum coatings depends on the formation of agglomerates between the fibers and aluminum powder, which provide effective spraying. Mixing via mechanical means is insufficient. Low porosity coatings with a fiber content of roughly 8 wt.% are produced under ideal spraying circumstances [31].

Thermal spraying of silicon nitride-containing coatings requires special powders that ensure that the silicon nitride particles adhere well to one of the matrix components. The basis of the plasma spraying method is the melting of the metallic, ceramic, carbide, oxide, composite, or plastic powders to be coated by the plasma method and spraying them onto the surface. In order to create plasma, energy must be provided to the gas mass, the stable gas structure must be disrupted, and an unstable dense energy cloud must be created. The most common and simplest method is to provide electrical energy to the gas mass. The greatest advantage of the plasma spraying method is that it can easily melt ceramic and metal alloy powders that are difficult to melt by reaching very high temperatures. Ceramic powders have become important coating materials due to their high wear resistance and hardness, easily available and cheap raw materials, good corrosion resistance, and thermal properties [32].

4. Conclusion

The most appropriate ways for producing composite coatings are thermal spraying and electrochemical coating strategies. Their primary benefit is that they can handle a variety of technical applications due to the material's superior tribological characteristics. In terms of application areas, composite coatings are used as lightweight and durable coatings for aircraft bodies, rotor blades, and spacecraft in the aviation and space industry. In the automotive industry, they are preferred for providing lightness and durability in vehicle parts. Coatings are used in many areas, from ship bodies to military vehicles in the maritime and defense sector, and in the energy sector, they appear as durable coatings for wind turbines, solar panels, and the oil and gas industry. In construction and infrastructure projects, coatings are used in various structural applications, from bridges to buildings. In the electronics and telecommunications field, they provide electromagnetic shields and lightweight coatings. In the health and medical sector, they are an ideal choice for medical implants, prostheses, and dental restorations due to their biocompatibility properties. Finally, in the sports and recreation field, they are used to provide lightness and durability in products such as sports equipment, ski gear, and bicycle parts. Composite coatings have many advantages in terms of lightness, high strength, environmental friendliness, sustainability, and compatibility with nanotechnology; therefore, composite coating technology will develop in the future, and their areas of use will increase.

References

1. Cheng, Q., Zhao, H., Zhang, G., Gu, P., & Cai, L. (2014). An analytical approach for crucial geometric errors identification of multi-axis machine tool based on global sensitivity analysis. *The International Journal of Advanced Manufacturing Technology*, 75, 107-121.
2. Donnet, C., & Erdemir, A. (2004). Solid lubricant coatings: Recent developments and future trends. *Tribology Letters*, 17(3), 389-397.
3. Ouyang, J.H., Li, Y.F., Zhang, Y.Z., Wang, Y.M., & Wang, Y.J. (2022). High-temperature solid lubricants and self-lubricating composites: A critical review. *Lubricants*, 10(8), 177.
4. Scharf, T.W., & Prasad, S.V. (2013). Solid lubricants: A review. *Journal of Materials Science*, 48, 511-531.
5. Jakab, B., Panaitescu, I., & Gamsjäger, N. (2021). The action of fillers in the enhancement of the tribological performance of epoxy composite coatings. *Polymer Testing*, 100, 107243.
6. Yalınız, E.T. (2022). *Epoksi esaslı polimerik kaplamaların tribolojik özelliklerinin incelenmesi* (Master's thesis, Pamukkale Üniversitesi Fen Bilimleri Enstitüsü).
7. Liu, D., Zhao, W., Liu, S., Cen, Q., & Xue, Q. (2016). Comparative tribological and corrosion resistance properties of epoxy composite coatings reinforced with functionalized fullerene C60 and graphene. *Surface and Coatings Technology*, 286, 354-364.
8. Yang, M., Zhu, X., Ren, G., Men, X., Guo, F., Li, P., & Zhang, Z. (2015). Tribological behaviors of polyurethane composite coatings filled with ionic liquid core/silica gel shell microcapsules. *Tribology Letters*, 58, 1-9.
9. Han, J., Ding, S., Zheng, W., Li, W., & Li, H. (2013). Microstructure and anti-wear and corrosion performances of novel UHMWPE/graphene-nanosheet composite coatings deposited by flame spraying. *Polymers for Advanced Technologies*, 24(10), 888-894.
10. Nemati, N., Emamy, M., Yau, S., Kim, J.K., & Kim, D.E. (2016). High temperature friction and wear properties of graphene oxide/polytetrafluoroethylene composite coatings deposited on stainless steel. *RSC Advances*, 6(7), 5977-5987.
11. Lim, W.S., Khadem, M., Anle, Y., & Kim, D.E. (2018). Fabrication of polytetrafluoroethylene-carbon nanotube composite coatings for friction and wear reduction. *Polymer Composites*, 39(S2), E710-E722.

12. Wang, C., Wang, H., Li, M., Liu, Z., Lv, C., Zhu, Y., & Bao, N. (2018). Anti-corrosion and wear resistance properties of polymer composite coatings: Effect of oily functional fillers. *Journal of the Taiwan Institute of Chemical Engineers*, 85, 248-256.
13. Rajak, D.K., Pagar, D.D., Menezes, P.L., & Linul, E. (2019). Fiber-reinforced polymer composites: Manufacturing, properties, and applications. *Polymers*, 11(10), 1667.
14. Kappenthuler, S., & Seeger, S. (2021). Assessing the long-term potential of fiber reinforced polymer composites for sustainable marine construction. *Journal of Ocean Engineering and Marine Energy*, 7(2), 129-144.
15. Kanaginahal, G.M., Muniraju, A.K., & Murthy, M.M. (2018). Coatings for enhancement of properties of polymer matrix composites: A review. *Materials Today: Proceedings*, 5(1), 2462-2465.
16. Ren, Y., Zhang, L., Xie, G., Li, Z., Chen, H., Gong, H., ... & Luo, J. (2021). A review on tribology of polymer composite coatings. *Friction*, 9, 429-470.
17. Yang, M., Xu, C., Wu, C., Lin, K.C., Chao, Y.J., & An, L. (2010). Fabrication of AA6061/Al₂O₃ nano ceramic particle reinforced composite coating by using friction stir processing. *Journal of Materials Science*, 45, 4431-4438.
18. Priyadarshi, P., Katiyar, P.K., & Maurya, R. (2022). A review on mechanical, tribological and electrochemical performance of ceramic particle-reinforced Ni-based electrodeposited composite coatings. *Journal of Materials Science*, 57(41), 19179-19211.
19. Krishna, L.R., Somaraju, K.R.C., & Sundararajan, G. (2003). The tribological performance of ultra-hard ceramic composite coatings obtained through microarc oxidation. *Surface and Coatings Technology*, 163, 484-490.
20. Torrey, J.D., & Bordia, R.K. (2008). Processing of polymer-derived ceramic composite coatings on steel. *Journal of the American Ceramic Society*, 91(1), 41-45.
21. Emarati, S.M., & Mozammel, M. (2020). Efficient one-step fabrication of superhydrophobic nano-TiO₂/TMPSi ceramic composite coating with enhanced corrosion resistance on 316L. *Ceramics International*, 46(2), 1652-1661.
22. Walsh, F.C., & Ponce de Leon, C. (2014). A review of the electrodeposition of metal matrix composite coatings by inclusion of particles in a metal layer: An established and diversifying technology. *Transactions of the IMF*, 92(2), 83-98.

23. Rajak, D.K., Wagh, P.H., Menezes, P.L., Chaudhary, A., & Kumar, R. (2020). Critical overview of coatings technology for metal matrix composites. *Journal of Bio-and Tribo-Corrosion*, 6, 1-18.
24. Patscheider, J., Zehnder, T., & Diserens, M. (2001). Structure-performance relations in nanocomposite coatings. *Surface and Coatings Technology*, 146, 201-208.
25. Asmatulu, R. (2012). Nanocoatings for corrosion protection of aerospace alloys. In *Corrosion Protection and Control using Nanomaterials* (pp. 357-374). Woodhead Publishing.
26. Allcock, B.W., & Lavin, P.A. (2003). Novel composite coating technology in primary and conversion industry applications. *Surface and Coatings Technology*, 163, 62-66.
27. Wielage, B., Steinhäuser, S., & Henker, A. (1999). Manufacture and properties of composite coatings: An introduction. *Journal of Thermal Spray Technology*, 8, 512-516.
28. Steinhäuser, S., & Wielage, B. (1997). Composite coatings: Manufacture, properties, and applications. *Surface Engineering*, 13(4), 289-294.
29. Akçin, Y., Osman, A.S.İ., & Yeşil, Ö. (2013). Kompozit malzemelerin kaplanabilirliğinin incelenmesi. *Pamukkale Üniversitesi Mühendislik Bilimleri Dergisi*, 19(7), 319-322.
30. Sathish, M., Radhika, N., & Saleh, B. (2023). Duplex and composite coatings: a thematic review on thermal spray techniques and applications. *Metals and Materials International*, 29(5), 1229-1297.
31. Zhao, Y., Zhang, T., Chen, L., Yu, T., Sun, J., & Guan, C. (2021). Microstructure and mechanical properties of Ti-C-TiN-reinforced Ni_2O_4 -based laser-cladding composite coating. *Ceramics International*, 47(5), 5918-5928.
32. Thiele, S., Berger, L. M., Herrmann, M., Nebelung, M., Heimann, R.B., Schnick, T., ... & Schnick, T. (2002). Microstructure and properties of thermally sprayed silicon nitride-based coatings. *Journal of Thermal Spray Technology*, 11, 218-225.


Chapter 4


BIBLIOMETRIC ANALYSIS FOR ROBOTS USING ARTIFICIAL INTELLIGENCE

Tayfun Abut¹

İhsan Tuğal²

¹ Department of Mechanical Engineering, Mus Alparslan University, 49100, Mus, Turkey

 1 0000-0003-4646-3345

² Department of Software Engineering, Mus Alparslan University, 49100, Mus, Turkey, 

2 0000-0003-1898-9438

Introduction

With the desire of people to find helpers and the development of technology, robotics studies have gained momentum. Human-machine or computer interaction is an interdisciplinary field that focuses on the connection between humans and machines and computers, and aims to examine software, hardware and human events. Robots have a wide range of applications ((Asimov, 2004; Lewis et al., 2018; Song and Guo, 2006; Abut and Huseyinoglu, 2019; Abut and Soyguder, 2019; Abut and Soyguder, 2022). The emergence and rapid development of artificial intelligence in recent years has become more important for robots to think, perceive their environment and make decisions. In this research, various studies have been conducted on the use of artificial intelligence in robotic studies. One of the first studies on the use of artificial intelligence in robotics was conducted by Brady in 1985 (Brady, 1985). A study on setting up a robotics laboratory for teaching artificial intelligence was conducted (Kumar and Meeden, 1998). Jacobsen et al, (2004) studied research robots for artificial intelligence, teleoperation and entertainment applications. Brady et al. (2012) conducted another study on robotics and artificial intelligence. A study on the role of artificial intelligence in robotics has been carried out (Bogue, 2014). A study was conducted on behalf of artificial intelligence and robot responsibilities (Ashrafian, 2015). A study on the basics of artificial intelligence and robotics (Raj and Seamans, 2019). A literature study on artificial intelligence used for long-term robot autonomy has been patched (Kunze et al. 2018). A study presented an overview of the field of artificial intelligence and robotics (Perez et al., 2018). A study was presented in response to the questions of whether robots developing with artificial intelligence will take your job (Rampersad, 2020). Grischke et al.,(2020). He conducted a study on robotics and artificial intelligence applications in dentistry. A systematic review on artificial intelligence in robot-assisted surgery is presented (Moglia et al., 2021). Ribeiro et al., (2021), presented a literature review on the use of robotic process automation and artificial intelligence in industry 4.0. Sarker et al., (2021) presented a systematic review on robotics and artificial intelligence in healthcare during the COVID-19 pandemic. They conducted a systematic search following the Preferred Reporting Items for Systematic Reviews and Meta-analyses (PRISMA) method. A systematic review of selected SSCI publications with AI-based robots in education is presented (Chu et al., 2022). Borboni et al. (2023) presented a systematic review of recent studies on the expanding role of AI in collaborative robots for industrial applications. A review on AI, machine learning and deep learning in advanced robotics (Soori et al., 2023). Akpuokwe et al. (2024) presented a comprehensive review on legal challenges in AI and robotics. Liang et al. (2024) conducted a study

on ethics in the field of AI and robotics in the architecture, engineering and construction industry. Zhang et al. (2024) conducted a review on the use of artificial intelligence in robotic surgery operations. The fact that the field of robotics is quite wide and there are different types of artificial intelligence expands the literature studies. In addition, the fact that robots have new areas of use and that they desire to work in an intelligent way has caused an increase in studies.

This research presents a bibliometric analysis of scientific studies on the use of artificial intelligence in the field of robotics. In this study, keywords, citations, publication years, journals, links, countries, authors, and review articles were analyzed in a new way. The data obtained from Web of Science was analyzed using the Biblioshiny web-based interface running the “bibliometrix” package in the R programming language. Analyzing 15935 studies from 1980-2024, the analysis reveals research trends, international collaboration networks and the geographical distribution of scientific production on the topic. The findings of the study show the important position of China in research on the use of artificial intelligence in robotics, followed by the USA and Japan. The research is a valuable tool for prospective researchers investigating the use of artificial intelligence in robotics to predict trends and improve utilization. In conclusion, this study highlights the importance of increasing global collaboration and interdisciplinary approaches in research on the use of artificial intelligence in robotics and reveals trends that will contribute to its development.

Material and Method

In this study, we conducted a bibliometric analysis of academic studies on the use of Artificial Intelligence in robotics in the Web of Science (WOS) database. WOS has more than 21,000 peer-reviewed journals and is one of the most frequently used and reliable global citation databases for academic article analysis (Yeung, 2023). We searched the WOS database for studies on the use of artificial intelligence in robotics between 1980 and 2024. The oldest publication year on the subject in the database was determined as 1980. We downloaded all the data on the same day to avoid deviations due to database updates. Before downloading the data, we filtered the year, document type and working language respectively. While filtering the words, we searched for studies that included both “Artificial Intelligence”, “Artificial Intelligent” and “Robot” as topics. For bibliometric analyses, we used the Biblioshiny web-based interface that works with the “bibliometrix” package in the R programming language (Aria and Cuccurullo, 2017; R Core Team, 2021). To perform the analysis by connecting to the web interface via R, we first installed the package required for bibliometric analysis using the following commands: `install.packages(“devtools”)`, `devtools::install_github (massimoaria/bibliometrix)`. We

then ran the package's library using the "library(bibliometrix)" command. Finally, we accessed the database using biblioshiny(). We selected WOS as the file type in the biblioshiny database and imported the prepared text file into the program. We then analyzed key statistics, journals, keywords, authors, institutions, countries and studies.

Results and Discussion

In the research, studies in which the words "Artificial Intelligence", "Artificial Intelligent" and "Robot" were mentioned together were scanned and 15935 studies were identified. Then, the year (1980-2024), document type (Article) and language (English) options were filtered respectively. As a result of the filtering, it was seen that the studies obtained cover the period 1980-2024. There are 3385 studies by 26909 authors and 860 of these studies are single authored. The total number of sources used was found to be 15935. When we look at the study production by years, in general, the number of articles reached a peak in 2008. However, a decline is observed afterwards. From 2016 onwards, there is an increasing trend until 2022 (Figure 1). Between 2022 and 2024, the number of studies produced decreased (from around 1600 to around 1200). This probably indicates that the topic of interest has received more attention over time, but that there has been an increase and decrease in the publication of relevant research resources. The journals and conferences that have contributed the most to research using Artificial Intelligence in robotics are given in Figure 2. With the resource menu in the most relevant resource unit, the 'World Congress on Intelligent Control' conference is the most visible work with 1367 times, followed by the 'Proceedings of the 3rd Congress on Intelligent Control' conference series in second place with 841 times and the 'Proceedings of the 10th World Congress on Intelligent Control' conference series in third place with 495 times (Figure 2). Other contributing conferences are "2022 41st Chinese Control Conference", "Icmit 2007 Mechatronics, Mems and Smart Material" and "Icmit 2005 Control Systems and Robotics". "Intelligent Autonomous Systems", "Engineering Applications of Artificial Intelligence" and "Journal of Intelligent & Robotic Systems" are other journals contributing to the related field.

The authors who have contributed the most to research using Artificial Intelligence in robotics are given in Figure 3. "Wang Y" emerged as the most prolific author in this discipline and produced the most publications. This author has emerged as a leading name in this field with 357 published papers on the Artificial Intelligence method in Robotics. This showcases the author's deep expertise and remarkable achievements in this particular field and highlights his work as an important reference source for researchers exploring this topic. "Zhang X" and 'Liu Y' are the other authors who made significant contributions, publishing 327 and 312 documents

respectively. “Li Y” (279 documents), ‘Zhang Y’ (271 documents), and ‘Wang X’ (257 documents) have also made important contributions in this field, but they are slightly behind the first three authors. “Wang H” (235 documents), ‘Wang J’ (234 documents) and ‘Liu H’ (233 documents) also have a similar number of documents each. “Liu H” is also on the list with 221 documents. The works of these authors can be sources that should be taken into consideration in research on the subject. Researchers can direct their own studies by examining the works of these authors.

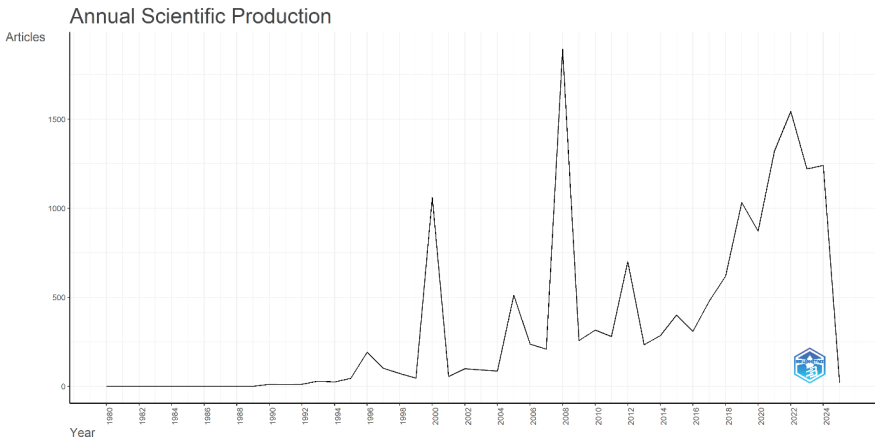


Figure 1. *Scientific production of articles on related topics by year.*

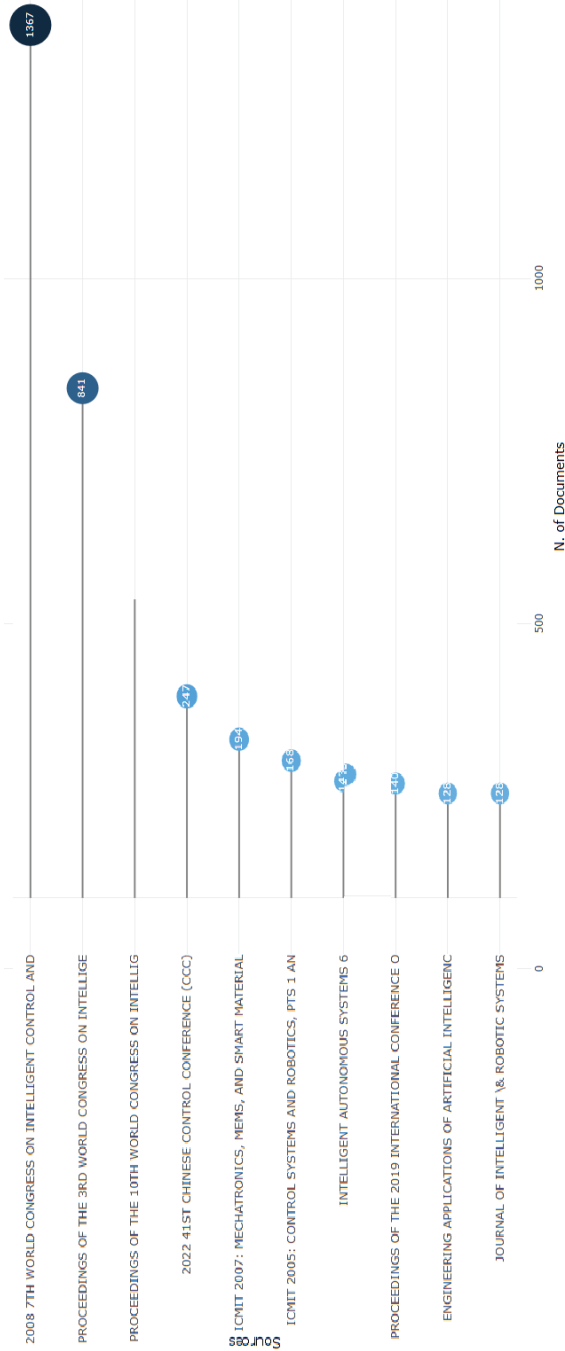


Figure 2. *The top 10 journals that published the most studies on the subject.*

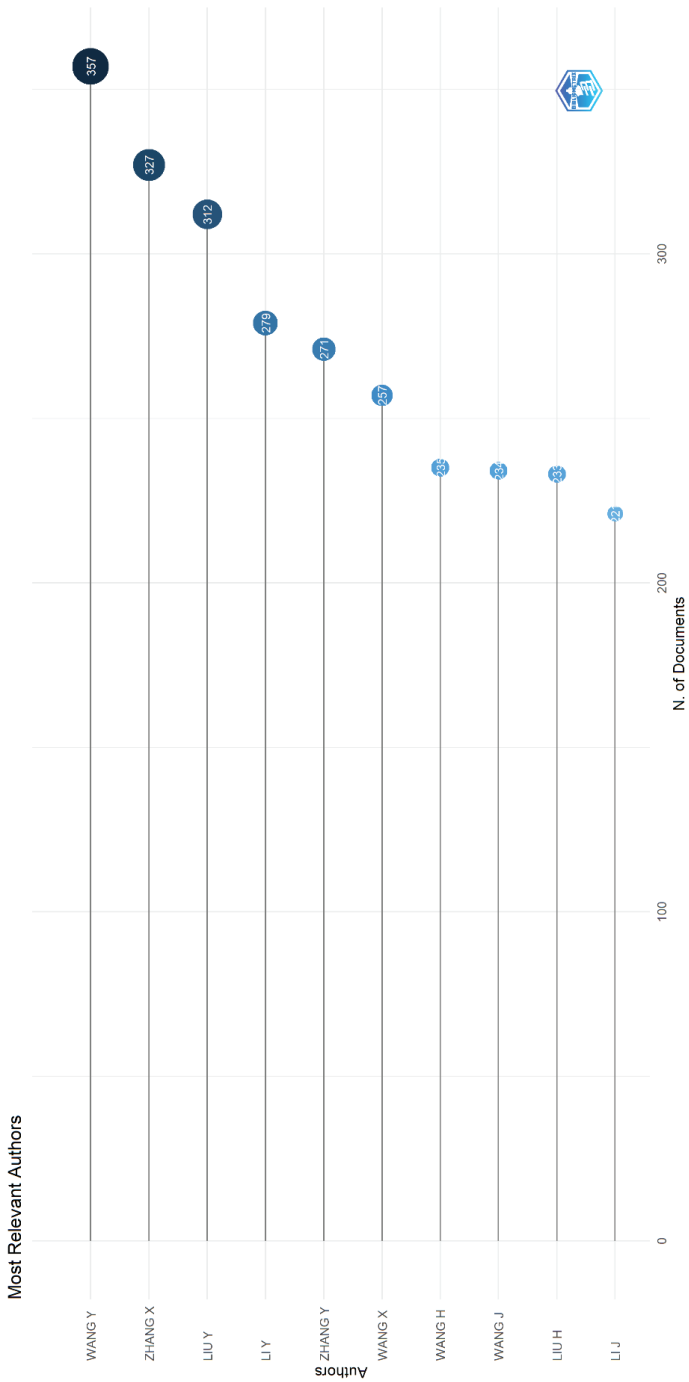


Figure 3. Top 10 authors who published the most studies on the topic.

“Proceedings CVPR IEEE” conference is the most common with 8698 citations, followed by “IEEE Intellignt Conference Robot” in second place with 6795 citations, “Arxiv” with 4839 citations and “Lecture Notes Computer Science” with 4555 citations (Figure 5).

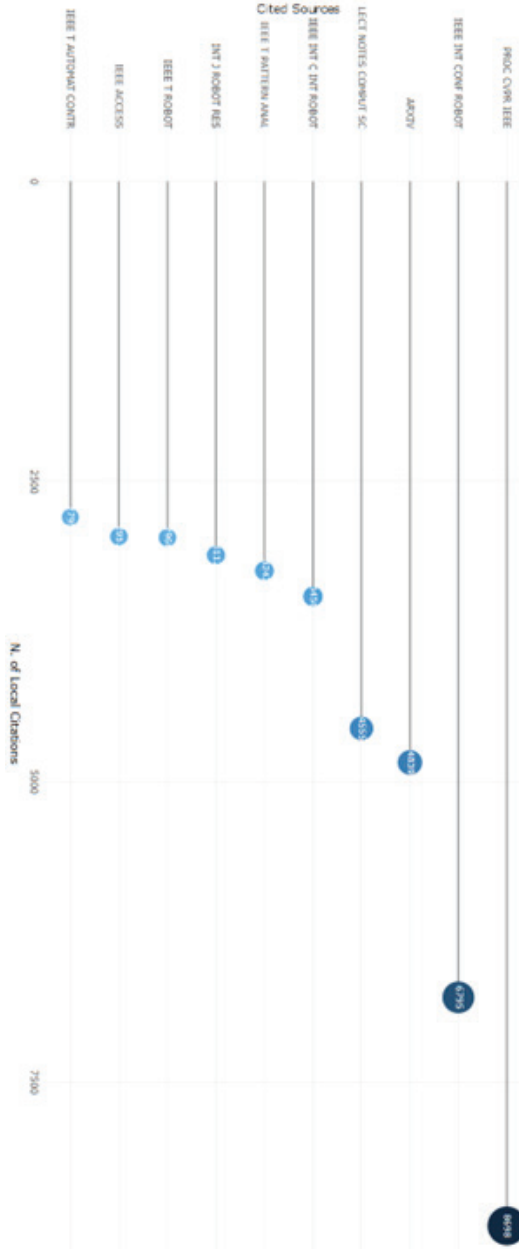


Figure 5. Most Local Cited Sources

Below are the Top 10 Most Globally Cited Papers, with Brooks RA ranked first with 2143 citations, followed by Pratta GA with 1350 citations and Hamet P with 1026 citations (Figure 6).

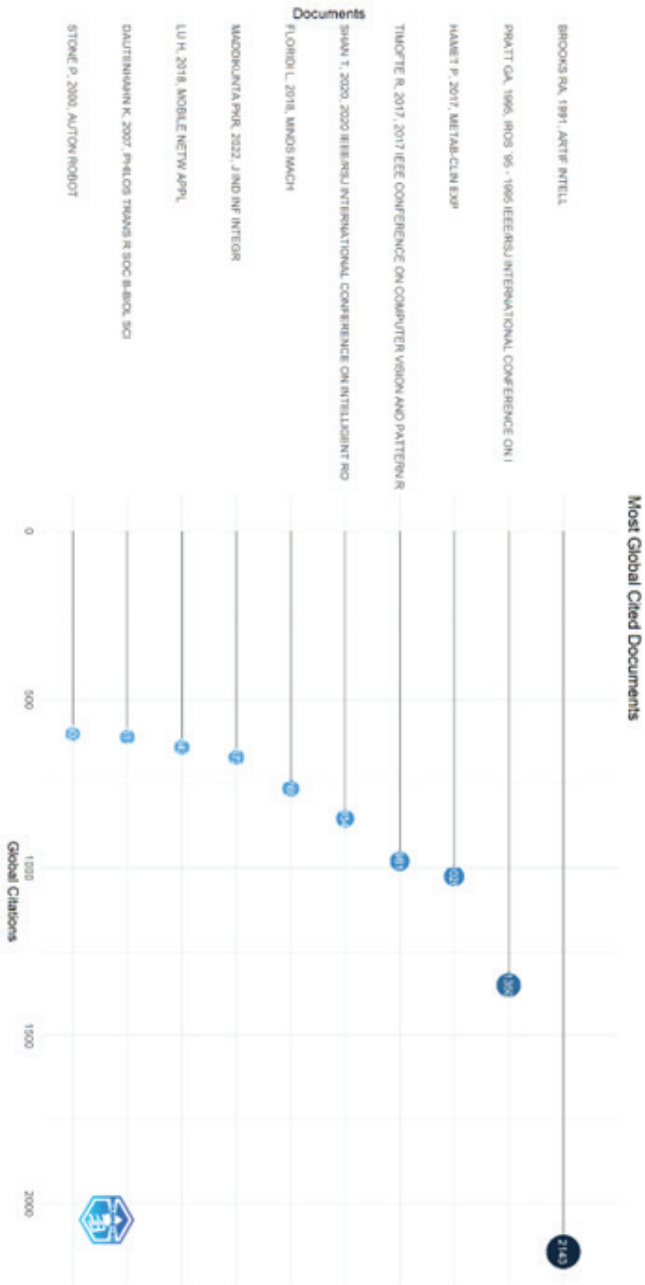


Figure 6. The top 10 documents with the most globally cited publications on the subject.

In publications where Artificial Intelligence is used in the field of robotics, the countries of the authors responsible for the correspondence and how these countries are distributed between single country publications (SCP - Single Country Publications) and multi-country publications (MCP - Multi-Country Publications) are given in Figure 7.

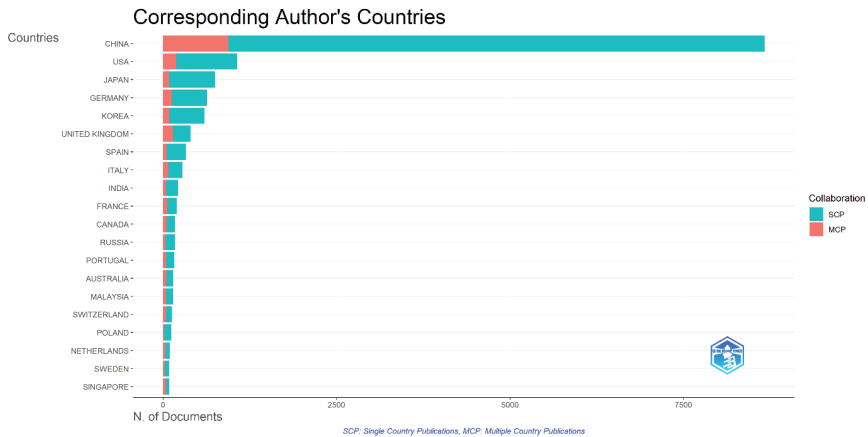


Figure 7. Countries of corresponding authors

China has the largest number of publications in this field. Authors in China are leaders not only in single country contributions but also in multi-country collaborations. The vast majority of publications from China are single country contributions. These show that China plays a leading role in research in this field and has a wide network of international collaborations. Following China, the USA and Japan also have a significant number of publications in this field. While the USA has focused more on single country publications, Japan has played a more active role in international collaboration. This suggests that both countries have made significant contributions to research in this field, but have pursued different strategies in terms of collaborations. Germany and Korea also have a significant number of publications in this field. Both countries have a significant number of publications in SCP, indicating that they are both active in national research. The United Kingdom and Italy are more prominent in multi-country publications (MCP), emphasizing the importance they attach to international collaborations. These countries seem to be integrated into international scientific networks and make global contributions in this field. The other countries on the list appear to be prominent in a similar number of multi-country publications (MCP). Here, Figure 8 shows the word cloud and Figure 12 shows the treemap. Figure 8, in Figure 9 a) and Figure 9 b), shows the keywords used by the



Figure 9. Treemap for the top a) 20 and b) 50 keywords.

Among the top 20 keywords, “Design” has a share of 14% and “System” has a share of 9%. “Model” and ‘Systems’ have a similar share of 8%. This shows that these terms are the most frequently used keywords in the research literature and that the relationship between the Artificial Intelligence method in the field of Robotics is the most focused topic in the studies. “Design” and ‘System’ are keywords with a share of 10% and 6% respectively. Similarly, “Model” and “Systems” have a share of 5%. This shows that these terms are the most frequently used keywords in the research literature and the most focused topic in studies on the use of Artificial Intelligence in robotics. In the Collaboration network in academic studies menu, we can see the network of collaboration in scientific journal writing. As we know, most of the authors of scientific journals are academics or professionals. Therefore, this collaboration is a place for authors to conduct studies or work for agencies or companies to establish good collaborative relationships. This development has been able to create a network when there is a relationship between the author and other authors and thus they become co-authors (Figure 10) and Co-occurrence Network (Figure 11) can be presented. Thus from the social structure can be derived the exchange of ideas and knowledge in the development of journal publication writing depicted in the world collaboration map (Figure 12).

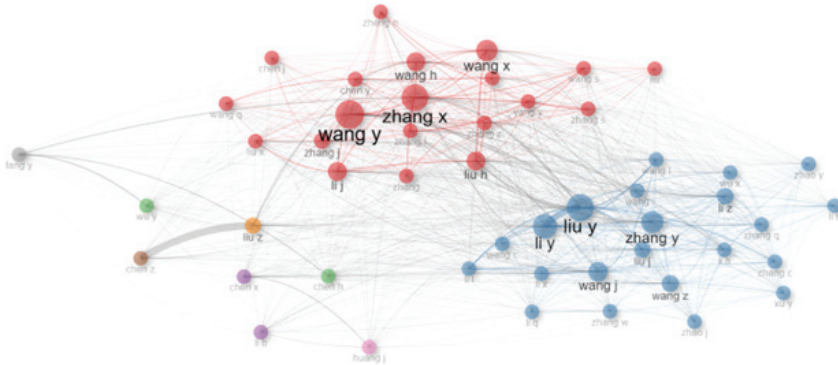


Figure 10. *Collaboration Network Author*

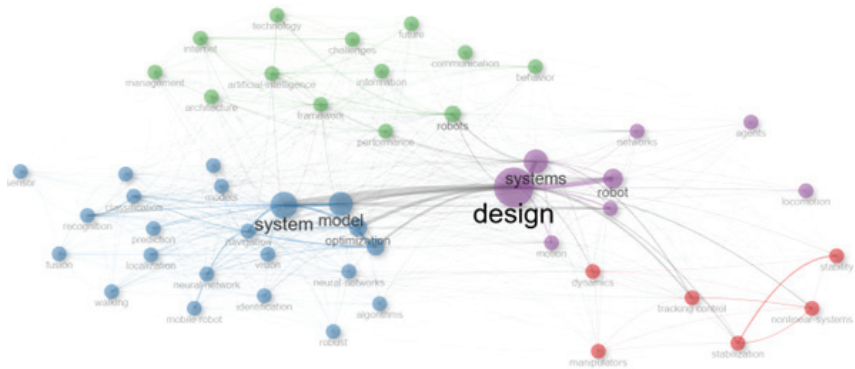


Figure 11 Co-occurrence Network

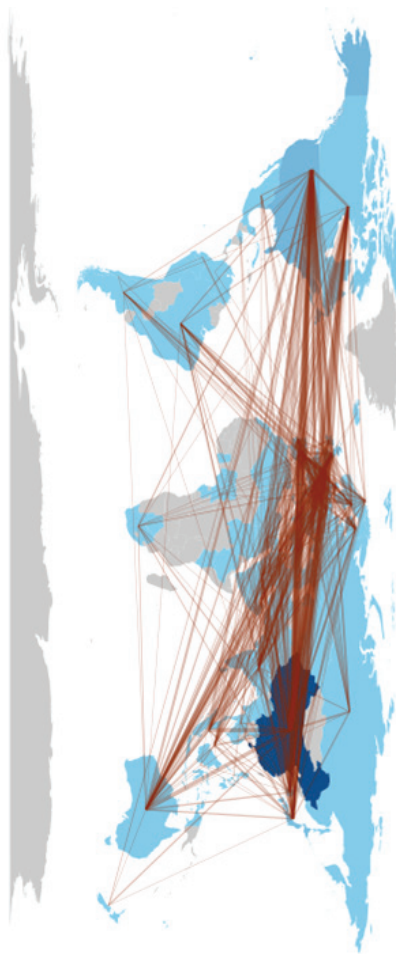


Figure 12. Collaboration world map

The results of this study extend to developers of the use of artificial intelligence in robotics and offer insights into competitors and emerging trends. The paper's bibliometric approach fills knowledge gaps, providing valuable insights to practitioners and researchers and facilitating innovation.

Conclusions

In this study, a bibliometric analysis of scientific publications using Artificial Intelligence methods in the field of Robotics was conducted. There is a significant gap in the literature regarding the historical study of this field using bibliometric methodologies. This research presents a new methodology that uses the Web of Science (WOS) database to analyze key dimensions, which are then integrated into bibliometric.org tools. The graph of annual scientific production shows a significant increase in the number of articles published in this field since the 1980s. Looking at the study production by year, it is shown that, in general, the number of articles over the years reached a peak in 2008. In particular, the "World Congress on Intelligent Control" conference stands out as the conference with the highest number of papers in this field and seems to be the focal point in this field. "Wang Y" emerged as the most prolific author and produced the most publications. In terms of most locally cited sources, the "Proceedings CVPR IEEE" conference was the most locally cited work. The findings of the study show the important position of China in research on the use of artificial intelligence in robotics, followed by the USA and Japan. Collaboration networks across countries reveal the global nature of research on the use of artificial intelligence in robotics. Keyword analysis and thematic maps show how the relationship to the use of artificial intelligence in robotics has evolved over time and which themes are prominent. "Design" and 'System' are among the most used keywords and these two concepts play a central role in the research. In conclusion, this bibliometric analysis shows that research on the use of artificial intelligence in robotics studies covers a wide range of topics and that knowledge in this field is enriched by international collaborations. This study can encourage further strengthening of international collaborations, knowledge sharing and development of innovative solutions in this field. Using bibliometric analysis is a valuable tool for potential researchers to predict trends and develop the use of artificial intelligence in robotics studies. It has the potential to be an important guide for future studies.

References

- Abut, T., & Huseyinoglu, M. (2019). Modeling and optimal trajectory tracking control of wheeled a mobile robot. *Caucasian journal of science*, 6(2), 137-146.
- Abut, T., & Soyguder, S. (2019). Real-time control and application with self-tuning PID-type fuzzy adaptive controller of an inverted pendulum. *Industrial Robot: the international journal of robotics research and application*, 46(1), 159-170.
- Abut, T., & Soyguder, S. (2022). Optimal adaptive computed torque control for haptic-teleoperation system with uncertain dynamics. *Proceedings of the Institution of Mechanical Engineers, Part I: Journal of Systems and Control Engineering*, 236(4), 800-817.
- Akpuokwe, C. U., Adeniyi, A. O., & Bakare, S. S. (2024). Legal challenges of artificial intelligence and robotics: a comprehensive review. *Computer Science & IT Research Journal*, 5(3), 544-561.
- Aria, M., & Cuccurullo, C. (2017). bibliometrix: An R-tool for comprehensive science mapping analysis. *Journal of informetrics*, 11(4), 959-975.
- Ashrafian, H. (2015). Artificial intelligence and robot responsibilities: Innovating beyond rights. *Science and engineering ethics*, 21, 317-326.
- Asimov, I. (2004). *I, robot* (Vol. 1). Spectra.
- Bogue, R. (2014). The role of artificial intelligence in robotics. *Industrial Robot: An International Journal*, 41(2), 119-123.
- Borboni, A., Reddy, K. V. V., Elamvazuthi, I., AL-Quraishi, M. S., Natarajan, E., & Azhar Ali, S. S. (2023). The expanding role of artificial intelligence in collaborative robots for industrial applications: A systematic review of recent works. *Machines*, 11(1), 111.
- Brady, M. (1985). Artificial intelligence and robotics. *Artificial intelligence*, 26(1), 79-121.
- Brady, M., Gerhardt, L. A., & Davidson, H. F. (Eds.). (2012). *Robotics and artificial intelligence* (Vol. 11). Springer Science & Business Media.
- Chu, S. T., Hwang, G. J., & Tu, Y. F. (2022). Artificial intelligence-based robots in education: A systematic review of selected SSCI publications. *Computers and education: Artificial intelligence*, 3, 100091.
- Grischke, J., Johannsmeier, L., Eich, L., Griga, L., & Haddadin, S. (2020). Dentronics: Towards robotics and artificial intelligence in dentistry. *Dental Materials*, 36(6), 765-778.

- Jacobsen, S. C., Olivier, M., Smith, F. M., Knutti, D. F., Johnson, R. T., Colvin, G. E., & Scroggin, W. B. (2004). Research robots for applications in artificial intelligence, teleoperation and entertainment. *The International Journal of Robotics Research*, 23(4-5), 319-330.
- Kumar, D., & Meeden, L. (1998). A robot laboratory for teaching artificial intelligence. *ACM SIGCSE Bulletin*, 30(1), 341-344.
- Kunze, L., Hawes, N., Duckett, T., Hanheide, M., & Krajník, T. (2018). Artificial intelligence for long-term robot autonomy: A survey. *IEEE Robotics and Automation Letters*, 3(4), 4023-4030.
- Lewis, F., Abdallah, C., & Dawson, D. (1993). Control of robot. *Manipulators, Editorial Maxwell McMillan, Canada*, 25-36.
- Liang, C. J., Le, T. H., Ham, Y., Mantha, B. R., Cheng, M. H., & Lin, J. J. (2024). Ethics of artificial intelligence and robotics in the architecture, engineering, and construction industry. *Automation in Construction*, 162, 105369.
- Moglia, A., Georgiou, K., Georgiou, E., Satava, R. M., & Cuschieri, A. (2021). A systematic review on artificial intelligence in robot-assisted surgery. *International Journal of Surgery*, 95, 106151.
- Perez, J. A., Deligianni, F., Ravi, D., & Yang, G. Z. (2018). Artificial intelligence and robotics. *arXiv preprint arXiv:1803.10813*, 147, 2-44.
- Raj, M., & Seamans, R. (2019). Primer on artificial intelligence and robotics. *Journal of Organization Design*, 8(1), 11.
- Rampersad, G. (2020). Robot will take your job: Innovation for an era of artificial intelligence. *Journal of Business Research*, 116, 68-74.
- Ribeiro, J., Lima, R., Eckhardt, T., & Paiva, S. (2021). Robotic process automation and artificial intelligence in industry 4.0—a literature review. *Procedia Computer Science*, 181, 51-58.
- R Core Team. (2013). R: A language and environment for statistical computing. *Foundation for Statistical Computing, Vienna, Austria*.
- Sarker, S., Jamal, L., Ahmed, S. F., & Irtisam, N. (2021). Robotics and artificial intelligence in healthcare during COVID-19 pandemic: A systematic review. *Robotics and autonomous systems*, 146, 103902.
- Song, G., & Guo, S. (2006, December). Development of a novel tele-rehabilitation system. In *2006 IEEE International Conference on Robotics and Biomimetics* (pp. 785-789). IEEE.
- Soori, M., Arezoo, B., & Dastres, R. (2023). Artificial intelligence, machine learning and deep learning in advanced robotics, a review. *Cognitive Robotics*, 3, 54-70.

Yeung, A. W. K. (2023). A revisit to the specification of sub-datasets and corresponding coverage timespans when using Web of Science Core Collection. *Heliyon*, 9(11).

Zhang, C., Hallbeck, M. S., Salehinejad, H., & Thiels, C. (2024). The integration of artificial intelligence in robotic surgery: A narrative review. *Surgery*.

Chapter 5



THE EFFECTS OF USING GRAPHENE NANOFLUIDS AND ITS DERIVATIVES ON THERMAL PERFORMANCE IN HEAT EXCHANGER

Fatma OFLAZ¹

¹ Dr., Firat University, Orcid ID: 0000-0002-9636-5746

1. Introduction

Heat exchangers are devices that enable heat transfer between two fluids at different temperatures. These devices are widely used in various industries, such as energy production plants, chemical factories, and oil refineries. Traditional heat exchangers typically use single-phase fluids, which limit the thermal efficiency of the system. However, researchers have turned to nanofluid technology to improve the energy efficiency of these systems. This technology is highly promising for the miniaturization of heat exchangers and the improvement of energy efficiency (Sundar 2023). Traditional heat exchangers typically use single-phase fluids, such as water, oil, and ethylene glycol, as heat carriers. These fluids are limited in terms of thermal conductivity, which restricts heat transfer efficiency to a certain level (Ciloglu and Bolukbasi 2015). Single-phase fluids offer lower heat transfer efficiency, which may require larger heat exchanger surface areas or longer operating times. These factors lead to larger system sizes and higher energy consumption. This issue is particularly a significant limitation in energy-intensive industries, such as thermal power plants, chemical factories, and oil refineries. Making heat exchangers smaller and more efficient has the potential to save energy while also reducing costs. Miniaturized heat exchangers offer more compact designs, saving both space and materials. This contributes to lighter equipment and helps reduce overall system costs. However, innovative fluids with high thermal conductivity are needed to achieve these goals.

Nanofluids are fluids obtained by adding nanoscale particles (typically 1-100 nm in size) to base fluids such as water, oil, or ethylene glycol (Said et al. 2022). These particles can be metal oxides (Al_2O_3 , CuO), metals (copper, silver), carbon-based materials (graphene, carbon nanotubes), or hybrid components. Thanks to the nanoparticles, the thermal conductivity of the fluids significantly increases. This property of nanofluids can greatly enhance the thermal performance of heat exchangers. The contributions of using nanofluids in heat exchangers to energy efficiency can be summarized as follows:

The high thermal conductivity of nanoparticles enhances the heat transfer capability of the base fluid. This means faster heat transfer, enabling efficient heat exchange even with smaller surface areas (Modi, Patel, and Patel 2023).

Compared to single-phase fluids, nanofluids offer a higher heat-carrying capacity, meaning that more heat can be transferred by the fluid, resulting in a more efficient heat exchanger (Barai, Kumar, and Wankhade 2023).

Nanofluids increase the convective heat transfer coefficient by enhancing the molecular motion within the fluid (Apmann et al. 2022). This leads to better heat transfer and reduces the operating time of the heat exchanger.

Nanofluids can be effective even at very low nanoparticle concentrations (Bacha et al. 2024). This increases system efficiency while limiting the amount of material used, thus controlling costs.

Thanks to the high efficiency provided by nanofluids, heat exchangers can be produced in smaller sizes, which is a significant advantage, particularly in applications with limited space. The use of nanofluids reduces energy consumption due to more efficient heat transfer, providing energy savings, especially in cooling and heating systems. In addition to these advantages, nanofluids also have challenges and disadvantages such as the cost of production, the expense of the nanoparticles used, the difficulty in maintaining long-term stability, and the fact that constant contact with surfaces can lead to wear and tear on equipment over time.

2. Properties of Graphene Nanofluids

Graphene (Gr) is a two-dimensional structure composed of a single layer of carbon atoms arranged in a hexagonal lattice. Each carbon atom is bonded to three other carbon atoms, forming a honeycomb pattern. This structure gives graphene its unique mechanical, thermal, and electrical properties. Graphene and its derivatives exist in various forms as a result of different production processes and chemical modifications. Common graphene derivatives such as graphene, graphene oxide (GrO), reduced graphene oxide (rGrO) and Gr quantum dots have distinct differences in their properties and are used in a variety of applications (Elsaid et al. 2021). Figure 1 shows the structure of Gr, GrO, rGrO and Gr quantum dots.

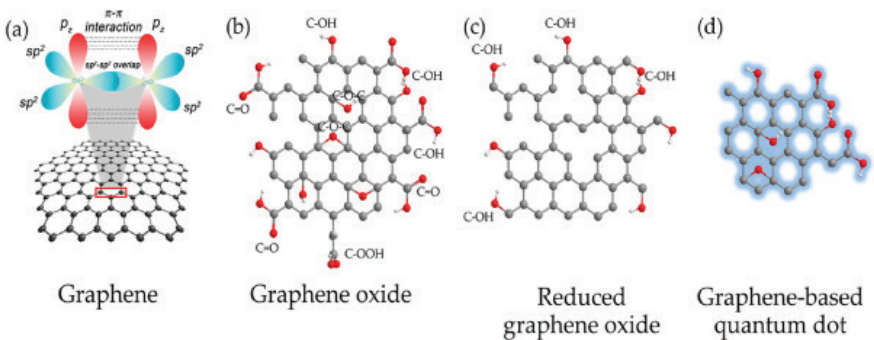


Fig. 1. Structure of Graphene and its derivatives (Elsaid et al. 2021)

Different graphene derivatives are produced using various synthesis methods. In this context, two main approaches are used in the synthesis of graphene and other nanomaterials: bottom-up and top-down approaches. Both methods allow for the production of graphene and its derivatives in different qualities and quantities, depending on the application. Bottom-up methods are suitable for producing purer and thinner graphene, while top-down methods produce larger quantities but generally result in multi-layered graphene (Pavia et al. 2021).

2.1. Preparation methods of nanofluids

The preparation of nanofluids can be classified similarly to nanofluids in general, using either one-step methods or two-step methods. Each approach has its specific processes and advantages. Figure 2 represents these two distinct techniques utilized in nanofluid preparation. The one-step method for preparing nanofluids involves the simultaneous synthesis and dispersion of nanoparticles in base fluids, which can include various techniques such as liquid and vapor chemical deposition. This approach minimizes issues related to drying, storage, transportation, and dispersion, thereby enhancing nanoparticle stability and reducing agglomeration (Arshad et al. 2019). The advantages of the one-step method include the production of evenly distributed nanoparticles, which leads to improved suspension stability in base fluids. Additionally, the elimination of multiple processing steps results in reduced production costs. However, the disadvantages of the one-step method include the possibility of incomplete chemical reactions, which can leave residual reactants in the nanofluid, potentially affecting performance. Moreover, achieving effective large-scale synthesis using one-step methods can be complex (Wei et al. 2009). The most widely used method for synthesizing nanofluids is the two-step method. This method utilizes various nanomaterials such as nanoparticles, nanofibers, nanorods, nanowires, nanosheets, nanotubes, and droplets. In the first step, the dry powder of these nanomaterials is prepared.

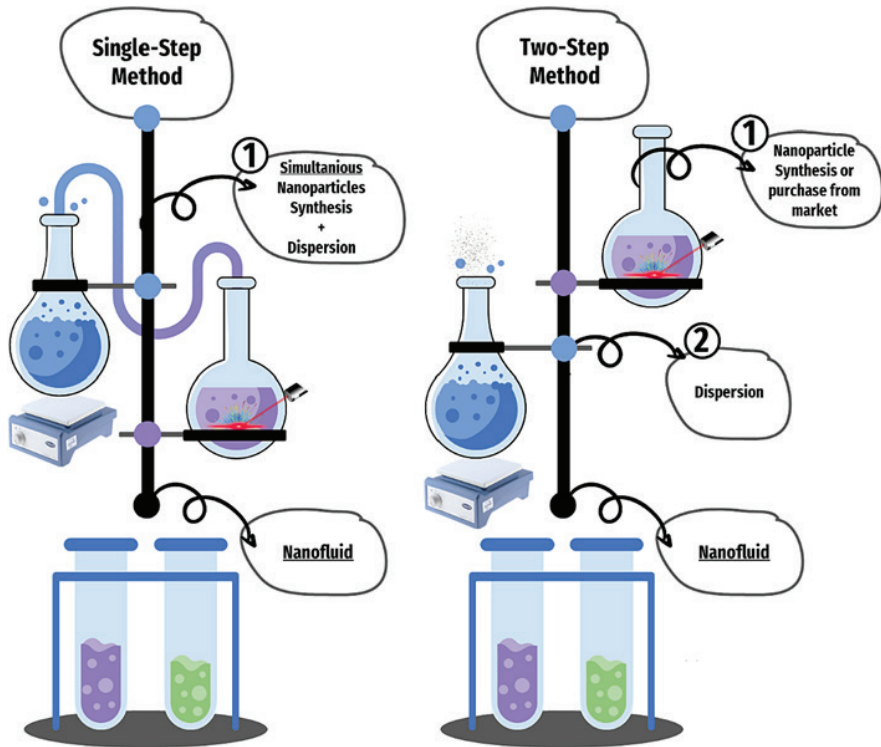


Fig. 2. Nanofluid Preparation Methods a) Single-step method, b) Two-step method (Babar et al. 2024)

The powder is reduced to nanoscale using mechanical and chemical methods, such as milling, sol-gel method, or vapor phase techniques. In the second step, this nanosized powder is mixed with a carrier fluid such as water, ethylene glycol, or oil. This mixing process is carried out using techniques like ultrasonic vibrations, magnetic force stirring, high-shear mixing, homogenization, and ball milling. Constant stirring at this stage helps reduce agglomeration, a common issue in the synthesis of nanofluids, where particles tend to clump together (Wang and Mujumdar 2008).

2.2. Thermal conductivity of nanofluids

The increase in thermal conductivity of nanofluids can be attributed to two key factors: Brownian motion and liquid layering at the liquid-particle interface. In Brownian Motion nanoparticles suspended in a fluid undergo random, erratic motion due to collisions with the molecules of the surrounding fluid. This phenomenon is known as Brownian motion. As nanoparticles move and collide within the fluid, they help transfer energy (in the form of heat) more effectively. This energy exchange enhances

the overall thermal conductivity of the nanofluid (Dhar et al. 2013; P. Keblinski, S.R. Phillpot, S.U.S. Choi 2002). The degree of Brownian motion increases with decreasing particle size and higher temperatures, both of which contribute to better heat transfer in nanofluids. In Liquid Layering at Liquid-Particle Interface; At the boundary between the solid nanoparticles and the surrounding fluid, a layer of liquid molecules forms that behaves differently from the bulk fluid. This is known as liquid layering. This liquid layer has a more ordered, structured arrangement of molecules compared to the rest of the fluid. This ordered layer conducts heat more efficiently than the disordered bulk fluid (Keblinski, Eastman, and Cahill 2005). The interaction between the liquid molecules and the surface of the nanoparticle enhances heat transfer across the interface, contributing to the increased thermal conductivity of the nanofluids. Together, these two mechanisms—Brownian motion and liquid layering—allow nanofluids to exhibit enhanced thermal conductivity compared to conventional fluids. In addition to this, several parameters significantly affect the thermal conductivity of nanofluids. These factors influence how efficiently heat is transferred within the fluid. Key parameters include nanoparticle concentration, nanoparticle size, nanoparticle shape, base fluid properties, temperature, pH and stability, nanoparticle material, ultrasonic and mechanical stirring, time and aging. Figure 3 shows the thermal conductivity change of graphene-based nanofluids compared to other nanofluids at different volume concentrations. The graph shows that even a very small volume concentration of Graphene exhibits a significant increase in thermal conductivity. Also, the effects of the base liquid on thermal conductivity are shown in Figure 3.

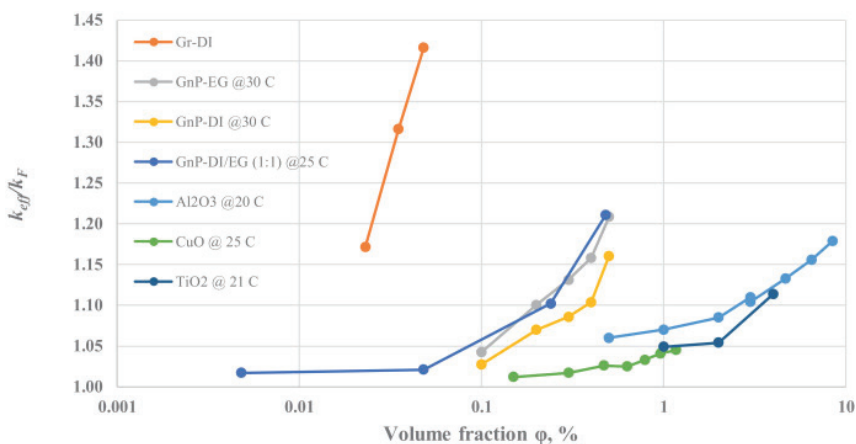


Fig.3. Thermal conductivity change of graphene-based nanofluids compared to other nanofluids at different volume concentrations (Elsaid et al. 2021).

Commonly used thermal conductivity equations for nanofluids are given in the following equations (1), (2), (3).

The Maxwell model (Xu, Gao, and Kang 2016) given in Equation 1 can be applicable for dilute concentration (low nanoparticle fraction) nanofluids. This model predicts the thermal conductivity of the nanofluid based on the thermal conductivities of the nanoparticles and the base fluid.

$$k_{nf} = k_{bf} \left(\frac{k_{np} + 2k_{bf} + 2\varphi(k_{np} - k_{bf})}{k_{np} + 2k_{bf} - \varphi(k_{np} - k_{bf})} \right) \quad (1)$$

Where: k_{nf} : Thermal conductivity of the nanofluid, k_{bf} : Thermal conductivity of the base fluid, k_{np} : Thermal conductivity of the nanoparticles, φ : Volume fraction of the nanoparticles.

The Bruggeman model (Wang, Zhou, and Peng 2003) given in Equation 2 can be applied to mixtures with higher concentrations of nanoparticles. This model is based on the symmetrical distribution of nanoparticles within the base fluid.

$$\varphi \cdot \frac{k_{np} - k_{nf}}{k_{np} + 2k_{nf}} + (1 - \varphi) \cdot \frac{k_{bf} - k_{nf}}{k_{bf} + 2k_{nf}} = 0 \quad (2)$$

The Hamilton-Crosser model given in Equation 3 was developed to predict thermal conductivity by taking into account the shape of the nanoparticles. This model is particularly used for non-spherical nanoparticles.

$$k_{nf} = k_{bf} \left(\frac{k_{np} + (n-1)k_{bf} + (n-1)\varphi(k_{np} - k_{bf})}{k_{np} + (n-1)k_{bf} - \varphi(k_{np} - k_{bf})} \right) \quad (3)$$

Where: n : Shape factor of the nanoparticles ($n = 3$ for spherical particles, higher values for non-spherical particles),

$k_{nf}, k_{bf}, k_{np}, \varphi$: Same as in Maxwell's equation.

2.3. Viscosity of nanofluids

The viscosity of nanofluids is a critical parameter for both fluid dynamics and heat transfer. Viscosity expresses a fluid's resistance to flow. One of the key parameters affecting the viscosity of nanofluids is temperature. Temperature has a significant effect on the viscosity of

nanofluids. As temperature increases, the kinetic energy of the fluid rises, which enhances fluidity and leads to a decrease in viscosity. This condition can improve the heat transfer performance of nanofluids (Mena et al. 2013). However, the physical properties of nanoparticulates can also change with temperature, which can affect viscosity. Viscosity is directly related to pressure drop and pumping power. A nanofluid with high viscosity requires more energy to be pumped, which affects energy efficiency (Gaganpreet and Srivastava 2012). Therefore, optimizing viscosity is crucial for reducing energy consumption while enhancing heat transfer performance. Additionally, the viscosity of the base fluid (such as water or oil) is an important parameter that determines the effect of nanoparticulates on viscosity. Nanoparticulates can increase or decrease the viscosity of the base fluid. Furthermore, the volume fraction of nanoparticulates in the fluid is one of the most significant factors influencing viscosity. Generally, as the volume fraction of nanoparticulates increases, viscosity also tends to increase. The size of the nanoparticulates has a significant effect on viscosity. Larger particles offer more resistance to the flow of the fluid, while smaller particles generally provide less resistance. Different types of nanoparticulates (such as metals, metal oxides, and carbon nanotubes) possess varying physical and chemical properties, making them important factors affecting viscosity (Arshad et al. 2019). Commonly used Viscosity equations for nanofluids are given in the following equations (4), (5), (6).

Einstein's equation (4) is one of the earliest models used to estimate the viscosity of dilute suspensions. It assumes that the suspended particles are spherical, rigid, and uniformly distributed in the base fluid. This equation is valid for low nanoparticle volume fractions ($\varphi < 0.02$).

$$\mu_{nf} = \mu_{bf} (1 + 2.5\varphi) \quad (4)$$

Where: μ_{nf} : Viscosity of the nanofluid, μ_{bf} : Viscosity of the base fluid, φ : Volume fraction of the nanoparticles.

Batchelor extended Einstein's equation to account for higher particle concentrations. It includes a second-order term to capture the effects of particle-particle interactions in suspensions with moderate nanoparticle volume fractions. This model, given in equation (5) is more accurate for nanofluids with slightly higher nanoparticle concentrations than Einstein's model.

$$\mu_{nf} = \mu_{bf} (1 + 2.5\varphi + 6.2 \varphi^2) \quad (5)$$

Brinkman's model given in equation (6) further extends the Einstein equation to predict the viscosity of nanofluids with relatively higher nanoparticle concentrations. It is especially useful for volume fractions of nanoparticles up to 30%.

$$\mu_{nf} = \mu_{bf} \left(\frac{1}{(1-\varphi)^2} \right) \quad (6)$$

This equation accounts for the increased resistance to flow caused by the increased concentration of nanoparticles.

2.4. Density of nanofluids

The density of nanofluids is critically important for fluid dynamics and heat transfer. Density is directly related to Reynolds number, friction factor, pressure drop, and Nusselt number (Babar et al. 2024). It expresses the amount of mass in a unit volume and is generally considered a fundamental parameter that affects the flow and heat transfer properties of fluids. Density influences the Reynolds number, determining whether the flow is laminar or turbulent. An increase in density can lead to a decrease in the Reynolds number, potentially causing the flow to become turbulent. An increase in density can also affect the friction factor, altering the interaction of the fluid with the surface. Typically, higher-density nanofluids exhibit an increase in the friction factor, while lower-density fluids may show a decrease. Additionally, an increase in density can raise pressure drop, impacting energy consumption, which is a crucial factor to consider in pump and system design. Furthermore, an increase in density can generally influence the Nusselt number, enhancing heat transfer performance. High-density nanofluids are expected to contain more nanoparticulates that enhance heat transfer, leading to an increase in the Nusselt number. The density of nanofluids were calculated through equations (7) created by Pak and Cho (Pak and Cho 1998).

$$\rho_{nf} = \varphi \rho_p + (1 - \varphi) \rho_f \quad (7)$$

2.5. Specific heat of nanofluids

The specific heat of nanofluids (NF) plays a significant role as an important thermal property, indicating how much heat can be absorbed or released per unit temperature change. Especially for nanofluids used as

Heat Transfer Fluids (HTF), specific heat directly affects the performance of the fluid. Increasing the heat carrying capacity of an HTF is directly related to its high specific heat. A higher specific heat allows more heat to be transferred, thus enhancing the cooling or heating capacity of the fluid. The addition of nanoparticles (NP) to a base fluid (BF) generally leads to a decrease in the specific heat capacity of nanofluids (NF). This is because the specific heat capacity of base fluids, such as water or ethylene glycol, is much higher than that of nanoparticles. Water has a specific heat capacity of approximately 4.18 J/g·K, while ethylene glycol has a specific heat capacity of about 2.35 J/g·K. In contrast, graphene's specific heat ranges from 0.643 to 2.10 J/g·K, which is significantly lower than that of water and ethylene glycol (Cardellini et al. 2016; Krishna et al. 2020). When nanoparticles are added to the base fluid, the nanofluid's overall specific heat capacity is a combination of the specific heat of the base fluid and the nanoparticles. Since the specific heat of nanoparticles is lower, the total specific heat capacity decreases. There are two commonly used specific heat models to determine the specific heat of nanofluids:

✓ **Classical Mixture Rule**

This model assumes that the specific heat of a nanofluid is the weighted average of the specific heats of the base fluid and the nanoparticles. In other words, the specific heat of the nanofluid depends on the mass fractions of the base fluid and the nanoparticles. The equation (8) (Ofiaz, Keklikcioglu, and Ozceyhan 2022) is expressed as:

$$c_{p,nf} = (1 - \varphi) \cdot c_{p,bf} + \varphi \cdot c_{p,np} \quad (8)$$

Where: $c_{p,nf}$: Specific heat of the nanofluid, φ : Volume fraction of the nanoparticles, $c_{p,bf}$: Specific heat of the base fluid, $c_{p,np}$: Specific heat of the nanoparticles.

This equation shows that the specific heat of the nanofluid is the sum of the mass contributions of the base fluid and the nanoparticles. However, this model is a simplified approach and may not fully account for complex interactions within the nanofluid.

✓ **Hamilton-Crosser Model**

The Hamilton-Crosser model expands on the classical mixture rule and places more emphasis on the thermal conductivity properties of the nanoparticles. This model also considers the effects of the shape and distribution of the nanoparticles on heat transfer in the nanofluid. The specific heat formula is expressed as (Ofiaz et al. 2022):

$$c_{p,nf} = (1 - \varphi) \cdot c_{p,bf} + \varphi \cdot \left(\frac{\rho_{np} c_{p,np}}{\rho_{bf}} \right) \quad (9)$$

Where: ρ_{np} : Density of the nanoparticles, ρ_{bf} : Density of the base fluid.

The Hamilton-Crosser model aims to more accurately predict the effect of nanoparticle concentration on specific heat. Since it accounts for the density of the nanoparticles, this model may be more suitable for complex nanofluid systems. Both models can be used to calculate the specific heat of nanofluids, but while the classical mixture rule offers a simpler, more straightforward approach, the Hamilton-Crosser model allows for a more detailed analysis. The choice of model depends on the properties of the nanofluid and its intended application.

3. Applications of graphene nanofluids in heat exchangers

In the modern era, energy consumption and environmental pollution are becoming increasingly critical due to the increase in emissions from fuel usage and the rapid growth of the thermal and cooling industries. Particularly in industrial and energy production processes, traditional cooling and heat transfer methods are insufficient in terms of efficiency, leading to increased energy consumption and harmful emissions to the environment. This highlights the importance of optimizing production systems (Behrozifard et al. 2024). Nanofluids offer an effective solution to this problem. Nanofluids, which are fluids enriched with nanoparticles, can significantly improve heat transfer performance compared to traditional fluids. This can reduce energy consumption and allow systems to operate more efficiently. The development of nanofluids has the potential to enhance the thermal conductivity of fluids used in both cooling and heat transfer systems, enabling greater cooling or heating with less energy. Therefore, the application of nanofluids presents a great opportunity for optimizing thermal management systems. This application can increase energy efficiency while reducing emissions, contributing to the prevention of environmental pollution and supporting the goal of sustainable energy use. Graphene nanofluids have become a preferred option in heat exchangers to enhance energy efficiency and performance due to their thermal properties. They can be used in both next-generation and existing systems, offering a revolutionary advancement in thermal management. Xian et al. studied how a surface activator impacted the stability of a GO-TiO₂ hybrid in an ethylene glycol-water fluid. They examined weight concentrations ranging from 0.025% to 0.1% and temperatures between 30°C and 70°C. The findings revealed that the activator choice affected the zeta potential, while the higher concentrations led to increased thermal

conductivity and viscosity compared to the base fluid. Additionally, they observed that thermal conductivity improved as the temperature increased (Xian, Sidik, and Saidur 2020). Zolfalizadeh et al. examined how different concentrations of graphene-water nanosheets affected heat exchanger performance. They found that the most significant improvements in heat transfer coefficient, efficiency, and rate occurred at a concentration of 0.06% by weight, with increases of 22.47%, 8.88%, and 15.65%, respectively, compared to the base fluid. However, as the flow rate and concentration of the nanofluid increased, there was a noticeable rise in pressure drop within the system. Naddaf (Naddaf and Zeinali Heris 2018) explored the effects of combining carbon nanotubes and graphene on the thermophysical properties of nanofluids, with particular attention to changes in the base fluid. Their research examined how the design of the heat exchanger and its plates impacted heat transfer, pressure drop, and the efficiency of the nanofluid. Additionally, they assessed how these factors influenced the overall performance of the heat exchanger system. Selvam (Selvam, Mohan Lal, and Harish 2017) examined the convective heat transfer and pressure drop of graphene nanoplatelet nanofluids in a water-ethylene glycol mixture flowing through an automobile radiator. Graphene nanoplatelet volume concentrations ranged from 0.1% to 0.5%, and the mass flow rate varied between 10 g/s and 100 g/s. Results showed that the convective heat transfer coefficient increased with higher nanoplatelet concentrations, inlet temperature, and mass flow rate. However, they found that pressure drop also increased with nanoplatelet loading and flow rate.

4. Conclusions

The use of graphene nanofluids in heat exchangers presents the potential for energy savings due to their superior thermal conductivity, making them a highly active area of research. Graphene nanofluids provide more efficient energy transfer compared to traditional cooling and heat transfer fluids, which enhances system performance while reducing energy consumption. For this technology to be adopted more widely, both the formulation of graphene nanofluids and the design of heat exchangers need to be further developed and optimized. For instance, research can focus on the size, density, and distribution of graphene particles to achieve greater stability, lower viscosity, and more efficient heat transfer in nanofluids. Additionally, heat exchanger designs can be improved to better accommodate the flow characteristics of graphene nanofluids, further boosting system efficiency. These advancements will help reduce energy costs in industrial and commercial applications, contributing to the adoption of more eco-friendly and sustainable solutions.

References

- Apmann, Kevin, Ryan Fulmer, Branden Scherer, Sawyer Good, Jake Wohld, and Saeid Vafaei. 2022. "Nanofluid Heat Transfer: Enhancement of the Heat Transfer Coefficient inside Microchannels." *Nanomaterials* 12(4). doi: 10.3390/nano12040615.
- Arshad, Adeel, Mark Jabbal, Yuying Yan, and David Reay. 2019. *A Review on Graphene Based Nanofluids: Preparation, Characterization and Applications*. Vol. 279. Elsevier B.V.
- Babar, Hamza, Hongwei Wu, Wenbin Zhang, Tayyab Raza Shah, Daniel McCluskey, and Chao Zhou. 2024. "The Promise of Nanofluids: A Bibliometric Journey through Advanced Heat Transfer Fluids in Heat Exchanger Tubes." *Advances in Colloid and Interface Science* 325(December 2023):103112. doi: 10.1016/j.cis.2024.103112.
- Bacha, Habib Ben, Naeem Ullah, Aamir Hamid, and Nehad Ali Shah. 2024. "A Comprehensive Review on Nanofluids: Synthesis, Cutting-Edge Applications, and Future Prospects." *International Journal of Thermofluids* 22(November 2023):100595. doi: 10.1016/j.ijft.2024.100595.
- Barai, Rohinee, Devesh Kumar, and Atul Wankhade. 2023. "Heat Transfer Performance of Nanofluids in Heat Exchanger: A Review." *Journal of Thermal Engineering* 9(1):86–106. doi: 10.18186/thermal.1243398.
- Behrozifard, A., Hamid Reza Goshayeshi, Iman Zahmatkesh, Issa Chaer, Soheil Salahshour, and D. Toghraie. 2024. "Experimental Optimization of the Performance of a Plate Heat Exchanger with Graphene Oxide/Water and Al₂O₃/Water Nanofluids." *Case Studies in Thermal Engineering* 59(January):104525. doi: 10.1016/j.csite.2024.104525.
- Cardellini, Annalisa, Matteo Fasano, Masoud Bozorg Bigdeli, Eliodoro Chiavazzo, and Pietro Asinari. 2016. "Thermal Transport Phenomena in Nanoparticle Suspensions." *Journal of Physics Condensed Matter* 28(48). doi: 10.1088/0953-8984/28/48/483003.
- Ciloglu, Dogan, and Abdurrahim Bolukbasi. 2015. "A Comprehensive Review on Pool Boiling of Nanofluids." *Applied Thermal Engineering* 84:45–63. doi: 10.1016/j.applthermaleng.2015.03.063.
- Dhar, Purbarun, Soujit Sen Gupta, Saikat Chakraborty, Arvind Pattamatta, and Sarit K. Das. 2013. "The Role of Percolation and Sheet Dynamics during Heat Conduction in Poly-Dispersed Graphene Nanofluids." *Applied Physics Letters* 102(16):1–16. doi: 10.1063/1.4802998.
- Elsaid, Khaled, Mohammad Ali Abdelkareem, Hussein M. Maghrabie, Enas Taha Sayed, Tabbi Wilberforce, Ahmad Baroutaji, and A. G. Olabi.

2021. "Thermophysical Properties of Graphene-Based Nanofluids." *International Journal of Thermofluids* 10. doi: 10.1016/j.ijft.2021.100073.
- Gaganpreet, and Sunita Srivastava. 2012. "Effect of Aggregation on Thermal Conductivity and Viscosity of Nanofluids." *Applied Nanoscience* 2(3):325–31. doi: 10.1007/s13204-012-0082-z.
- Kebllinski, Pawel, Jeffrey A. Eastman, and David G. Cahill. 2005. "Nanofluids for Thermal Transport." *Materials Today* 8(6):36–44. doi: 10.1016/S1369-7021(05)70936-6.
- Krishna, Yathin, M. Faizal, R. Saidur, K. C. Ng, and Navid Aslfattahi. 2020. "State-of-the-Art Heat Transfer Fluids for Parabolic Trough Collector." *International Journal of Heat and Mass Transfer* 152. doi: 10.1016/j.ijheatmasstransfer.2020.119541.
- Mena, Jesús Betancourt, Anderson Antonio Ubices De Moraes, Yipsy Roque Benito, Gherhardt Ribatski, and José Alberto Reis Parise. 2013. "Extrapolation of Al₂O₃-Water Nanofluid Viscosity for Temperatures and Volume Concentrations beyond the Range of Validity of Existing Correlations." *Applied Thermal Engineering* 51(1–2):1092–97. doi: 10.1016/j.applthermaleng.2012.11.002.
- Modi, K. V., P. R. Patel, and S. K. Patel. 2023. "Applicability of Mono-Nanofluid and Hybrid-Nanofluid as a Technique to Improve the Performance of Solar Still: A Critical Review." *Journal of Cleaner Production* 387(November 2022):135875. doi: 10.1016/j.jclepro.2023.135875.
- Naddaf, Atiyeh, and Saeed Zeinali Heris. 2018. "Experimental Study on Thermal Conductivity and Electrical Conductivity of Diesel Oil-Based Nanofluids of Graphene Nanoplatelets and Carbon Nanotubes." *International Communications in Heat and Mass Transfer* 95(May):116–22. doi: 10.1016/j.icheatmasstransfer.2018.05.004.
- Oflaz, Fatma, Orhan Keklikcioglu, and Veysel Ozceyhan. 2022. "Investigating Thermal Performance of Combined Use of SiO₂-Water Nanofluid and Newly Designed Conical Wire Inserts." *Case Studies in Thermal Engineering* 38(August):102378. doi: 10.1016/j.csite.2022.102378.
- P. Kebllinski, S.R. Phillpot, S.U.S. Choi, J. A. Eastman. 2002. "Mechanisms of Heat Flow in Suspensions of Nano-Sized Particles (Nanofluids)." *International Journal of Heat and Mass Transfer* 45:855–63. doi: 10.1109/icosp.2004.1441590.
- Pak, Bock Choon, and Young I. Cho. 1998. "Hydrodynamic and Heat Transfer Study of Dispersed Fluids with Submicron Metallic Oxide Particles." *Experimental Heat Transfer* 11(2):151–70. doi: 10.1080/08916159808946559.
- Pavía, Mauricio, Khoder Alajami, Patrice Estellé, Alexandre Desforges, and Brigitte Vigolo. 2021. "A Critical Review on Thermal Conductivity

Enhancement of Graphene-Based Nanofluids.” *Advances in Colloid and Interface Science* 294. doi: 10.1016/j.cis.2021.102452.

- Said, Zafar, L. Syam Sundar, Arun Kumar Tiwari, Hafiz Muhammad Ali, Mohsen Sheikholeslami, Evangelos Bellos, and Hamza Babar. 2022. “Recent Advances on the Fundamental Physical Phenomena behind Stability, Dynamic Motion, Thermophysical Properties, Heat Transport, Applications, and Challenges of Nanofluids.” *Physics Reports* 946:1–94. doi: 10.1016/j.physrep.2021.07.002.
- Selvam, C., D. Mohan Lal, and Sivasankaran Harish. 2017. “Enhanced Heat Transfer Performance of an Automobile Radiator with Graphene Based Suspensions.” *Applied Thermal Engineering* 123:50–60. doi: 10.1016/j.applthermaleng.2017.05.076.
- Sundar, L. Syam. 2023. “Synthesis and Characterization of Hybrid Nanofluids and Their Usage in Different Heat Exchangers for an Improved Heat Transfer Rates: A Critical Review.” *Engineering Science and Technology, an International Journal* 44:101468. doi: 10.1016/j.jestch.2023.101468.
- Wang, Bu Xuan, Le Ping Zhou, and Xiao Feng Peng. 2003. “A Fractal Model for Predicting the Effective Thermal Conductivity of Liquid with Suspension of Nanoparticles.” *International Journal of Heat and Mass Transfer* 46(14):2665–72. doi: 10.1016/S0017-9310(03)00016-4.
- Wang, Xiang Qi, and Arun S. Mujumdar. 2008. “A Review on Nanofluids - Part II: Experiments and Applications.” *Brazilian Journal of Chemical Engineering* 25(4):631–48. doi: 10.1590/S0104-66322008000400002.
- Wei, Xiaohao, Haitao Zhu, Tiantian Kong, and Liqiu Wang. 2009. “Synthesis and Thermal Conductivity of Cu₂O Nanofluids.” *International Journal of Heat and Mass Transfer* 52(19–20):4371–74. doi: 10.1016/j.ijheatmasstransfer.2009.03.073.
- Xian, Hong Wei, Nor Azwadi Che Sidik, and R. Saidur. 2020. “Impact of Different Surfactants and Ultrasonication Time on the Stability and Thermophysical Properties of Hybrid Nanofluids.” *International Communications in Heat and Mass Transfer* 110(November 2019). doi: 10.1016/j.icheatmasstransfer.2019.104389.
- Xu, J. Z., B. Z. Gao, and F. Y. Kang. 2016. “A Reconstruction of Maxwell Model for Effective Thermal Conductivity of Composite Materials.” *Applied Thermal Engineering* 102:972–79. doi: 10.1016/j.applthermaleng.2016.03.155.
- Zolfalizadeh, Mehrdad, Saeed Zeinali Heris, Hadi Pourpasha, Mousa Mohammadpourfard, and Josua P. Meyer. 2023. “Experimental Investigation of the Effect of Graphene/Water Nanofluid on the Heat Transfer of a Shell-and-Tube Heat Exchanger.” *International Journal of Energy Research* 2023. doi: 10.1155/2023/3477673.

Chapter 6

WIND TURBINE DESIGNS AND NUMERICAL ANALYSES AT VERY LARGE POWERS¹

*Faruk KÖSE*²

*Mohamed DWEDAR*³

¹ This publication is derived from master's thesis entitled "Investigation of Different Blade Profiles for High-Capacity Wind Turbines by Cfd Method" conducted by Mohamed Dwedat, under the supervision of Prof. Dr. Faruk KÖSE, Konya Technical University, Institute of Graduate Studies, Department of Mechanical Engineering.

² Prof. Dr., Konya Technical University, Faculty of Engineering and Natural Sciences, Department of Mechanical Engineering Department, Konya/Türkiye, Orcid: 0000-0003-2171-9148, fkose@ktun.edu.tr

³ Mech. Engineer., Intelligent Cyber Physical Systems Institute (ICPS) University of Heilbronn/Germany, Orcid: 0009-0002-9490-837X, Mohamed.dwedat@hs-heilbronn.de

1. INTRODUCTION

As a result of the increasing use of fossil fuels, global warming caused by the greenhouse effect caused by the increase in carbon dioxide emissions in the atmosphere has become a threat to the ecological balance of the world. All these situations have increased the demand for renewable energy, especially wind and solar energy. While the developments in large wind turbines used in electricity generation with wind energy continue rapidly in the world, a domestic turbine with MW power has not yet been commercially produced in Turkey.

Recent scientific studies on turbine power have been carried out to design and manufacture wind turbines with 20, 25, and 50 MW power capacity. With the development of science and technology, the Computational Fluid Dynamics (CFD) method is used to obtain the lowest error rate in wind turbine analyses. With the 'blade element momentum' method, which is generally used in the blade design of turbines, the most commonly used different airfoils (such as NACA 2215, 4415, and LS(1)) are analyzed, and the lightest and most efficient ones are determined and used. At the end of the dynamic analysis, the forces acting on the blade in each different profile and the amount of energy generated from each different turbine are calculated.

In the example design and analysis, the mechanical design of the load, voltage, and lengths of the 50 MW turbine will be made using computational fluid dynamics. The possibility of manufacturing and installing 50 MW turbines will be investigated using CFD, and the annual amount of electrical energy that can be generated from the turbines will be calculated. On the other hand, the main turbine parts, such as the blades, hub, main shaft, cabin, and tower, will also be mechanically designed. The study will be a model to show that large turbines can be built after the complete design of each turbine and to determine the different loads from wind and part weight acting on the turbine parts.

The most commonly used nominal wind speed value for the nominal power value in the design of large commercial wind turbines is determined in the range of 10-14 m/s. At this wind speed, the turbine reaches maximum operating turbine and generator power. At nominal wind speed, the lift and drag forces acting on the blades and other turbine parts are calculated. These lift and drag forces are also calculated at 25 m/s, at which the turbine will be deactivated, and at 55 m/s, which is the maximum endurance wind speed.

As a sample design study, the turbine blades with the two most optimum profiles are to be determined for a nominal power of 50 MW, which may be possible in the coming years, and the main parts, such as

the hub, main shaft, casing, and tower, will be designed. In addition, the design of the turbine parts and the turbine system will be simulated by the CFD method in a suitable atmosphere, and flow and strength analyses will be performed. As a result of this, the design and main dimensions of the 50 MW power capacity turbine, which has not yet been produced under today's conditions, will be determined. In case these dimensions reach very large values, in order to reduce the dimensions, the use of materials with better properties, such as carbon fiber in blades and other turbine parts, should be investigated.

The CFD method is a highly accurate method used in many industrial applications to numerically determine the properties of liquid and gas flows, such as velocity and pressure. In wind energy applications, energy generation with turbines in an atmospheric flow environment is an application of CFD. Wind energy includes a large number of different values of the flow consisting of the aerodynamics of the turbine blades and the traces generated from the microclimate and atmospheric boundary layer weather conditions. Furthermore, the different values interact as atmospheric flows define wind conditions at the wind farm scale and further down to a turbine scale. CFD can be integrated with optimization algorithms in the search for optimal shape design or optimal control. Examples of model-based optimization include, for example, optimal design of blade geometry and micro-layout in complex terrain (Lalit, 2015).

CFD simulations for wind turbines focus on numerical simulations and model-based optimizations at the turbine scale. In the case study, it will be established as a research basis that it is easy to select suitable blades for wind turbines with large and medium loads in terms of efficiency, annual power generation amount, and wind loads on the blade and turbine. Geometry design for two or three different airfoils (such as NACA 2225, 4415, LS(1)) will be performed for comparison in turbine analyses. For each different turbine, the wind loads on it should be analyzed at different design wind speeds (11-14 m/s). By dynamic analysis of the turbine in motion, the blades that carry more wind load and are more efficient in wind energy production should be examined.

1.1. Wind Turbine Design Studies in the World and Turkey

Scientific studies in the literature on the design of wind turbines have been going on for about 1.5 centuries and have increased more in recent years with the increasing interest in renewable energy systems. While the studies on this subject were in the power sizes of 1-2 kW in the first years, today, power values of 20,000 kW have been exceeded.

Tong (2010) stated in his book that it will be useful as a resource for researchers and engineers working on the design of all main parts of small,

medium, and large wind turbines, such as blades, hubs, shafts, cabins, and towers. Cox and Andreas (2012) develop structural properties of a 70 m long blade on a downwind, horizontal-axis wind turbine in this paper for use in a high wind speed location. A hybrid composite structure using glass and carbon fiber layers was created, achieving a lightweight design with low tip deflection. Schubel and Crossley (2012) presented a detailed review of the current state-of-the-art for wind turbine blade design, including theoretical maximum efficiency, practical efficiency, horizontal-axis wind turbine blade design, and blade loads. A detailed review of aerodynamic design principles for a modern wind turbine blade, blade shape/quantity, profile selection and optimal angles of attack, aerodynamic, gravitational, centrifugal, gyroscopic, and operating conditions of design loads on the blades is presented. In their study, Lingling and Fan (2015) provide important information about the modelling, analysis, control, space vectors, complex vectors, and other frequency domain variables-based machine transducer modelling strategies of wind energy systems.

Rajakumar and Ravindran (2016) investigated different NACA airfoils at low wind turbine blade speeds and various angles of attack. They investigated the overall aerodynamic performance of profile NACA 6409 at various angles of attack. Aerodynamic parameters were found to be strongly influenced by Reynolds number and angle of attack. As a result, in the future, efforts will be made to design, develop, and install a large scope of low wind speed turbines in urban and rural locations at low power requirements. Lalit (2017) used ANSYS Fluent software for CFD analysis of the wind turbine blade and the static structure module for static analysis. He designed blade designs with S809 as a horizontal-axis wind turbine blade profile in different parameters and analyses of wind flow. Ananda et al. (2018) carried out the aerodynamic design of a 13.2 MW wind turbine blade in their study. Designing such large-scale turbines using conventional methods will result in a significant amount of technical obstacles. For example, at these scales, primary design limitations apply due to the large rotor weight and large rotor weight. loads on the blade due to the combination of gravity and aerodynamic loads, and extreme blade root diameters are required for robust structural performance in all wind conditions. Some of the other challenges are that such extreme powers (50 MW) will involve a blade length of about 200 m and very large rotor weight, high blade stiffness required to prevent blade impact with the tower, and increased energy cost in the construction and transportation of rotor blades due to the large blade size.

Corke and Nelson (2018) cover basic wind energy concepts, wind characteristics and modelling, rotor aerodynamics, lightweight flexible structures, wind farms, aerodynamics, wind turbine control, acoustics, energy storage, and economics.

These issues will be implemented to produce a new conceptual wind energy design that shows the interaction of various design aspects in a complete system. Mauro et al. (2019) showed the possibility of obtaining a reliable CFD 2D model of such micro rotors by modeling a micro wind turbine Eddy Simulation approach for turbulence modeling. The modeling methodology was developed through an accurate grid and time step sensitivity study and by comparing different approaches for turbulence closure. Subham et al. (2019) investigated various noise generation mechanisms in wind turbines and potential noise reduction techniques in their article. Special attention was given to reviewing the aerodynamic noise sources and recent developments in aerodynamic noise reduction. Many studies on the impact of wind turbine noise on human health have linked wind turbine noise to discomfort and sleep disturbance. Therefore, there is a need to reduce these noise emissions, which can be achieved by targeting specific noise sources.

Mansour and Rola (2020) numerically investigated the performance of the IceWind turbine in their publication. In the study, three-dimensional numerical simulations were performed for the full-scale model using the SST K- ω model at a wind speed of 15.8 m/s. As a result, the static torque, speed distributions and streamlines, and pressure distributions were compared with previous data. In their study, Sy et al. (2020) looked at the effect of wingtip devices, especially a split blade, to reduce the drag caused by wind vortices at the blade tip and thus improve performance. The split blade application was performed using CFD on the National Renewable Energy Laboratory (NREL) Phase VI array H. In total, the results for the four simulated blade configurations, an extended version of the previous blade, a base blade with blades, and a split-blade base blade at wind speeds between 7 m/s and 15 m/s, showed that adding a blade increased the power output by an average of 1.23%, while adding a split-blade increased the power output by 2.53% compared to the extended blade, while the cost increase was 0.83% and 2.05%, respectively. In their paper, Yao et al. (2021) presented a critical assessment of the technology pathways and challenges for a series of aero-structural blade designs and very large-scale rotors to demonstrate that a 50 MW wind turbine design is indeed feasible from a detailed engineering perspective. They started with Monte Carlo simulations focusing on optimizing the 50 MW turbine rotor design, carbon spar cover, and root design, and obtained a baseline design, a blade length of 250 m with a mass of 502 tons. Then, by determining the optimum chord and blade thickness for the best aerostructural performance, an aerostructural design and optimization were carried out to reduce the blade mass by more than 25% and its cost by more than 30%.

Papi et al. (2021) aimed to provide a descriptive procedure for a complete preliminary design process of the wind turbine to the scientific and industrial community. Secondly, a special focus was given to the arrangement methods, which are usually some of the critical points of a real design. Modern pitch arrangement strategies, the results of the selected case study showed how an increase of more than 12% in annual energy production can be achieved with a proper aerodynamic optimization combined with step-by-step arrangement according to a traditional approach. Carrero et al. (2022) compared 2D and 3D CFD modeling of wind turbine blades to identify reduced sequential patterns of worn leading edge arrangements. In particular, after an extensive validation campaign of the adopted numerical models, a first qualitative comparison is performed on 2D and 3D flow fields by looking at turbulent kinetic energy color maps. Promising similarities ultimately push the analysis to quantitative comparisons. Thus, the differences and commonalities between the pressure, drag coefficients, and polar diagrams of the 3D blade and the simplified eroded 2D setup are highlighted. The analysis reveals that the viscous properties of the system (i.e., pressure field and lift coefficients) are fully described by the reduced sequential 2D setup. On the other hand, inconsistencies in wall friction and drag coefficients are systematically observed. The 2D model consistently underestimates the drag contribution by about 17%, inducing flow separation over different downstream locations. However, the proposed 2D model is very accurate in dealing with the more important aerodynamic performance of the blade and is 30 times faster than the 3D evaluation in providing the same information. Therefore, the proposed 2D CFD setup is of fundamental importance for use in the digital twin of any physical wind turbine. The aim is to plan maintenance carefully and accurately, while also taking into account the leading edge erosion (Carrero et al., 2022).

In the research of Tarhan and Çil (2022), the aerodynamic performances of different airfoils used in wind turbines were simulated using Qblade software, and their numerical analyses were performed. The analyses were carried out at angles of attack between 0° and 20° and at Reynolds numbers of 5×10^4 , 2×10^5 , and 1×10^6 . As a result of the study, it was determined that NACA 6412, NACA 6415, and NACA 4415 airfoils had the highest aerodynamic efficiency, and a three-bladed wind turbine was created using these airfoils. The maximum efficiency was obtained for these airfoils in the tip-speed ratio range of 6.5 to 7.8. As a result, it was seen that the efficiency to be obtained from the turbine would be at the maximum level when NACA 6412, NACA 6415, and NACA 4415 airfoils were used in wind turbines. According to the results of this research, the NACA 4415 airfoil was considered a suitable choice, and this profile was used in the thesis study. In this study, Q-blade and ANSYS Fluent programs were used to

calculate different effects on large turbines. Each turbine was examined at different angles for the first profile types, NACA 4415 and NACA 2215. These two profile types were selected to break down the current market usage. Through this study, it was determined that different profile types are suitable for use in large turbines. For example, the NACA 4415 profile type is preferred to be used in places where people do not live, while the NACA 2215 profile type is preferred to be used in places near people due to its low noise level. However, the amount of energy obtained from the NACA 4415 profile type is higher compared to the NACA 2215 profile type.

A 16 MW offshore wind turbine with the lightest weight per megawatt made in China has a rotor diameter of 252 meters and a swept area of approximately 50,000 m², which is equivalent to about seven standard football fields. The hub height is 146 meters. Under nominal operating conditions, according to the annual average energy production design value, a single unit will be able to produce more than 66 million kWh of clean electricity per year (Richard, 2022). In 2024, the increases in terrestrial and offshore wind turbine powers continued, and in a news source dated October 10, 2024, it was reported that a 270 m diameter 15 MW wind turbine was built as a terrestrial turbine (Akpınar, 2024), and in the news dated October 15, the turbine designed as an offshore turbine has a blade diameter of 310 m, a hub height of 185 m, and a wind speed of 10 m/s with 26 MW power, and will be able to produce 100 GWh of electricity per year and meet the electricity needs of 55,000 homes. It will also reduce 30,000 tons of coal consumption and 80,000 tons of carbon dioxide emissions. It is stated that the turbine has a typhoon (hurricane) resistant structure (Çakmak, 2024).

2. DESIGN AND ANALYSIS OF VERY LARGE POWER (50 MW) WIND TURBINE

2.1. Design of 50 MW Wind Turbine

Wind turbines are designed according to the nominal power value. In the preliminary design, average values for mechanical and electrical losses are taken or neglected, and according to Betz's law, 48% can be taken as the maximum possible power coefficient from wind energy. Taking the air density as 1.225 kg/m³, the diameter of the rotor of the wind turbine is found to be 260 m from the power expression. As we have stated before, when the losses are neglected, it is seen that the loss rate actually increases up to 35%, and the total diameter of the rotor of the 50 MW turbine can reach 260 m. For this power, the loads on the wings should be calculated for NACA 4415 and NACA 2215 wing profiles; strength analysis and calculation of the amount of energy that can be produced annually in both cases should be done. In very large wind turbines, the turbine shaft rotation

speed should be taken as 0.2-0.8 rpm due to the very high centrifugal forces created by the large blade weights.

$$P_{WT} = 0.5 (\rho \times A_{WT} \times C_p \times V^3 \times \eta_d) \tag{2.1}$$

Therefore, in equation (2.1), the total mechanical and electrical losses (η_d) are calculated by taking 80% of the nominal power, the wind speed as 14 m/s, and the power coefficient (C_p) as 45%, and the total swept area is calculated as 70,000 m². The turbine blade length (approximate rotor radius) for a nominal power of 50 MW is found to be 157 m.

The height of a 50 MW wind turbine tower is taken as 301.4 m as a reference. The radius of the blade is designed as 157 m, and the diameter of the hub is 5 m. In contrast, when designing the blade, the blade consists of 24 parts, each approximately 7 m long. Using the blade element momentum method, the dimensions of the turbine blades will be as in Table 2.1 below. According to Table 2.1, in the same wing sections of NACA 4415 and NACA 2215 profiles, while the shell thicknesses and beam lengths have the same values, the slope degrees are different in many position lengths.

Table 2.1. NACA 4415 and NACA 2215 profiles blades values table of a 50 MW wind turbine

Location length [m]	Shell Thickness [mm] NACA 4415 and NACA 2215	Beam length [m] NACA 4415 and NACA 2215	Slope degree [degree] NACA 4415	Slope degree [degree] NACA 2215
0	240	12	30	20
6	300	12	30	20
12	282	15	39.17	29.17
18	265	14.12	39.17	29.17
24	257	13.112	39.17	29.17
30	256	12.312	41.89	38.89
36	236	12.418	47.66	37.66
42	232	11.377	46.93	36.93
47	228	10.684	46.20	36.20
52	214	9.236	45.47	45.47
58	199	9.679	44.74	44.74
64	184	8.095	44.01	44.01
70	170	7.525	33.28	43.28
76	156	7.043	32.55	42.55
82	143	7.643	31.82	31.82
88	130	6.517	31.22	31.22
96	120	5.6	30.73	30.73
104	112	5.601	30.11	30.11
110	103	5.317	30.05	30.05
116	101	5.984	30.04	30.04

122	98.1	5.754	30.0311	30.031
128	93.7	5.341	30.0211	30.021
134	89.2	5.211	30.013	30.013
146	80.1	4.99	30	30
152	76.00	4.678	30	30
157	66.11	4.012	30	30

Figure 2.1 shows the NACA 4415 profile blade and sections of a 50 MW wind turbine.

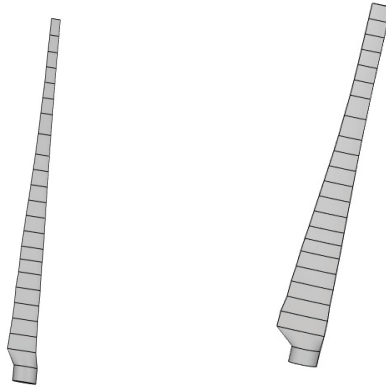


Figure 2.1. Sections of 50 MW wind turbine NACA 4415 profiled blade (swept area $71,127.67 \text{ m}^2$) (left) and NACA 2215 profiled blade (swept area $69,492 \text{ m}^2$) (right)

The behavior of the wind turbine will be analyzed at different wind speeds by taking the rotor rotation speed as 0.2 rpm for 50 MW turbine power, and the power graph of the turbine’s operating range for different wind speeds is given in Figure 2.2.

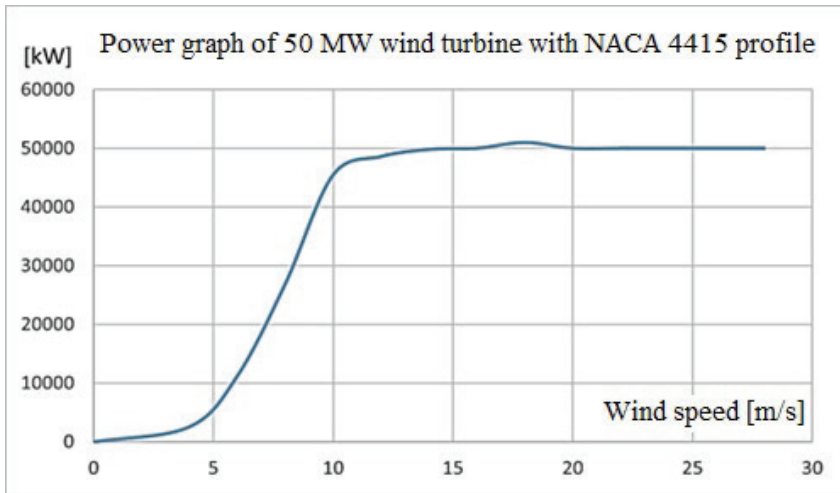


Figure 2.2. Turbine powers [kW] with 50 MW wind turbine NACA 4415 profiled blade

In Figure 2.2, the lowest power that can be obtained from the turbine at a wind speed of 4 m/s is shown as 180 kW. The amount of power that can be obtained increases as the wind speed increases.

2.2. Analysis of a 50 MW Wind Turbine With a NACA 4415 and NACA 2215 Profiled Blades

In Figure 2.3, during the analysis of the forces acting on different parts of the blade, it is analyzed that the most severe effect is in the section between 30-37 m. These parts should be reinforced with the necessary materials to prevent cracks and collapses. The least effective parts of the wing are on the sides, and the effect gradually increases as it moves away from the 33-37 m section where it is affected by the highest force effect. The height of the wind turbine tower is designed as 301.3 m, the rotor rotation speed is taken as 0.2-0.8 rpm, and the gravitational acceleration is taken as 9.81 m/s^2 per second. The maximum power coefficient that the turbine can reach at the beginning of the first operation is 1.1. The stability of the turbine is observed 30 seconds after it starts to work to stabilize it. The maximum power coefficient that can be reached after stabilization is 59%.

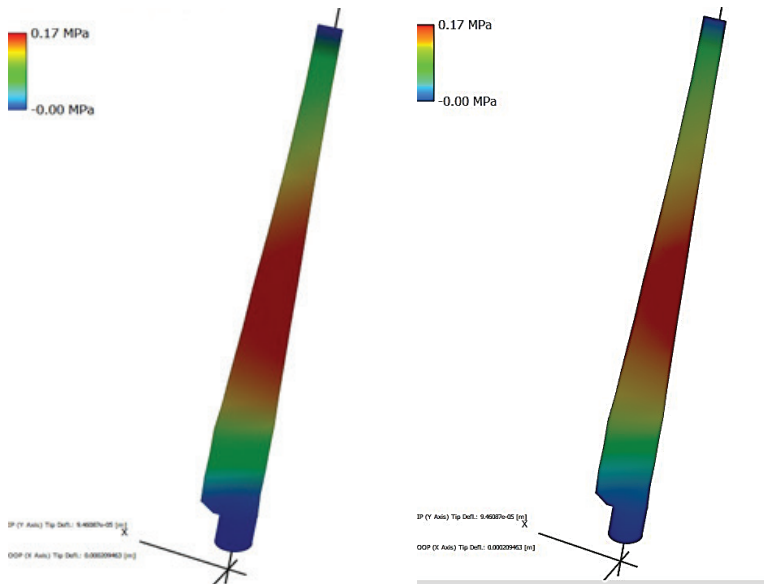


Figure 2.3. Strength analysis of 50 MW wind turbine blades with NACA 4415 profile (left) and NACA 2215 profile blades (right)

The beginning of the NACA 2215 profiled wing edge has the lowest pressure, because in this part there is a lot of supporting material, and also the profile section has not yet started. Gradually, the wing profile begins to scale, and starting from this area, the pressure on the wing parts increases. During the analysis of the forces acting on different parts of the wing, it is analyzed that the most severe effect is in the section between 30-36 m. These parts should be reinforced with the necessary materials to prevent cracks and collapses. The least effective parts of the wing are at the bottom, and the effect gradually increases as we move away from the section of 30-36 m, where it is affected by the highest force effect.

Figures 2.4 and 2.5 show the turbine simulation for an air density of 1.225 kg/m^3 . The wind speed is taken as 10 m/s in this simulation. The atmospheric pressure is taken as 100 kPa . Atmospheric pressure can vary from one place to another depending on the altitude above sea level.

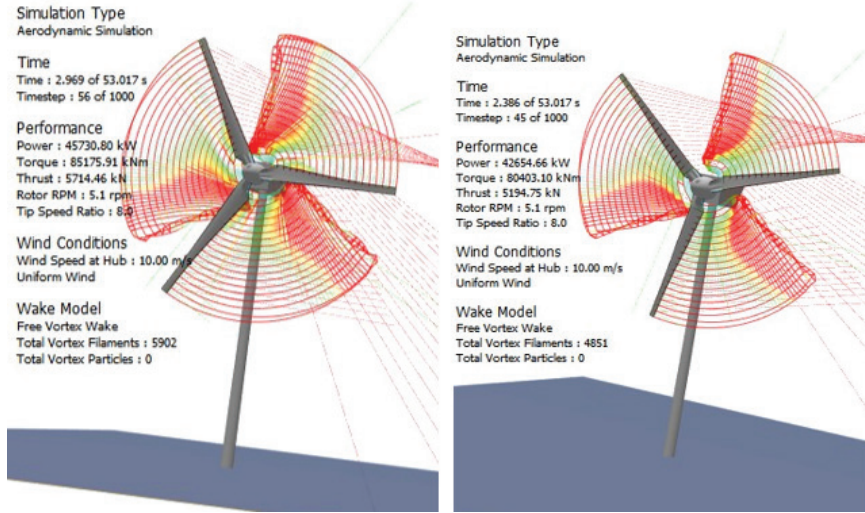


Figure 2.4. Simulation of regularly analysis of the NACA 4415 profile (left) and NACA 2215 profile (right) blades 50 MW wind turbines

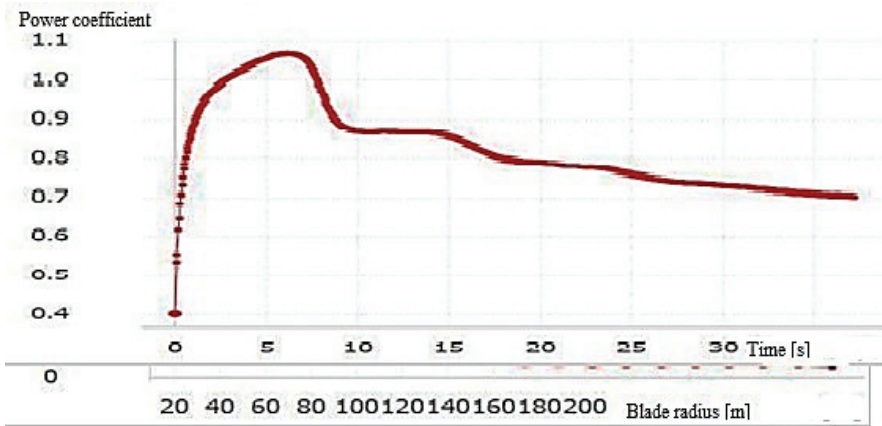


Figure 2.5. Power coefficient of 50 MW wind turbine NACA 4415 profile

Figure 2.6 shows the final shape of the angle of attack. The angle of attack is as large as possible between 0 (m) and 56 degrees at the beginning of the blade, and the angle of attack changes with the increase in the length of the blade; the angle of attack, which is quite large in the first 20 m of the blade, decreases rapidly until about 50 m and reaches the lowest value of 4 degrees after 160 m.

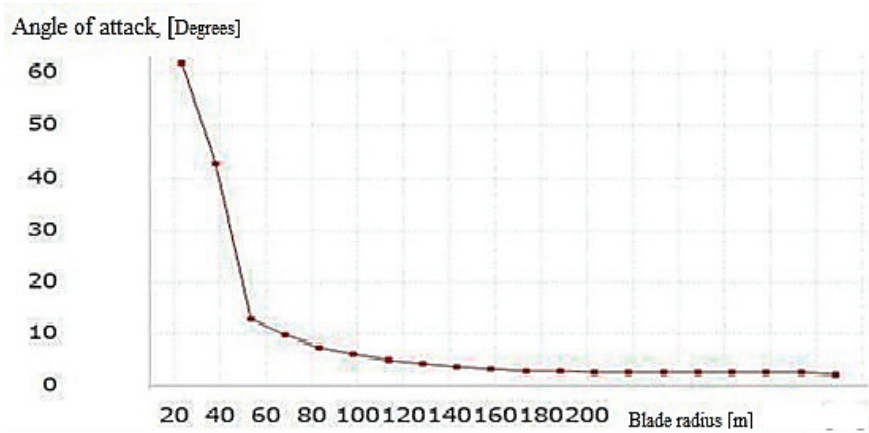


Figure 2.6. Angle of attack of 50 MW wind turbine NACA 4415 profile

2.3. Annual Energy Production of 50 MW Wind Turbine With NACA 4415 and NACA 2215 Profiled Blades

50 MW wind turbine It is assumed that the annual operating hours of the turbine are 8760 hours, and the minimum wind speed is 7.5 m/s and 14 m/s. In this way, the annual average wind speed is 11 m/s. Considering that the total efficiency of the turbine is 48%, considering the total losses due to heat and pressure in addition to the internal mechanical losses and losses in the electrical generator by 95%. According to the total energy output simulation system, for an average wind speed of 11 m/s, the average electrical output power of the NACA 4415 profile blade turbine is 46.5 MW and for the NACA 2215 profile blade turbine it is 43.5 MW. The amounts of electrical energy that can be produced annually are approximately calculated as follows.

For NACA 4415 profile blades: $AEP = 46.5 \text{ MW} \times 8760 = 407,340,000 \text{ kWh}$

For NACA 2215 profile blades: $AEP = 43.5 \text{ MW} \times 8760 = 381,060,000 \text{ kWh}$

As a result, 7% more electricity was produced with the NACA 4415 profile blades than with the 2215 profile blade turbine.

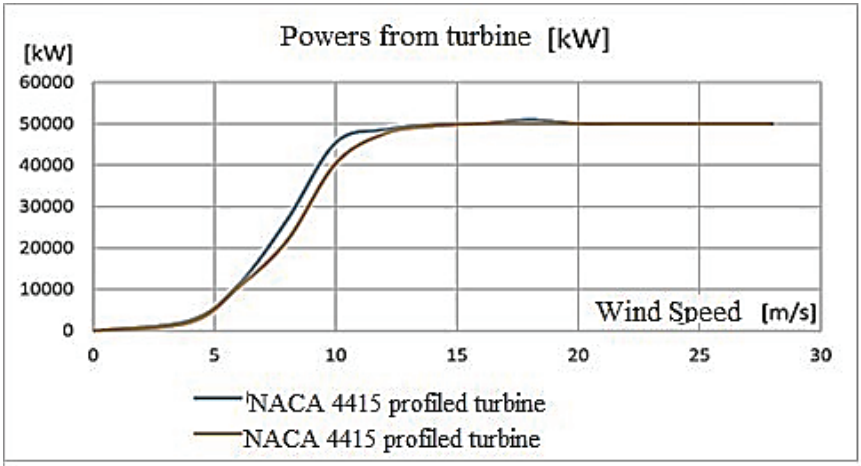


Figure 2.9. NACA 2215 profile of a 50 MW wind turbine [kW]

In Figure 2.9, the rotor rotation speed is determined as 0.2 rpm and the behaviour of the wind turbine is analysed at different wind speeds. It is seen that the nominal turbine power of 50 MW is reached at a wind speed of approximately 13 m/s for both profiled blades.

When the turbine first starts to operate, the maximum achievable power coefficient in Figure 2.10 approaches 1.1 for the 4415 profile. In order to stabilise the turbine, its stability is observed 90 seconds after it starts to operate. After stabilisation, the maximum achievable power coefficient is around 59%. Figure 2.10 shows the comparison of the strength coefficient of both profiles. It is found that the power coefficient of the NACA 2215 profile is 15% lower than that of the NACA 4415 profile. In the 50 MW wind turbine, the maximum power coefficient reached by the NACA 2215 profile at the beginning of the first operation is 0.9, while the maximum power coefficient reached by the NACA 4415 profile is 1.1.

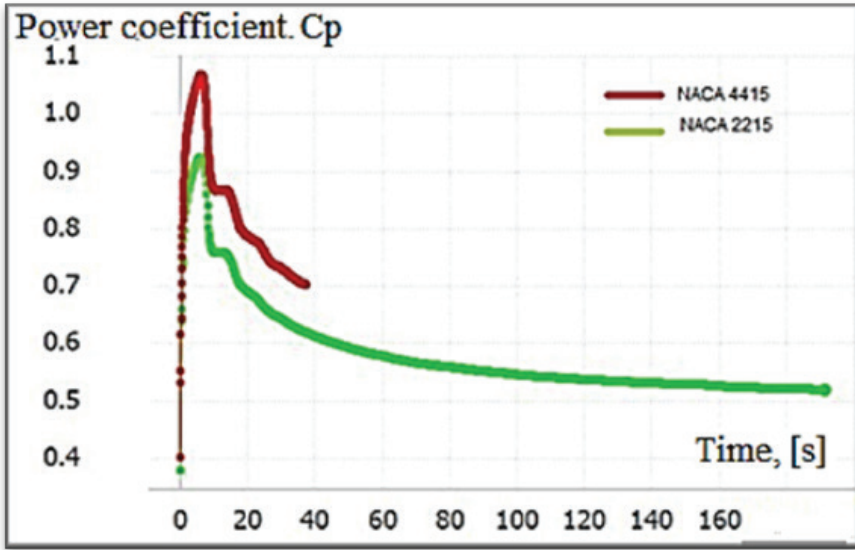


Figure 2.10. Power coefficient changes of NACA 4415 and NACA 2215 profiles of 50 MW wind turbine

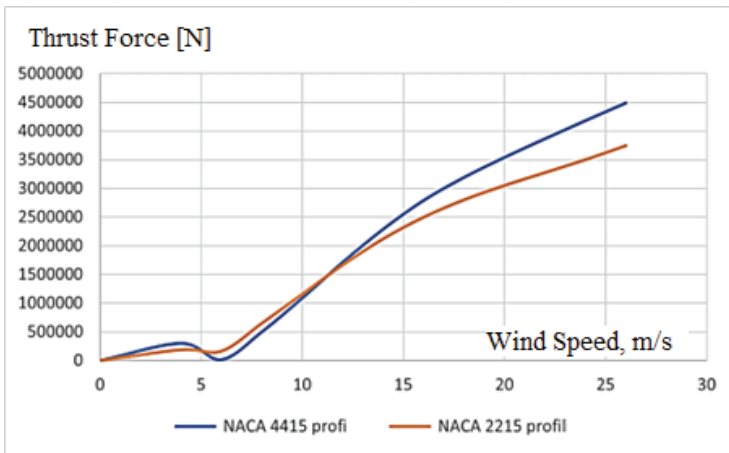


Figure 2.11. Thrust forces of 50 MW wind turbines with NACA 5515 and 2215 profiled blades

Figure 2.11 shows that the NACA 2215 profile does not require much thrust to move the turbine compared to the NACA 4415 profile. The thrust force starts to increase from about 6 m/s wind speed and increases with the wind speed. After 12 m/s wind speed, the rate of increase decreases for the blade with NACA 2215 profile and reaches 3.5 million Newton for 2215 profile and 4.4 million Newton for 4415 profile at 25 m/s.

2.4. Power Generated at Different Wind Speeds in a 50 MW Wind Turbine

Table 2.2 shows that the NACA 4415 profile is capable of generating and absorbing approximately 18% more energy from the wind than the NACA 2215 profile at 8 m/s wind speed. And this percentage difference between the blades decreases as the wind speed increases. When the wind speed is 14 m/s, this difference percentage reaches 3%.

Table 2.2. Power obtained at different wind speeds in a 50 MW wind turbine

Wind Speed [m/s]	NACA 4415 profile 50 MW WT generated power [kW]	NACA 2215 profile 50 MW WT generated power [kW]
4	2580.44	2112.69
6	11219.29	10637.1
8	26883.4	21856.6
10	45463.49	40445.7
12	48599.17	47569.71
14	49802.20	49451.6
16	50301	50454
20	50301	50454
24	50301	50454
26	50301	50454

2.5. Strength Analysis of a 50 MW Wind Turbine

Boundary conditions are a very important factor when using the Ansys FLUENT programme and the maximum boundary speed was taken as 50 m/s wind speed. The average Reynolds number was used as 2400 and the air density was used as 1.225 kg/m^3 . The meshing size was set to 0.05 to obtain the maximum accuracy of the simulation.

In Figures 2.12, the total pressures affecting the entire turbine casing are analysed. When the acting forces are analysed, it is found that the parts of the flow that are most exposed to pressure are especially in the blades.

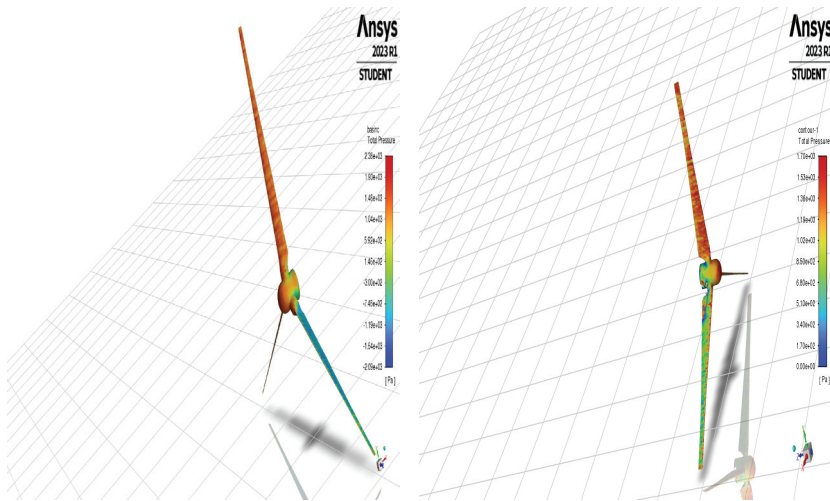


Figure 2.12. Strength analysis of 50 MW wind turbine blade NACA 4415 (left) and NACA 2215 (right) profiles with ANSYS Fluent programme

The most effective stress on the profile itself is at the ends of the profile. Therefore, there is little difference in the forces along the body of the profile. Thus, the pressure colour along the air-foil body is almost the same. However, for the blade with NACA 4415 profile, the upper limit value of the pressure scale seems to be higher.

2.6. Design And Strength Analysis of the Main Shaft of a 50 MW Wind Turbine

The rotor is always made of strong steel to carry high loads. The rotor (hub) diameter of the 50 MW turbine was calculated as 6.402 m (Table 2.5). The torques and different resistances obtained for different rotation speeds of the turbine shaft were analysed.

Table 2.5 Characteristics of the rotor shaft and hub of a 50 MW wind turbine

Turbine Section	Value and unit
Mass of the rotor hub	631.22 tonne
Rotor hub moment of inertia	$17.48 \cdot 10^5 \text{ kgm}^2$

The rotor weight of the example 50 MW turbine given in Table 2.5, including the blades, is 632.22 tons, which is quite high compared to the existing turbines. This shows that in order to obtain high powers, turbines must be made in larger sizes and as a result, turbine parts with large weights must be made.

Recently, due to the importance of renewable energy field, attention has been directed to large power wind turbines. In this study, an important and effective method has been found in the design and analysis of various large wind turbines using CFD method. CFD simulations for wind turbines focus on numerical simulations and model-based optimizations at turbine scale. In the sample study, the dimensions of the blades and some main parts of the turbines to be manufactured with two different blade profiles of NACA 2414 and 4415 for 50 MW power were designed. Design calculations and CFD analyses were made for each turbine for 11-14 m/s nominal wind speeds. With the dynamic analysis of the turbine in motion, the blades that carry more wind load and are more efficient in wind energy production were examined with CFD method.

In the study, the selection of suitable blades and other main parts for wind turbines with large and medium loads in terms of efficiency, annual electric energy production amount, wind loads on the blade and turbine was taken as the research basis. It is a model for selecting the large wind turbine blade profiles taken as reference. When designing large wind turbines, the blades were first designed and the flow analysis and the best selection were examined in detail. It was found that the blade length would be 250 m in a 50 MW wind turbine, the weight would be around 480-500 tons and the rotor rotation speed should be 0.2-0.8 rpm to prevent high centrifugal forces. When the forces formed on the blades designed with both NACA profiles were analyzed, it was shown that the part that is 15% away from the hub of the blade is the most sensitive part in terms of strength. It was concluded that this part of the blade should be reinforced with lighter and stronger materials than glass fiber, such as carbon fiber.

REFERENCES

- Akpınar, M. (2024) (Technology Editor), <https://forum.donanimhaber.com/15-mw-lik-dunyanin-en-buyuk-kara-ruzgar-turbini-kuruldu--159763288> (Kaynak:<https://www.rechargenews.com/wind/-world-s-largest-15mw-onshore-wind-turbine-installed-in-china/2-1-1722161>) Access date: 10-15.10.2024.
- Ananda, G. K., Bansal, S. and Selig, M. S., 2018, Aerodynamic Design of the 13.2 MW SUMR-13i Wind Turbine Rotor, *2018 Wind Energy Symposium*, 346-357.
- Carraro, M., V., F.D., Zweiri, F., Benini, E., Heidari, A., Hadavinia, H., 2022, CFD Modeling of CFD Modeling of Wind Turbine Blades with Eroded Leading Edge, *Fluids*, 7, 302.
- Corke, T., Nelson, R., 2018. *Wind Energy Design*, First edition, *CRC Press*. 1-353.
- Cox, Kevin and Andreas, Echtermeyer, 2012, Structural Design and Analysis of a 10MW Wind Turbine Blade, *Energy Procedia*, 24: 194-201.
- Çakmak, D., (2024) url: <https://www.donanimhaber.com/cin-26-mw-gucunde-dunyanin-en-buyuk-ruzgar-turbini-tanitti--183089#26-mw-guce-ve-310-metre-kanat-capina-sahip>. Access date: 10.10.2024.
- Lalit, K., 2017. CFD Analysis On Wind Blade, *IJARSE*, Vol. No.4, Issue 04, 67-79.
- Lingling, F., 2015. Modeling and Analysis of Doubly Fed Induction Generator Wind Energy Systems, *Academic Press*, 15.25-36.
- Mansour, H., and Rola A., 2020. Design and 3D CFD Static Performance Study of a Two-Blade IceWind Turbine, *Energies*, 13, 53-65.
- Mauro, S., Sebastian B., Rosario L. and Michele M., 2019. Micro H-Darrieus wind turbines: CFD modeling and experimental validation, *Second International Conference on Material Science, Smart Structures and Applications: Icmss*, 2019, 85-97.
- Papi, F., Alberto N., Giovanni F., and Alessandro B., 2021. On the Use of Modern Engineering Codes for Designing a Small Wind Turbine: An Annotated Case Study, *Energies*, 14, 110-122.
- Rajakumar, S., and Ravindran D., 2016. Computational Fluid Dynamics of Wind Turbine Blade At Various Angles Of Attack And Low Reynolds Number, *International Journal of Engineering Science and Technology*, 15, 56-67.
- Richard, C., 2022, Goldwind And China Three Gorges Roll Out Nacelle For 16MW Offshore Wind Turbine, *WindPower Montly, News*, 24 November 2022.

- Schubel, P. J., and Crossley, R.J., 2012, Wind Turbine Blade Design, *Energies*, 2012, 5, 3425-3449.
- Sy, M. S., Binoe, E. A., and Louis, A. M. D., 2020. Aerodynamic Investigation of a Horizontal Axis Wind Turbine with Split Winglet Using Computational Fluid Dynamics, *Energies*, 13, 45-58.
- Subham, S. A. A., 2019, Wind turbine noise and its mitigation techniques: A review. *Energies* 02, 2-19.
- Tarhan, C., Çil, M.A., 2022, Numerical Investigation of Different Blade Profiles Used in Wind Turbines, *Engineer and Machinery*, vol.63, no.706, pp.1-22, 2022.
- Tong, W., 2010, Wind Power Generation and Wind Turbine Design, *WIT Press*, Ashurst Lodge, Ashurst, Southampton, SO40 7AA, UK.
- Yao, S., Mayank C., Griffith, D.T., Mendoza, A.S.E., Selig, M.S., Martin, D., Kianbakht, S., Johnson, K., and Loth, E., 2021. Aero-Structural Design and Optimization of 50MW Wind Turbine With Over 250-m Blades, *Wind Engineering*, 46: 273-295.

Chapter 7

ENERGY AND EXERGY ANALYSIS OF A 1 MW MONOCRYSTALLINE PHOTOVOLTAIC SOLAR POWER PLANT PROPOSED FOR INSTALLATION IN ORDU PROVINCE

Oguz Ozan YOLCAN¹

Ahmet DAYANÇ²

1 Asst. Prof. Dr., Kutahya Dumlupinar University, oguzozan.yolcan@dpu.edu.tr,

ORCID: 0000-0002-6664-5675

2 Res. Asst., Kutahya Dumlupinar University, ahmet.dayanc@dpu.edu.tr,

ORCID: 0000-0002-5214-9021

INTRODUCTION

Energy can be defined as the capacity to do work or the potential to transfer heat in physical systems (Lower, 2024). Essentially, the concept of energy can be utilized to understand and explain many interactions in the universe. Energy can exist in various forms such as mechanical, thermal, chemical, electrical, nuclear, and electromagnetic (EIA, 2024). According to the first law of thermodynamics, known as the “Conservation of Energy,” energy can neither be created from nothing nor destroyed; it can only be transformed from one form to another (NASA, 2021).

In thermodynamic systems, energy can be analyzed through components such as internal energy, kinetic energy, and potential energy (MIT, 2024). Research on the form and amount of energy used (ranging from industrial processes to simple everyday tasks) helps increase system efficiency and reduce energy costs.

Renewable Energy refers to energy sources that continuously renew themselves through natural processes or become accessible again within a very short time (UN, 2024). The most common examples of these sources include solar, wind, hydroelectric, biomass, and geothermal energy (National Grid, 2022).

Because fossil fuels (such as oil, coal, and natural gas) have limited reserves, their recovery can take millions of years once consumed (Kuo, 2019). Therefore, unlike fossil fuels, renewable sources support sustainable development goals and have generally lower environmental impacts compared to fossil fuels. Renewable energy technologies are particularly important in efforts to reduce greenhouse gas emissions and combat climate change.

Solar Energy is energy obtained by collecting and utilizing electromagnetic radiation from the Sun through various methods (energy.gov, 2024). Although only a very small portion of the energy released

by fusion reactions in the Sun's core reaches the Earth, it is still sufficient to potentially meet humanity's total energy needs many times over (Roy, 2024).

Solar energy can be harnessed through two main methods: solar thermal systems and photovoltaic systems. In solar thermal systems, solar radiation is converted into heat, which can be used to produce hot water. In photovoltaic systems, solar radiation is converted directly into electrical energy (Solar N Plus, 2024).

Photovoltaic Panels are devices that use semiconductor materials to directly convert the photons in sunlight into electrical energy (Wikipedia, 2024). This conversion is based on a physical principle known as the photovoltaic effect. Although silicon is the most common material for photovoltaic cells, panels are also produced using alternative materials such as thin-film technologies, gallium arsenide (GaAs), and perovskite (Rourke, 2024).

The efficiency level of photovoltaic panels indicates how much of the sunlight is converted into useful electrical energy (Vourvoulias, 2024). As technology advances, these efficiency values increase while costs decrease. Factors such as location, tilt, orientation, and shading play important roles in the installation of photovoltaic panels. Furthermore, panel quality and environmental conditions (e.g., temperature, humidity) also affect durability and performance.

Photovoltaic Solar Power Plants are systems that generate large amounts of electricity through photovoltaic panels installed over wide areas (PVCASE, 2023). Such plants can be deployed as large-scale, grid-tied installations, or they can be utilized in off-grid or hybrid solutions.

Large-scale photovoltaic power plants are equipped with additional components such as inverters, transformers, grid connection components, and monitoring systems. Through these components, the generated direct current (DC) electricity is converted into alternating current (AC) and integrated into the grid (Lozanova, 2024). Due to technological

advancements, the decreasing cost of installations is making these power plants increasingly attractive for many countries.

Exergy refers to the maximum theoretical potential for a system or energy source to perform work, taking into account the ambient conditions (Mukherjee, 2023). In other words, exergy is a quantity based on the second law of thermodynamics that represents the amount of “useful energy.”

While energy analysis relies solely on the “conservation of energy” principle, exergy analysis evaluates the system from a more comprehensive perspective. Even though the total amount of energy is conserved, a reduction in availability or “quality” is unavoidable according to the second law. Therefore, exergy analysis is critical for identifying irreversibilities within a process or system, improving system efficiency, and conducting design optimization.

Energy and Exergy Analyses are comprehensive assessment methods used to understand, enhance, and optimize system performance in power plants or similar industrial facilities. By employing an energy analysis, one can quantitatively determine energy inputs, outputs, and losses (e.g., heat losses) in a system, based on the first law of thermodynamics. Although it indicates how much energy conversion occurs in the system, it may be insufficient to explain the reasons and mechanisms behind losses according to the second law of thermodynamics. Exergy analysis, on the other hand, takes into account irreversibilities across the entire system and within each component. Within the framework of the second law of thermodynamics, it reveals the level of “available energy” or “energy convertible to work.” Particularly in facilities with multi-stage processes, such as power plants, it identifies which components or process steps experience the greatest losses, thereby guiding measures to increase efficiency.

By applying both energy and exergy analyses together, one can evaluate the overall performance of a power plant or system much more clearly. These analyses help identify deficiencies in power plant design,

bottlenecks within the system, and areas where economic improvements can be made. They are especially useful in renewable energy power plants (e.g., solar, wind, and hydroelectric) for improving environmental sustainability and economic feasibility. In contemporary technological applications aimed at energy efficiency and system optimization, the role of exergy is steadily increasing, and the design and operational strategies of power plants are being developed accordingly.

The efficiency of photovoltaic panels can vary significantly depending on environmental conditions. For example, in a study by Jena and Naikin (Jena, S., Kumar, & A., 2021), natural factors affecting the output of PV panels were examined experimentally. The study analyzed how temperature, irradiation, dust, and shading influence PV performance. It emphasizes that such environmental factors play a critical role in the energy production of PV panels.

Within the scope of this study, based on the geographical location examined for the photovoltaic solar power plant, Figure 1 below presents the long-term (2004–2021) average global solar radiation distribution ($\text{kWs/m}^2/\text{day}$) in Turkey.



Figure 1. Long-term (2004–2021) average global solar radiation distribution ($kWs/m^2/day$) in Turkey (MGM, 2024a).

Because the province of Ordu is located in northern Turkey, its solar energy potential is observed to be lower compared to the provinces in southern Turkey. According to the Solar Energy Potential Atlas, Ordu’s solar energy potential ranges between $1250 kWh/m^2/year$ and $1300 kWh/m^2/year$.

In Figure 2 below, the long-term (2004–2021) average global solar radiation distribution ($kWs/m^2/day$) for Ordu is presented.

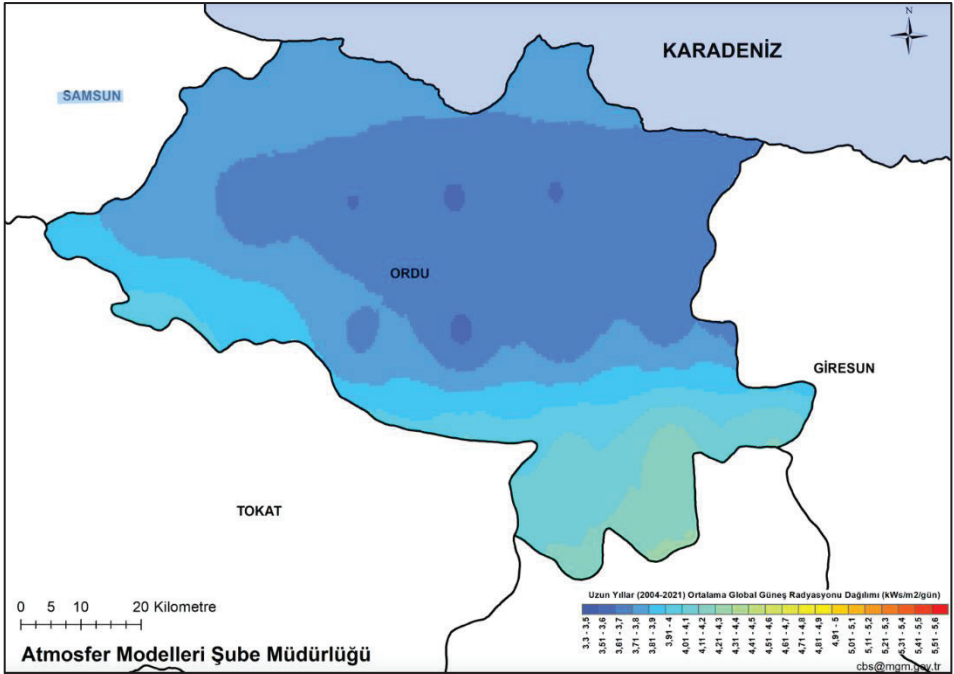


Figure 2. Long-term (2004–2021) average global solar radiation distribution ($\text{kWs/m}^2/\text{day}$) for Ordu (MGM, 2024b).

According to the “Monthly Sector Report” published by the Energy Market Regulatory Authority in September 2024, Ordu’s licensed installed capacity is 543.97 MW as of September 2024. Similarly, as of September 2024, licensed electricity generation from the licensed installed capacity reached 22544.54 MWh (EPDK | Republic of Turkey Energy Market Regulatory Authority, 2024). As stated in the same report, as of September 2024, Ordu’s unlicensed solar power installed capacity stands at 9.14 MW (EPDK | Republic of Turkey Energy Market Regulatory Authority, 2024). Finally, Ordu’s electricity consumption in September 2024 was recorded as 136005.79 MWh (EPDK | Republic of Turkey Energy Market Regulatory Authority, 2024).

MATERIAL AND METHOD

In this study, an energy and exergy analysis was conducted for a 1 MW photovoltaic (PV) solar power plant. The chosen geographic location for the analyzed PV solar power plant is the province of Ordu in Turkey. The main reason for selecting Ordu is that its unlicensed solar energy installed capacity is considerably lower than the average in Turkey. As of September 2024, the unlicensed solar energy installed capacity of Ordu stands at 9.14 MW (EPDK | Republic of Turkey Energy Market Regulatory Authority, 2024).

The design of the PV solar power plant for Ordu province was performed using the System Advisor Model software (National Renewable Energy Laboratory (NREL), 2024). During the simulated design of the PV solar power plant, monocrystalline panels with a capacity of 400 W were selected.

In calculating the energy and exergy efficiencies of a photovoltaic panel, meteorological data are utilized in addition to the values obtained through panel measurements. Below are the mathematical expressions related to the energy and exergy analysis of a PV panel.

Equation 1 represents the panel efficiency equation. It shows that, for PV panels, the product of the maximum voltage (V_m) and the maximum current (I_m) is directly proportional to the panel efficiency, whereas it is inversely proportional to the solar radiation (S_t [W/m^2]) incident on the panel area (A [m^2]).

$$\eta = \frac{V_m \cdot I_m}{S_t \cdot A} \quad (1)$$

Exergy transfer is calculated via Equations 2 and 3:

$$\sum \dot{Ex}_g = \sum \dot{Ex}_c + \sum \dot{Ex}_d + \sum \dot{Ex}_k \quad (2)$$

$$\dot{E}x_{\zeta} = \dot{E}x_m - \sum \dot{\Gamma} - \dot{E}x_k \quad (3)$$

In Equations 2 and 3, the following are indicated:

- $\Rightarrow \dot{E}x_g$: The total exergy input to the panel,
- $\Rightarrow \dot{E}x_{\zeta}$: The total exergy output from the panel,
- $\Rightarrow \dot{E}x_d$: The exergy destruction,
- $\Rightarrow \dot{E}x_k$: The thermal exergy,
- $\Rightarrow \dot{E}x_m$: The maximum exergy output,
- $\Rightarrow \dot{\Gamma}$: The irreversibilities.

The system's electrical exergy output can be computed by subtracting the irreversibilities from the maximum exergy output using Equation 4:

$$\dot{E}x_m - \sum \dot{\Gamma} = V_{ad} I_{kd} - (V_{ad} I_{kd} - V_m I_m) = V_m I_m \quad (4)$$

In Equation 4:

- $\Rightarrow V_{ad}$: The open-circuit voltage,
- $\Rightarrow I_{kd}$: The short-circuit current.

Additionally, the heat transfer through convection from the panels can be calculated using Equation 5:

$$Q = h_c \cdot A \cdot (T_{huc} - T_0) \quad (5)$$

In Equation 5:

- $\Rightarrow h_c$: The convective heat transfer coefficient,
- $\Rightarrow T_{huc}$: The cell temperature,

$\Rightarrow T_0$: The ambient temperature.

Subsequently, the convective heat transfer coefficient is calculated using Equation 6:

$$h_c = 5,7 + 3,8.V \tag{6}$$

In Equation 6:

$\Rightarrow V$: The wind speed.

Moreover, the thermal exergy is calculated using Equation 7:

$$\Sigma \dot{Ex}_k = \left(1 - \frac{T_0}{T_{huc}}\right) [(5,7 + 3,8.V) \cdot A \cdot (T_{huc} - T_0)] \tag{7}$$

The exergy output from the system can be determined via Equation 8, and the exergy input to the system can be determined via Equation 9:

$$\Sigma \dot{Ex}_\zeta = V_m I_m - \left(1 - \frac{T_0}{T_{huc}}\right) \cdot [h_c \cdot A \cdot (T_{huc} - T_0)] \tag{8}$$

$$\Sigma \dot{Ex}_g = S_t \cdot A \cdot \left(1 - \frac{T_0}{T_G}\right) \tag{9}$$

In Equation 9:

$\Rightarrow T_G$: The sun's surface temperature.

Finally, the exergy efficiency of a photovoltaic panel can be calculated using Equation 10:

$$\Psi = \frac{\dot{Ex}_\zeta}{\dot{Ex}_g} = \frac{V_m I_m - \left(1 - \frac{T_0}{T_{huc}}\right) \cdot [h_c \cdot A \cdot (T_{huc} - T_0)]}{S_t \cdot A \cdot \left(1 - \frac{T_0}{T_G}\right)} \tag{10}$$

RESULTS AND DISCUSSION

The data obtained for Ordu province are provided on a monthly basis, covering all 12 months of the year. In this study, monthly data for cell temperature, ambient temperature, efficiency, and exergy efficiency were presented. These data are illustrated in Figure 3 below.

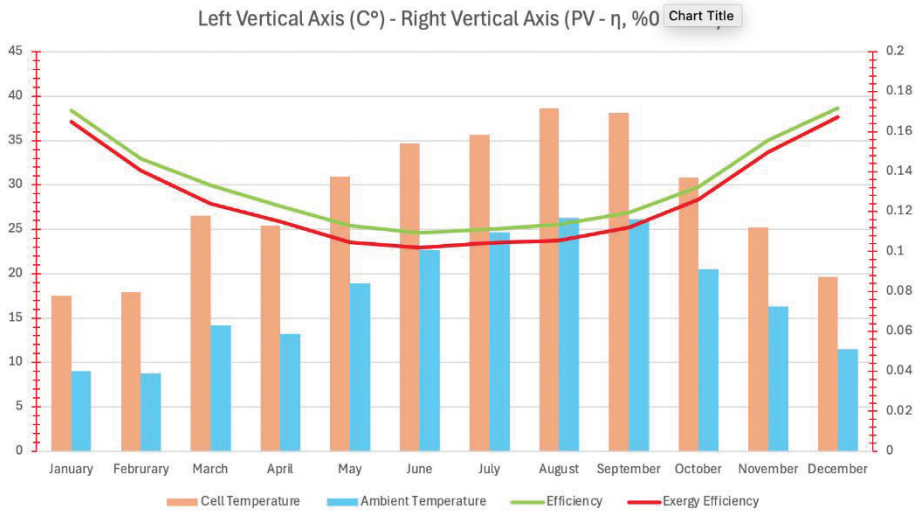


Figure 3. Cell Temperature, Ambient Temperature, Efficiency and Exergy Efficiency

Based on the theoretical data from the System Advisor Model software and the meteorological data of Ordu province, the annual average energy efficiency of the PV panels was calculated as 13.32%, while the annual average exergy efficiency was calculated as 12.63%. The monthly values of energy and exergy efficiencies are shown in Table 1 below.

Table 1. Efficiency and Exergy Efficiency

Months	Efficiency	Exergy Efficiency
January	0.1705	0.1649
February	0.1464	0.1405
March	0.1333	0.1239
April	0.1228	0.1149
May	0.1130	0.1045
June	0.1095	0.1020
July	0.1110	0.1044
August	0.1134	0.1056
September	0.1196	0.1122
October	0.1323	0.1261
November	0.1559	0.1498
December	0.1718	0.1672

Furthermore, as a result of the simulation and analysis in the System Advisor Model software, considering the one-year electricity production of the PV solar power plant, the total production was found to be 1245.9 MWh. The monthly variations are visualized in Figure 4 below.

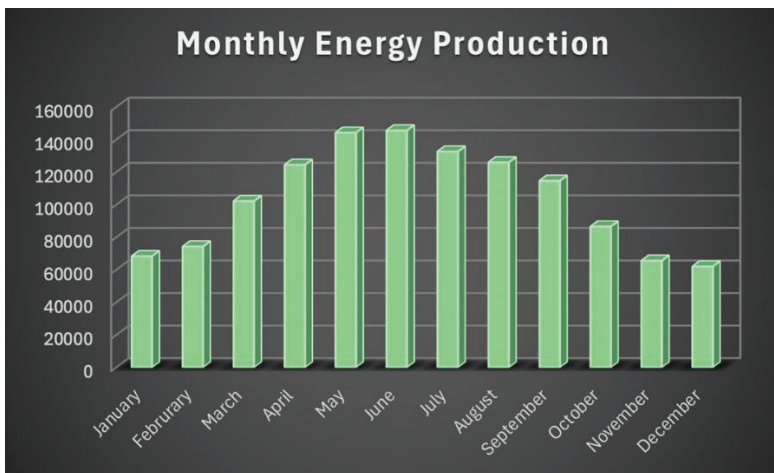


Figure 4. Monthly Energy Production (MEP)

Table 2 presents the monthly production values.

Table 2. Monthly Energy Production

MONTHS	MEP
January	68328.2
Februrary	74241
March	102164
April	124407
May	144134
June	145553
July	132559
August	125938
September	114589
October	86487.4
November	65535.9
December	61963.6

CONCLUSION

In this study, an energy and exergy analysis was carried out for a 1 MW-capacity PV solar power plant that could be installed in Ordu province, located in northern Turkey. The monthly electrical energy production values of the PV solar power plant, simulated in the System Advisor Model software, were examined, and the one-year electrical energy production was calculated to be 1245.9 MWh. Additionally, using the theoretical data from the System Advisor Model software and the meteorological data of Ordu province, the annual average energy efficiency of the PV panels was determined to be 13.32%, while the annual average exergy efficiency was found to be 12.63%. It was observed that as the temperature of the PV panels increases, both the energy and exergy efficiencies decrease, indicating an inverse relationship between temperature and efficiency.

REFERENCES

- EIA. (2024). Forms of energy - U.S. Energy Information Administration (EIA). Retrieved December 25, 2024, from <https://www.eia.gov/energyexplained/what-is-energy/forms-of-energy.php>
- energy.gov. (2024). Solar Radiation Basics | U.S. Department of Energy. Retrieved December 25, 2024, from <https://www.energy.gov/eere/solar/solar-radiation-basics>
- EPDK | Türkiye Cumhuriyeti Enerji Piyasası Düzenleme Kurumu. (2024). Elektrik Piyasası Aylık Sektör Raporu Listesi. Retrieved December 17, 2024, from <https://www.epdk.gov.tr/detay/icerik/3-0-23/elektrikaylik-sektor-raporlar>
- Kuo, G. (2019). When Fossil Fuels Run Out, What Then? - MAHB, Stanford. Retrieved December 25, 2024, from <https://mahb.stanford.edu/library-item/fossil-fuels-run/>
- Lower, S. (2024). 14.1: Energy, Heat and Work - Chemistry LibreTexts. Retrieved December 25, 2024, from [https://chem.libretexts.org/Bookshelves/General_Chemistry/Chem1_\(Lower\)/14%3A_Thermochemistry/14.01%3A_Energy_Heat_and_Work](https://chem.libretexts.org/Bookshelves/General_Chemistry/Chem1_(Lower)/14%3A_Thermochemistry/14.01%3A_Energy_Heat_and_Work)
- Lozanova, S. (2024). The Difference Between Solar Inverters Vs. Converters | Greenlancer. Retrieved December 25, 2024, from <https://www.greenlancer.com/post/solar-inverter-vs-converter>
- MGM. (2024a). Global Güneş Radyasyonu. Retrieved December 25, 2024, from https://www.mgm.gov.tr/kurumici/radyasyon_iller.aspx
- MGM. (2024b). Ordu ili | Global Güneş Radyasyonu. Retrieved December 25, 2024, from https://www.mgm.gov.tr/kurumici/radyasyon_iller.aspx?il=ordu
- MIT. (2024). 2.1 First Law of Thermodynamics. Retrieved December 25, 2024, from <https://web.mit.edu/16.unified/www/FALL/thermodynamics/notes/node15.html>
- Mukherjee, N. (2023). What is Exergy? | LinkedIn. Retrieved December 25, 2024, from <https://www.linkedin.com/pulse/what-exergy-nikhilesh-mukherjee>

- NASA. (2021). Conservation of Energy. Retrieved December 25, 2024, from <https://www.grc.nasa.gov/www/k-12/airplane/thermo1f.html>
- National Grid. (2022). What are the different types of renewable energy? Retrieved December 25, 2024, from <https://www.nationalgrid.com/stories/energy-explained/what-are-different-types-renewable-energy>
- National Renewable Energy Laboratory (NREL). (2024). *System Advisor Model - SAM*. Retrieved from <https://sam.nrel.gov/>
- UN. (2024). *What is renewable energy? | United Nations*. Retrieved from <https://www.un.org/en/climatechange/what-is-renewable-energy>
- PVCase. (2023). Solar plant design guide: the basics. Retrieved December 25, 2024, from <https://pvcase.com/blog/solar-plant-design-guide-the-basics/>
- Rourke, E. (2024). The Best New Solar Technology - Solar Advice UK. Retrieved December 25, 2024, from <https://solaradvice.co.uk/best-new-solar-technology/>
- Roy. (2024). Amount of Solar Energy Hitting Earth Every Second, Day, Week & Year. Retrieved December 25, 2024, from <https://gosolarquotes.com.au/amount-of-solar-energy-hitting-earth/>
- Satyaranjan Jena, Amiya Kumar Naik, . (2021). Impact of Environmental Factors on The Performance of Solar PV Cells: An Experimental Study. 2021 1st Odisha International Conference on Electrical Power Engineering, Communication and Computing Technology(ODICON). DOI: <https://doi.org/10.1109/odicon50556.2021.9428999>
- Solar N Plus. (2024). How PV Cells Harness the Sun to Generate Electricity. Retrieved December 25, 2024, from <https://www.solarnplus.com/how-pv-cells-harness-the-sun-to-generate-electricity/>
- Vourvoulias, A. (2024). How Efficient Are Solar Panels in December 2024? | Greenmatch. Retrieved December 25, 2024, from <https://www.greenmatch.co.uk/blog/2014/11/how-efficient-are-solar-panels>
- Wikipedia. (2024). Theory of solar cells. Retrieved December 25, 2024, from https://en.wikipedia.org/wiki/Theory_of_solar_cells

Chapter 8



WIND TUNNEL EXPERIMENTAL APPLICATIONS

*Samet Giray TUNCA*¹

*Kadir OLCAY*²

*Mustafa Arif ÖZGÜR*³

1 Dr., Kütahya Dumlupınar University Dumlupınar Vocational School Department of Electricity and Energy sgiray.tunca@dpu.edu.tr ORCID: 0000-0002-7632-8745

2 Dr., Kütahya Dumlupınar University Dumlupınar Vocational School Department of Electricity and Energy kadir.olcay@dpu.edu.tr ORCID: 0000-0001-7918-6482

3 Prof.Dr., Kütahya Dumlupınar University, Faculty of Engineering, Department of Mechanical Engineering, arif.ozgur@dpu.edu.tr ORCID: 0000-0001-5877-4293

Introduction

Wind tunnel tests provide direct measurements for optimization on aerodynamic designs and related models. Different stages are passed to perform these measurements. First, the scaled version of the model to be studied must be prepared according to the dimensions of the wind tunnel test chamber. Then, the speed to be applied in the wind tunnel and other parameters such as the angle if the structure is a wing must be adjusted to start the tests. In wind tunnel tests, measurements such as aerodynamic forces, pressure measurements, and laminar separation bubbles can be performed. These measurements are made with force devices, pressure sensors, smoke monitoring techniques, oil tests and devices such as MiniCTA. These and similar experimental tests must be performed to obtain aerodynamic characteristic data. With the obtained data, flow separations, laminar turbulence transition zones and aerodynamic performances are analyzed. These methods are used to optimize the aerodynamic performances of designs in many sectors such as aviation, automotive, construction and architecture (Greenblatt, D., & Wygnanski, I. 2020). In academic studies, numerical data obtained through simulations are compared with experimental data. Aerodynamic force measurements in wind tunnels are of critical importance for understanding and optimizing aerodynamic forces on aircraft, vehicles, buildings and other structures. These forces, especially lift and drag forces, determine the performance, efficiency and stability of an object. Accurate measurement of these forces in wind tunnel tests is vital for the development and improvement of aerodynamic designs.

Importance of Aerodynamic Force Measurement in Wind Tunnel

Design performance is important in measuring aerodynamic forces. Measuring lift and drag forces on aircraft wings, vehicles or building models allows us to understand the aerodynamic performance of designs. These forces indicate the interaction of the object with the air and these forces need to be optimized to achieve a more efficient design (Houghton, E. L., & Carpenter, P. W. 2003). Especially in the automotive and aviation sectors, measuring aerodynamic forces helps to make improvements to minimize energy consumption by reducing friction and air resistance. This increases the fuel efficiency of vehicles or allows aircraft to consume less fuel.

Structural stability and safety issues are another important issue in aerodynamic force measurements (Nielsen, J. N., & Wolf, D. R. 2012). Measuring aerodynamic forces in engineering structures such as buildings, bridges and tall buildings is a critical stage in testing the resistance of these structures to wind loads. Improperly designed structures can be subjected to excessive forces at high wind speeds, posing a risk of structural damage or collapse. Wind tunnel tests help identify laminar and turbulent

flow regions by examining the behavior of the flow over the object. Flow separation and turbulence can cause the aerodynamic forces to become unbalanced, resulting in reduced lift or increased drag (Fry, D. J., & Kline, S. J. 1957). Such analyses are necessary to optimize designs.

Direct force measurements are made in wind tunnel tests to verify theoretical results obtained with numerical simulations (CFD). This shows whether the simulation results are reliable and provides the opportunity to test how designs perform in reality.

Aerodynamic force measurements are essential for fine-tuning design processes. For example, redesigning the surface profile of a wing or the contours of a vehicle to reduce aerodynamic forces can contribute to significantly improved performance.

Measurement Methods

1. Force Measurement System

Force measurement devices are multi-component force scales placed on the object under test in the wind tunnel. These devices measure the total lift, drag and side forces on the object during the test. There are different designs of force devices. Although the measurement logic is generally the same, there are differences in the connection of the model to the device.

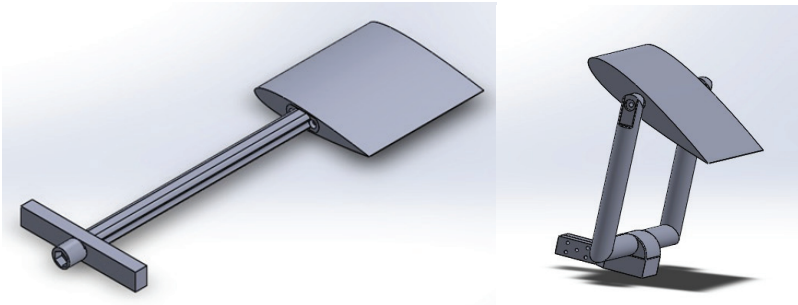


Figure 1. Different examples of connecting the model to the force device



Figure 2. Connecting the wing model to the force system

In order to understand the working principle of modern wind turbines, it is necessary to know the airfoil and the two important aerodynamic forces formed on this airfoil.

Drag Force: The force formed in the flow direction. For a flat plate, the maximum drag force occurs when the airflow is 90° perpendicular to the object, while the minimum drag force occurs when the airflow is parallel to the object surface. This force expresses the force on any area in the wind direction (Sarhat, E., & Ali, A. 2018).

$$D = C_D \frac{1}{2} \rho A V^2$$

D represents the drag force, ρ represents the density of the air, V represents the wind speed, A represents the surface area, and C_D represents the dimensionless drag coefficient. The change in C_D values is related to the aerodynamic quality of the surface. As C_D decreases, the drag force also decreases.

Lift Force: Lift force acts on the object in a direction perpendicular to the flow. This force is what causes airplanes to take off from the ground. Low pressure areas occur due to the increase in flow intensity at small angles to the direction of air flow (Richardson, E. G. 1961). Therefore, a relationship is created between air flow speed and pressure (Kähler, C. J., & Kompenhans, J. 2000). In other words, as air flow accelerates, pressure decreases, and as air combustion slows down, pressure increases. This phenomenon is called the “Bernoulli Effect”. This effect explains the suction or pulling effect of lift force on the object. Drag force is defined by the following formula;

$$L = C_L \frac{1}{2} \rho A V^2$$

Lift force, like drag force, depends on air density, wind speed and surface area.

2. Flow Visualization Methods

These techniques are used for the detection of flow separation, laminar-turbulent transitions and separation bubbles. These observations help us to better understand how aerodynamic forces are generated. Such force measurements in the wind tunnel are indispensable for the development of safer, more efficient and more environmentally friendly designs, especially in aeronautical and automotive engineering (Merzkirch, W. 1987).

2.1. Smoke Visualization Method

Wind tunnel smoke imaging is an important visualization method used in fluid dynamics tests. Smoke flow allows us to observe how air or fluids move, flow structures around objects, and aerodynamic features such as turbulence. Smoke image data helps improve designs by improving the quality of aerodynamic analysis. Thanks to this method, it is possible to directly observe the laminar-turbulent transition of the flow and flow separation. The transition points between laminar regions where the flow is regular and turbulent regions where it becomes irregular and mixed are critical for aerodynamic design. This visualization allows engineers to better understand the movement of fluids and their effects on objects. Flow separation is a phenomenon that seriously affects aerodynamic performance. Smoke imaging determines when and where the flow separates from the object surface by detecting these separation regions. In addition, the vortices formed as a result of separation and the effect of these vortices on the object are observed. Especially at low speeds or low Reynolds numbers, smoke imaging is used to detect laminar separation bubbles. These bubbles create turbulent regions that cause the flow to separate from the object surface and reattach. This phenomenon is important data for optimizing aerodynamic forces and performance. Smoke flow provides a visual understanding of how aerodynamic forces are generated. The processes of the flow impinging on the object, separating from the surface, and creating turbulent regions affect the generation of lift and drag forces. Smoke provides a clearer picture of how these forces are generated and how to optimize them. Flow visualization allows designs to be optimized to improve the aerodynamic properties of wings, vehicles, or structures used in wind tunnel tests. Smoke imaging helps engineers improve designs by showing where the flow is smoother and more efficient, and where flow disruptions or turbulence occur.

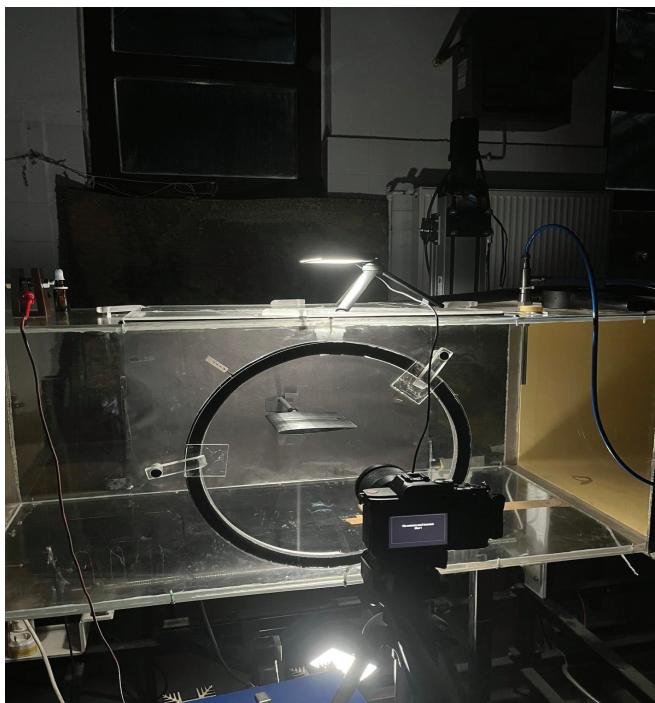


Figure 3. Smoke visualization method

In wind tunnel experiments, smoke flow is first created by placing a resistance wire vertically in front of the test chamber in the opposite direction of the flow. It is connected to the power source so that current passes through the tensioned resistance wire. Then, current is applied and an oil or similar substance, the density of which has been previously determined, is dropped onto the wire to obtain the necessary smoke. In this way, the substance burns and smoke is formed by the current passing through the wire. The wind tunnel is operated at the speed at which the experiment will be performed, allowing smoke filaments to pass over the model. A professional camera is used to view the smoke passing over the model. According to how the smoke moves around the object, the flow structure, vortices and flow separation are observed. The smoke image is obtained as data for interpretation.

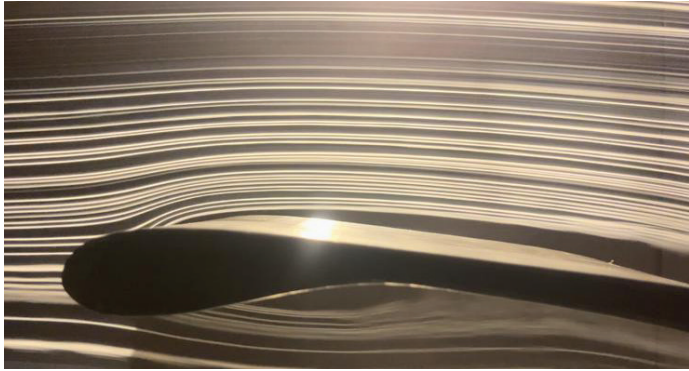


Figure 4. Smoke image on wing model

Smoke visualization is extremely valuable as a visual and qualitative component of aerodynamic analysis, alongside more quantitative methods such as numerical simulations and force measurements. This method finds wide application in engineering studies to improve designs and increase aerodynamic performance.

1.2. Oil Flow Visualization

Oil experiments in wind tunnels are used as one of the flow visualization techniques and are an important part of aerodynamic studies. These experiments provide critical information about the pressure distribution, drag forces and flow separation regions, especially on the surface of objects. The purpose of oil experiments is to study the complex structure of air flow by visualizing how a fluid interacts with a surface.

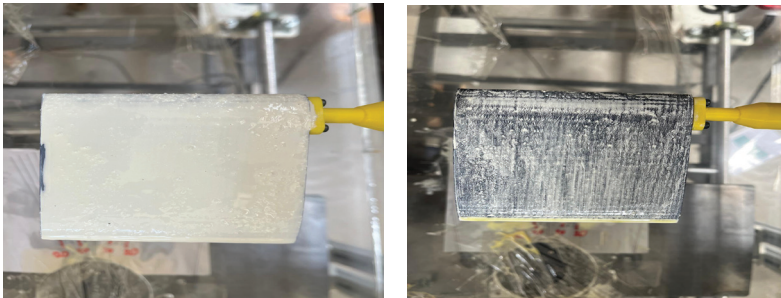


Figure 5. Oil flow visualization application: before and after

The oil is applied to the surface as a thin film and moves under the influence of the flow. As a result of this movement, information is obtained about the flow direction and velocity distributions formed on the surface. Oil experiments are also used to detect the regions where the flow separates and reconnects with the object surface. Flow separation is an important parameter for aerodynamic performance and accurate determination of these separation points is necessary to optimize lift and drag forces.

The oil film helps to identify the areas where laminar flow transitions to turbulent flow and the surface friction forces. In laminar flow, the oil film moves in a smooth and thin line, while in turbulent regions it shows a scattered and mixed movement. This helps to understand where the aerodynamic design is more efficient and where the flow is disrupted. The areas where the oil accumulates heavily or decreases indicate where the pressure is high or low. This information is very important to understand how the aerodynamic forces generated on the surface are distributed. The oil film visualizes how lift and drag forces are generated and provides direct information on how designs can be modified to minimize these forces. By examining the interaction of the flow with the surface, it helps to optimize the aerodynamic forces on the object.

Oil tests visualize the lines and directions of flow on an object. Streamlines show how the airflow progresses and where vortices or flow separation occur, allowing the design to be optimized to improve aerodynamic performance.

Complex geometries can create flow structures that can be difficult to understand with CFD simulations or other visualization methods. An oil film provides a direct view of how the flow is progressing over such complex geometries and where disturbances or turbulence occur. This is very useful in critical areas such as airfoils, vehicle bodies, or building corners. Oil experiments are also used to validate computational fluid dynamics (CFD) results. Simulations often theoretically predict how the flow will progress over the surface (Hesselink, L., et al, 1994). Oil experiments allow these predictions to be tested experimentally and increase the reliability of the modeling results. This method is particularly useful for understanding flow directions over the surfaces of wings, vehicles, or buildings.

A thin layer of oil is applied to the surface of the object to be tested. This oil will move under the influence of the flow. The object is placed in a wind tunnel and air is supplied at a specified speed. The wind flow causes the oil to move along the surface, leaving traces that show the direction and intensity of the flow. The traces formed by the oil film allow visual analysis of flow lines, separation zones and surface friction forces.

Oil flow visualization experiments contribute greatly to the improvement of aerodynamic designs by directly and visually examining the interaction of the flow with the surface. By visualizing critical aerodynamic factors such as flow separation, turbulence and surface friction, they enable engineers to optimize their design processes. Therefore, oil experiments in the wind tunnel are extremely important for both experimental validation and design improvements.

1.3. MiniCTA Surface Measurement Experiments

MiniCTA (Miniature Constant Temperature Anemometry) surface measurement probe is a highly sensitive and important measurement tool for aerodynamic studies. It is used to measure critical flow parameters such as velocity profiles, turbulence intensity, and flow separation, especially at low Reynolds numbers and in thin boundary layer regions (Zhang, X., & Liu, Y. 2022). The use of MiniCTA probe in wind tunnels is essential for understanding aerodynamic forces and optimizing designs. MiniCTA probe is used to measure thin boundary layer flows on the surface of the object. The boundary layer is the region where airflow slows down along the surface and has significant effects on aerodynamic performance. MiniCTA analyzes the flow characteristics by determining the velocity profiles and whether the flow is laminar or turbulent in this region.

It can precisely measure the levels of turbulence in the flow. Turbulent flows can cause aerodynamic forces to become unbalanced and lead to performance losses. Using the probe, it is possible to analyze the turbulence intensity and energy spectrum. Measuring the effect of turbulence is critical, especially in wind tunnel experiments at low speeds.

The MiniCTA probe is also used to detect regions where the flow separates and reattaches from the surface. Flow separation causes increased aerodynamic drag, so determining when and where the flow separates is vital information for optimizing performance.

In critical transition regions where laminar flow transitions to turbulent flow, it directly affects lift, drag, and surface friction. Using these measurements, engineers can optimize surface geometry and improve flow performance.

The MiniCTA probe is particularly useful for measuring flow at low speeds, for micro aircraft, small wings or for studying bio-inspired aerodynamic models. In wind tunnel studies, this probe provides high accuracy at low speeds and can capture even small details.

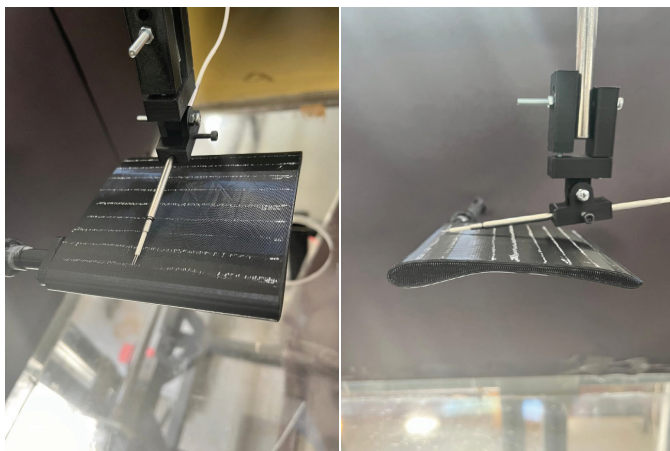


Figure 6. MiniCTA surface probe application

The MiniCTA probe is placed at a certain distance above or near the surface to be tested. This requires careful placement to ensure the most accurate measurement of the boundary layer and flow. The focus is usually on the boundary layer region, as this is the area where aerodynamic forces are most directly affected. In order for the MiniCTA probe to make accurate measurements, it must be calibrated before wind tunnel testing. This calibration increases the sensitivity of the probe, which is sensitive to temperature changes and wind tunnel speed, and allows for accurate data collection. When the wind tunnel is operated, the MiniCTA probe continuously measures the speed, turbulence and direction of the flow. The probe can quickly detect small fluctuations and velocity changes in the flow. This data is recorded at high frequency to provide a detailed analysis of the flow structure. The collected data is analyzed to determine critical parameters such as boundary layer thickness, velocity profile, turbulence intensity and flow separation. These analyses are compared with both experimental and numerical simulations, providing feedback for design improvement. The MiniCTA surface measurement probe is a highly sensitive instrument that enables detailed analysis of the flow in wind tunnel experiments. It helps optimize aerodynamic designs by accurately measuring critical parameters such as boundary layer flow, turbulent intensity, and flow separation. The sensitivity it provides, especially at low speeds and low Reynolds numbers, makes this probe an indispensable part of aerodynamic analysis.

Wind tunnel performance testing in different weather conditions is critical to understanding how aerodynamic designs behave in real-world conditions. Since aircraft, buildings, vehicles, and other structures often face changing weather conditions, simulations of these conditions help optimize the reliability, durability, and performance of the design.

Importance of Performance Tests in Different Weather Conditions

Real-world weather conditions are constantly changing. Parameters such as wind direction, speed, temperature, humidity, and air density change over time (Brown, T., & Smith, A. 2017). Different weather conditions can be simulated in a wind tunnel to see how objects perform under these conditions. These tests are important to verify that designs can work not only under ideal conditions but also under challenging and variable environments.

Tests at different wind speeds help measure the drag and lift forces, stability, and aerodynamic efficiency of objects. Turbulent flows at high speeds can increase aerodynamic forces on structures or vehicles. Low-speed tests are important to understand critical phenomena such as boundary layer behavior and flow separation. This allows design changes to be made to achieve optimal performance at low and high speeds.

Different weather conditions can create large changes in turbulence levels (Lee, J., & Park, S. 2019). By creating turbulent flows in a wind tunnel, it is examined how aircraft or other structures perform under these conditions. Turbulent flows can cause irregularities in lift and drag forces, which can cause imbalances and loss of performance, especially in aircraft. Understanding the effect of turbulence allows designs to be made resistant to turbulence.

Air temperature and density play an important role in the formation of aerodynamic forces (Settles, G. S. 2001). Hot air can reduce lift by decreasing air density, while cold air can affect aerodynamic forces differently by increasing density (Johnson, M., & Carter, R. 2018). By simulating different temperature conditions in a wind tunnel, the effects of these variables on the design can be analyzed. It is very important to perform performance tests at different altitudes and temperatures, especially for aircraft.

Rain, snow and icing conditions can be simulated in a wind tunnel. Such conditions can particularly affect the wing performance, surface friction and flow characteristics of aircraft. Snow and ice can accumulate on the surface, reducing lift and increasing drag. Rain disrupts the flow on the surface of the object and creates turbulence. These tests are critical for the safe and efficient operation of structures and aircraft in these difficult conditions. Tests conducted under different weather conditions are especially important for evaluating the stability and maneuverability of aircraft. The stability of aircraft or vehicles is examined in a wind tunnel under different conditions, thus testing the performance of control surfaces or aerodynamic forms in difficult conditions. This contributes to the optimization of designs in terms of both safety and performance.

The effects of climatic conditions are vital for structures or vehicles that will perform in different geographic regions. For example, high humidity in tropical regions, low temperatures in polar regions, or extreme heat in desert regions can affect the durability and functionality of designs. By simulating these climatic factors in a wind tunnel, structures or vehicles can be ensured to perform reliably around the world.

Performing performance tests in a wind tunnel under different weather conditions is critical to determining how a design will perform not only under ideal conditions but also in real-world conditions. These tests can be used in a wide range of applications from aircraft to building designs, and provide vital information to improve safety, durability, and aerodynamic performance. Therefore, simulating different weather conditions is an essential part of aerodynamic studies.

Wind Tunnel Experiments Different Application Examples

There are many studies in the literature conducted in wind tunnels. In these studies, measurements such as aerodynamic force, pressure, laminar and turbulent flows were made.

In a study conducted in a subsonic wind tunnel, aerodynamic force measurements were made using the Naca0012 wing profile. The smoke imaging method was used with this system. The results obtained with force measurements made at 3 different speeds show that they are compatible with the literature.

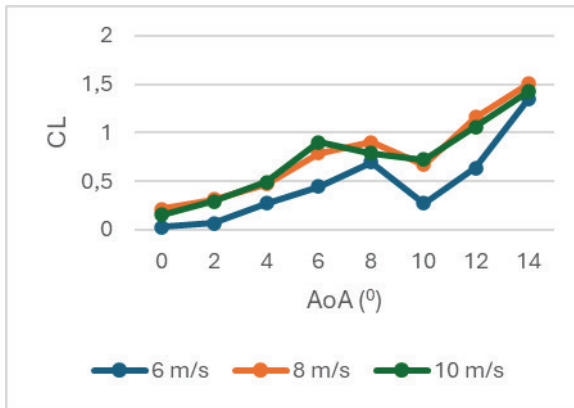


Figure 7. Lift coefficient measurement example (Yıldırım & Erbaş, 2023)

In another study, it was done with Naca0015 wing profile. In this study, the model was connected to the force system in different ways and analyses were made. Comments were made about the methods by considering the connection elements and the differences in the obtained results (Tunca S.G. & Özgür M.A.,2023). In another study, the aerodynamic force coefficients

of the Naca0015 wing profile were determined and the smoke image and the stall angle were compared. Aerodynamic analyses were made at the measured speed by determining the angle at which the smoke left the wing surface (Tunca S.G. & Özgür M.A.,2023).

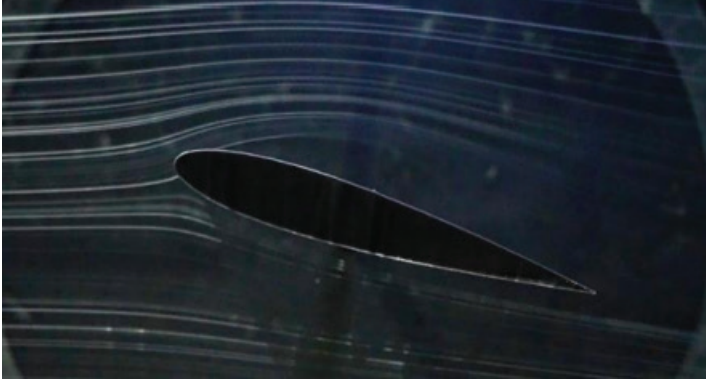


Figure 8. Smoke flow imaging experiment on Naca0015 airfoil

There are bio-inspired studies in the literature. Inspiration from nature is important in the development of designs in the field of aerodynamics. In a study conducted in this field, the pterosaur wing structure was examined and its aerodynamic characteristics were revealed. In the study, aerodynamic force measurements, smoke imaging and oil experiments were performed. Flow separation bubbles were detected with the MiniCTA surface probe (Tunca S.G. 2024).

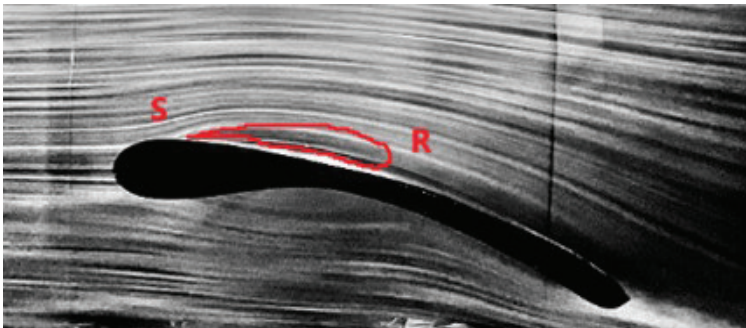


Figure 9. Detection of flow separation bubble on bio-inspired wing model

Wind tunnel experiments are an indispensable tool for optimizing aerodynamic performance, validating designs, and obtaining critical data in engineering applications. The different application examples examined in this study show that wind tunnel experiments can be effectively used in a wide range of applications from aircraft designs to energy production, from automotive aerodynamics to wind load analysis of building structures. The

results obtained reveal that these experiments not only validate theoretical analyses, but also inspire innovative design solutions. In the future, it is anticipated that wind tunnel experiments supported by developing sensor technologies and numerical modeling methods will increase their importance in different engineering disciplines by providing more precise and comprehensive analyses.

From aircraft design to wind turbines, these tests help understand airflow and aerodynamic forces. Studies on aircraft aerodynamics use wind tunnel tests to evaluate the performance of airfoils and structural designs. Lee and Park (2019), in a study examining how aircraft wings behave in different weather conditions, emphasized the role of wind tunnel experiments in improving flight stability. Similarly, in aerodynamic tests conducted for wind turbines, the efficiency and flow characteristics of turbine blades are examined in detail. Such experiments provide the necessary optimizations for wind turbines to operate more efficiently (Brown & Smith, 2017).

Wind tunnel experiments In automobile design, wind tunnel tests are conducted to reduce aerodynamic drag force and increase fuel efficiency, and aim to optimize the airflow of vehicles. In a study on automobile aerodynamics, Thompson and Davis (2020) examined how wind tunnel experiments contribute to efficiency increases in vehicle designs. As a result, wind tunnel experiments are an indispensable tool for improving aerodynamic performance and increasing efficiency in different engineering fields.

Reference

- Adrian, R. J. (1991). Particle-imaging techniques for experimental fluid mechanics. *Annual Review of Fluid Mechanics*, 23(1), 261-304. <https://doi.org/10.1146/annurev.fl.23.010191.001401>
- Brown, T., & Smith, A. (2017). *The impact of varying weather conditions on the performance of wind turbines*. *Renewable Energy*, 45(1), 56-65. <https://doi.org/10.1016/j.renene.2016.11.009>
- Fry, D. J., & Kline, S. J. (1957). Flow visualization by hydrogen bubble generation. *Review of Scientific Instruments*, 28(7), 584-588. <https://doi.org/10.1063/1.1715965>
- Greenblatt, D., & Wygnanski, I. (2020). Wind tunnel measurement systems for unsteady aerodynamic research. *Progress in Aerospace Sciences*, 119, 100633. <https://doi.org/10.1016/j.paerosci.2020.100633>
- Hesselink, L., Post, F. H., & Delmarcelle, T. (1994). Visualization of vector and tensor data sets. In *Computer Graphics Proceedings, Annual Conference Series* (pp. 319-328). ACM. <https://doi.org/10.1145/192161.192241>
- Houghton, E. L., & Carpenter, P. W. (2003). Measurement of aerodynamic forces and moments in wind tunnels. In *Aerodynamics for Engineers* (5th ed., pp. 100-150). Pearson Education. <https://doi.org/10.1002/9780470686652.eae078>
- Johnson, M., & Carter, R. (2018). *Weather-related factors affecting the efficiency of solar panels: A case study*. *Solar Energy*, 183, 125-133. <https://doi.org/10.1016/j.solener.2019.03.008>
- Kähler, C. J., & Kompenhans, J. (2000). Fundamentals of multiple plane stereo particle image velocimetry. *Experiments in Fluids*, 29(S1), S70-S77. <https://doi.org/10.1007/s003480070007>
- Lee, J., & Park, S. (2019). *Aerodynamic performance evaluation of airfoils under different atmospheric conditions*. *Journal of Wind Engineering and Industrial Aerodynamics*, 193, 42-53. <https://doi.org/10.1016/j.jweia.2019.01.003>
- Merzkirch, W. (1987). *Flow Visualization*. Academic Press.
- Nielsen, J. N., & Wolf, D. R. (2012). Wind-tunnel balance characterization for hypersonic research. *NASA Technical Reports*. <https://ntrs.nasa.gov>
- Richardson, E. G. (1961). *Visual Methods in Fluid Dynamics*. Macmillan.
- S. G. Tunca and M. A. Özgür, (2023) "Positioning analysis of the lift force sensor in subsonic wind tunnel test chamber design and its effect on naca0015

airfoil”, JSR-A, no. 055, pp. 193–205, December 2023, doi: 10.59313/jsr-a.1369969.

Sarhat, E., & Ali, A. (2018). The methods of drag force measurement in wind tunnels. *International Journal of Mechanical Engineering and Robotics Research*, 7(3), 275-280. <https://www.researchgate.net>

Settles, G. S. (2001). *Schlieren and Shadowgraph Techniques: Visualizing Phenomena in Transparent Media*. Springer. <https://doi.org/10.1007/978-3-642-56640-0>

Thompson, L., & Davis, P. (2020). *Wind tunnel tests for performance assessment of aircraft wings in different weather conditions*. *Aerospace Science and Technology*, 97, 102210. <https://doi.org/10.1016/j.ast.2019.102210>

Tunca S.G. Investigation of Aerodynamic Characteristics of Bio-Inspired Airfoil in Subsonic Wind Tunnel. Kütahya Dumlupınar University Graduate Education Institute Doctoral Thesis. Kütahya.2024

Tunca, S. G., & Özgür, M. A. (2023). Sesaltı Rüzgar Tünelinde Kanat Aerodinamiği Kuvvet Ve Akış Görüntüleme Analizleri. *Kirklareli University Journal of Engineering and Science*, 9(2), 516-527. <https://doi.org/10.34186/klujes.1391434>

Yıldırım, M., & Erbaş, O. (2023). *Naca0008 Kanat Yapısının Sesaltı Rüzgar Tünelinde Kuvvet Ve Akış Görselleştirme İle Aerodinamik Analizi*. 4. Ispen Uluslararası Modern Bilimsel Araştırmalar Kongresi .

Zhang, X., & Liu, Y. (2022). A new hypersonic wind tunnel force measurement system to investigate aerodynamic characteristics. *Aerospace Science and Technology*, 128, 107147. <https://doi.org/10.1016/j.ast.2021.107147>